Lockheed
Missiles & Space Company, Inc.
Huntsville Engineering Center

Cummings Research Park
4800 Bradford Drive
Huntsville, AL 35807

FILAMENT WOUND DATA BASE DEVELOPMENT

Revision 1

Final Report

May 1985

Contract NAS8-35054

Prepared for National Aeronautics and Space Administration
Marshall Space Flight Center, AL 35812

by

R. Scott Sharp
William F. Braddock

APPROVED C. Donald Andrews

C. Donald Andrews, Manager
Systems Anal. & Sim. Section

CONTENTS

NOMENCLATURE

C_A	axial force coefficient
C_D	drag coefficient
C_ℓ, C_R	rolling moment coefficient
C_M	pitching moment coefficient
C_N	normal force coefficient
C_n, C_{YM}	yawing moment coefficient
C_Y	side force coefficient
D_{Ref}	reference diameter, D_{Ref} = 146 in.
ET	external fuel tank
FWC	filament wound motor case
HPN	high performance nozzle extension
L_{Ref}	reference length, L_{Ref} = 1789.6 in.
M	freestream Mach number
MRP	moment reference point, $0.59L_{Ref}$ from nose
P_o	freestream total pressure, psi
P_∞, P_{STAT}	freestream static pressure, psi
q, Q	freestream dynamic pressure, psi
R_N	freestream Reynolds number, 1/ft
SRB	solid rocket booster
STD	standard nozzle extension
X, Y, Z	body axes

NOMENCLATURE (CONCLUDED)

X_M, Y_M, Z_M	missile axes
α	angle of attack, deg
α_T	trim angle of attack, deg
ΔC_p	center of pressure coefficient increment due to nozzle extension
ΔC_M	pitching moment coefficient increment due to nozzle extension
ΔC_N	normal force coefficient increment due to nozzle extension
ϕ, PHI	roll angle, deg

1. INTRODUCTION

The objective of this work was to update the present Space Shuttle Solid Rocket Booster (SRB) baseline reentry aerodynamic data base and to develop a new reentry data base for the filament wound case SRB along with individual protuberance increments. Lockheed's procedures for performing these tasks are discussed herein.

The Space Shuttle launch configuration consists of a delta wing Orbiter, a large External Tank (ET), and two Solid Rocket Boosters. At launch the Orbiter engines and the two SRBs are ignited. The SRBs burn out at an altitude of approximately 140,000 feet. After burnout, the SRBs separate from the Shuttle launch configuration and free-fall toward the ocean. At approximately 17,000 feet altitude, parachutes are deployed which lower each SRB into the ocean with an impact velocity of approximately 80 feet per second. The SRBs are designed to be recovered, refurbished, and reused.

Free-fall of the SRBs after separation from the Space Shuttle Launch Vehicle is completely uncontrolled. However, the SRBs must decelerate to a velocity and attitude that is suitable for parachute deployment. To determine the SRB reentry trajectory parameters, including the rate of deceleration and attitude history during free-fall, engineers at Marshall Space Flight Center are using a six-degree-of-freedom computer program to predict dynamic behavior. Static stability aerodynamic coefficients are part of the information required for input into this computer program.

Lockheed analyzed the existing reentry aerodynamic data tape (Data Tape 5) for the current steel case SRB. This analysis resulted in the development of Data Tape 7. The Data Tape 5 aerodynamic math model for the

1. INTRODUCTION

The objective of this work was to update the present Space Shuttle Solid Rocket Booster (SRB) baseline reentry aerodynamic data base and to develop a new reentry data base for the filament wound case SRB along with individual protuberance increments. Lockheed's procedures for performing these tasks are discussed herein.

The Space Shuttle launch configuration consists of a delta wing Orbiter, a large External Tank (ET), and two Solid Rocket Boosters. At launch the Orbiter engines and the two SRBs are ignited. The SRBs burn out at an altitude of approximately 140,000 feet. After burnout, the SRBs separate from the Shuttle launch configuration and free-fall toward the ocean. At approximately 17,000 feet altitude, parachutes are deployed which lower each SRB into the ocean with an impact velocity of approximately 80 feet per second. The SRBs are designed to be recovered, refurbished, and reused.

Free-fall of the SRBs after separation from the Space Shuttle Launch Vehicle is completely uncontrolled. However, the SRBs must decelerate to a velocity and attitude that is suitable for parachute deployment. To determine the SRB reentry trajectory parameters, including the rate of deceleration and attitude history during free-fall, engineers at Marshall Space Flight Center are using a six-degree-of-freedom computer program to predict dynamic behavior. Static stability aerodynamic coefficients are part of the information required for input into this computer program.

Lockheed analyzed the existing reentry aerodynamic data tape (Data Tape 5) for the current steel case SRB. This analysis resulted in the development of Data Tape 7. The Data Tape 5 aerodynamic math model for the

steel case SRB reentry trajectory was modified to eliminate previous anomalies in the data base and provide more accurate results by expanding the math model.

A Filament Wound Case (FWC) SRB is planned which is approximately 30,000 pounds lighter than the current steel case baseline SRB. Like the current Solid Rocket Booster, the FWC SRB will also be recoverable. Because the FWC SRB will incorporate several configuration changes, it was necessary to develop a new reentry aerodynamic data tape (Data Tape 8). The aerodynamic characteristics of the FWC booster were therefore determined by a scaled model wind tunnel test designated as TWT 691. This test was planned and implemented by MSFC and Lockheed-Huntsville personnel in MSFC's 14-Inch Trisonic Wind Tunnel (TWT). Lockheed's analysis of the results of this test culminated in the development of the FWC SRB reentry static stability coefficients, hereinafter referred to as Data Tape 8.

The configuration changes planned for the FWC SRB will alter both the total vehicle aerodynamics and the resulting dynamic behavior of the SRB during reentry. Lockheed has developed a math model for these configuration changes. Data from wind tunnel test TWT 691 were analyzed and aerodynamic increments for the systems tunnel, stiffener rings, external tank attach ring, and high performance nozzle were developed. These individual protuberance increments will enable configuration changes to be easily modeled.

Data Tape 7, Data Tape 8, and the individual configuration increments are available in magnetic tape form in MSFC's computer tape library. Data Tape 7 is available in tabular and graphical form in Appendixes A and B, respectively, of the Lockheed report which describes the development of that data base (Ref. 1). Tabular data for Data Tape 8 and the individual protuberance increments, as well as plots of the high performance nozzle increments, are contained in Appendix A of this report. Data Tape 8 is presented graphically in Appendix B of this report.

A complete description of the analyses performed to develop Data Tape 7, Data Tape 8, and the configuration increments, is presented herein along with a description of the procedures used in the development of the data base.

The TWT 691 test was planned and conducted by MSFC and Lockheed-Huntsville personnel in the MSFC 14-inch TWT. The purpose of this test was to provide data for development of the aerodynamic static stability characteristics of the Filament Wound Case (FWC) SRB configuration during reentry. The focus of the test was to obtain reentry data in the Mach range of 0.4 to 2.99 for the angle-of-attack range of 100 to 180 degrees at roll angles of 0, 45, and 90 degrees. Additional configurations were run to provide data for the development of aerodynamic coefficient increments for the attach rings, stiffener rings, systems tunnels, and high performance nozzle for both the steel case and FWC SRB configurations. These increments will enable flight configurations to be modeled by simply adding or subtracting the necessary increments. For further discussion on test TWT 691 see Section 5.1 and Ref. 3.

The TWT 694 test program was designed to obtain the aerodynamic roll characteristics of the Space Shuttle 146-inch diameter SRB reentry configuration with a redesigned systems tunnel and external tank attach ring over a portion of its reentry flight regime. The test was conducted in the MSFC 14-inch TWT for Mach numbers of 2.74, 3.48. and 4.96, angles of attack from 150 to 190 degrees, and roll angles from 0 to 360 degrees. A more detailed discussion of this test is available in Ref. 4. Data from tests TWT 694 and TWT 691 were used in the development of the FWC SRB reentry aerodynamic math model (Data Tape 8) and the individual protuberance increments.

The TWT 678 test program was designed to obtain high performance nozzle increments. This test was used along with the TWT 691 test program in the development of the high performance nozzle increment.

3. SRB AERODYNAMIC DATA TAPES

A number of wind tunnel tests have been conducted on SRB models in various wind tunnel facilities in order to supply static aerodynamic force and moment coefficients for input into the MSFC six-degree-of-freedom reentry computer simulations. The purpose of conducting the dynamic simulations is to predict the SRB attitude, velocity and deceleration rates, etc., of the reentry trajectory. These wind tunnel tests as described in Section 2 have been the basis for several iterations in the static stability reentry aerodynamic data base. In this section the history of the data tapes is traced to provide a background for future data base development.

Each of the following data tapes have recorded data listings of six-component aerodynamic coefficients (C_N, C_M, C_Y, C_n, C_A C_ℓ), in the missile axis system (see Fig. 3-1) for the right side Space Shuttle SRB with the nozzle extension removed. The data cover the Mach number range from 0.4 to 3.5. The angle of attack range is from zero to 180 degrees in five degree increments and the roll angle range is from zero to 360 degrees in 45 degree increments.

Data Tape 1 was developed from test TWT 640 (SA14F) in April 1976 by W.W. Boyle, W.F. Braddock, and Bobby Conine using a computer graphics system. Since this tape is the only aerodynamic math model of the SRB which was created from an analysis of a complete wind tunnel data base, it is the basis for all subsequent math models.

Data Tape 2 was developed by modifying Data Tape 1 data with wind tunnel test data from tests SA11F, SA16F, SA21F. These tests provided data for a large model, thin sting, and roll trim, respectively. This tape was developed in March 1977 by Boyle, Braddock, and Conine. The resulting aerodynamic math model (Data Tape 2) produced significantly better dynamic

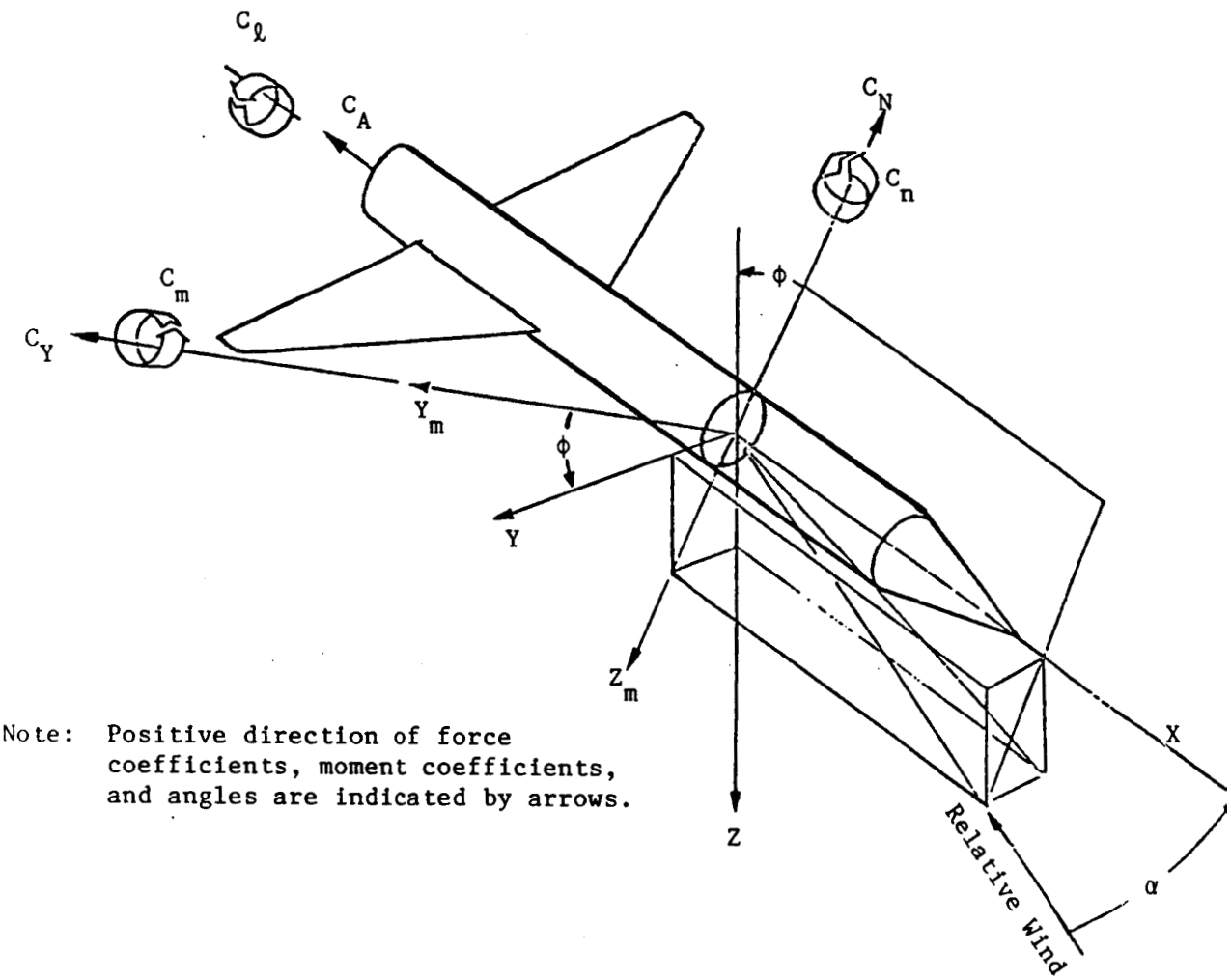

Note: Positive direction of force coefficients, moment coefficients, and angles are indicated by arrows.

Fig. 3-1 Missile Axis Systems for Right Side of SRB

4.1 STING INTERFERENCE DATA

Analysis results of the wind tunnel test data from SRB sting interference tests TWT 660 and HRWT 042 were used to evaluate the sting interference effects that should be removed from the Space Shuttle SRB reentry aerodynamic data. The wind tunnel tests consisted of a transonic test, in the MSFC 14-Inch Trisonic Wind Tunnel (TWT 660) and a subsonic test, in the MSFC High Reynolds Number Wind Tunnel (HRWT 042). The test program was designed to obtain six-component static stability data on a model of the Space Shuttle 146-inch diameter right SRB model mounted on various sting arrangements and combinations to determine the sting effects. The results of these tests provided a data base that can be used to increment force and moment coefficients to develop corrections due to sting effects in the SRB reentry aerodynamic data base.

These sting interference test programs were used to correct the Mach 0.5 data and to develop Mach 0.55 and 1.05 data base. Figure 4-1 shows normal force as a function of angle of attack for Mach 1.05. Data Tape 1 was used as the basic data which was then corrected for sting interference using the TWT 660 test results. The Data Tape 7 curve shows the results after Data Tape 1 was corrected for sting interference. Figure 4-2 depicts normal force as a function of Mach number. This plot was used as a check for the results found in Fig. 4-1. Figure 4-3 shows pitching moment as a function of angle of attack for Mach 1.05. The Data Tape 7 curve shows the results after Data Tape 1 was corrected for sting interference. Figure 4-4 shows pitching moment as a function of Mach number. These results correlate well with those of Fig. 4-3.

4.2 ADDITIONS TO DATA BASE

The flight angle of attack history superimposed on the predicted trim angle of attack is presented in Fig. 4-5. The flight data band shows a large pitch down below Mach 1.0 which indicates that near Mach 1.0 there must be a large negative pitching moment coefficient acting on the SRB

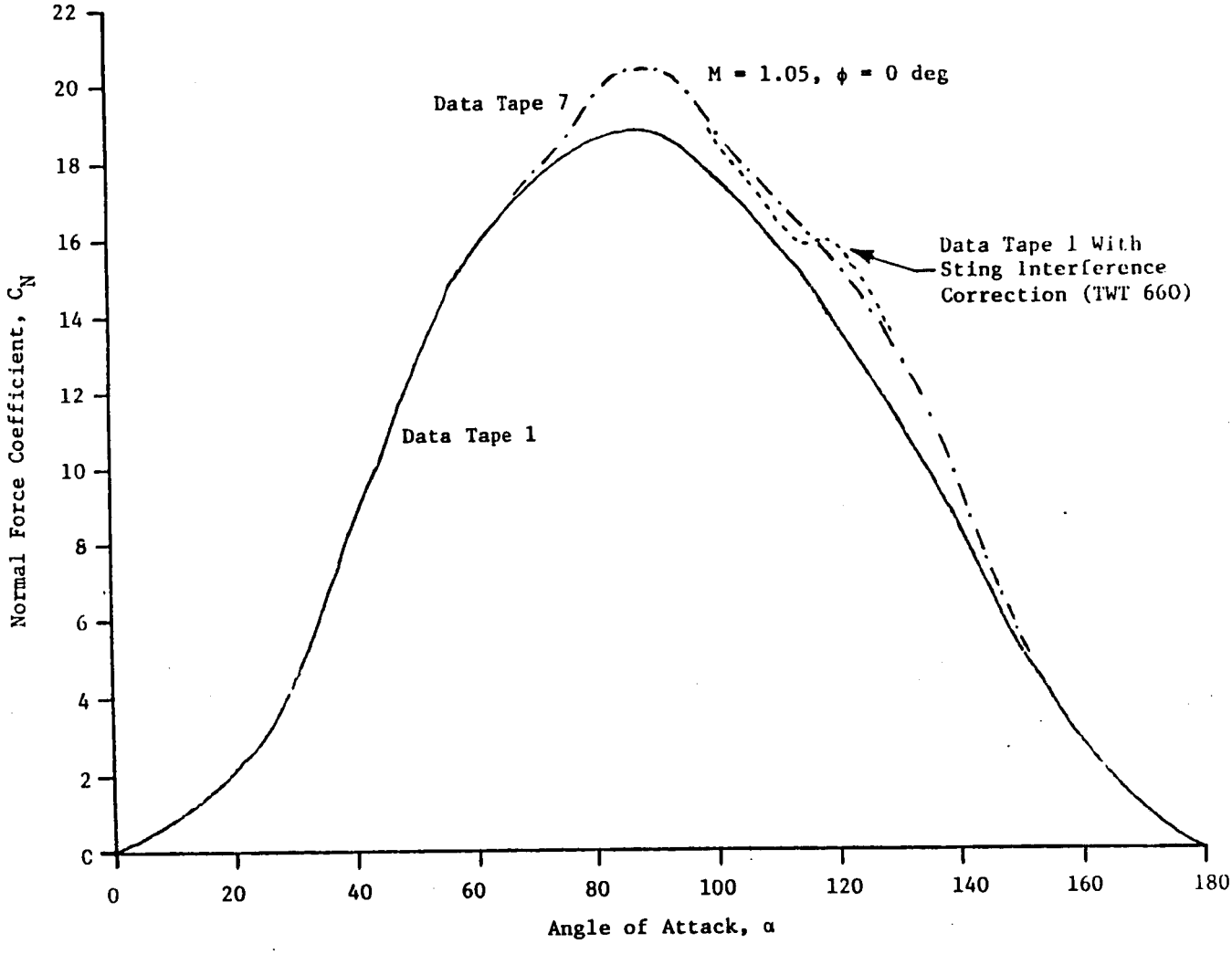

Fig. 4-1 C_N Sting Interference Correction vs α

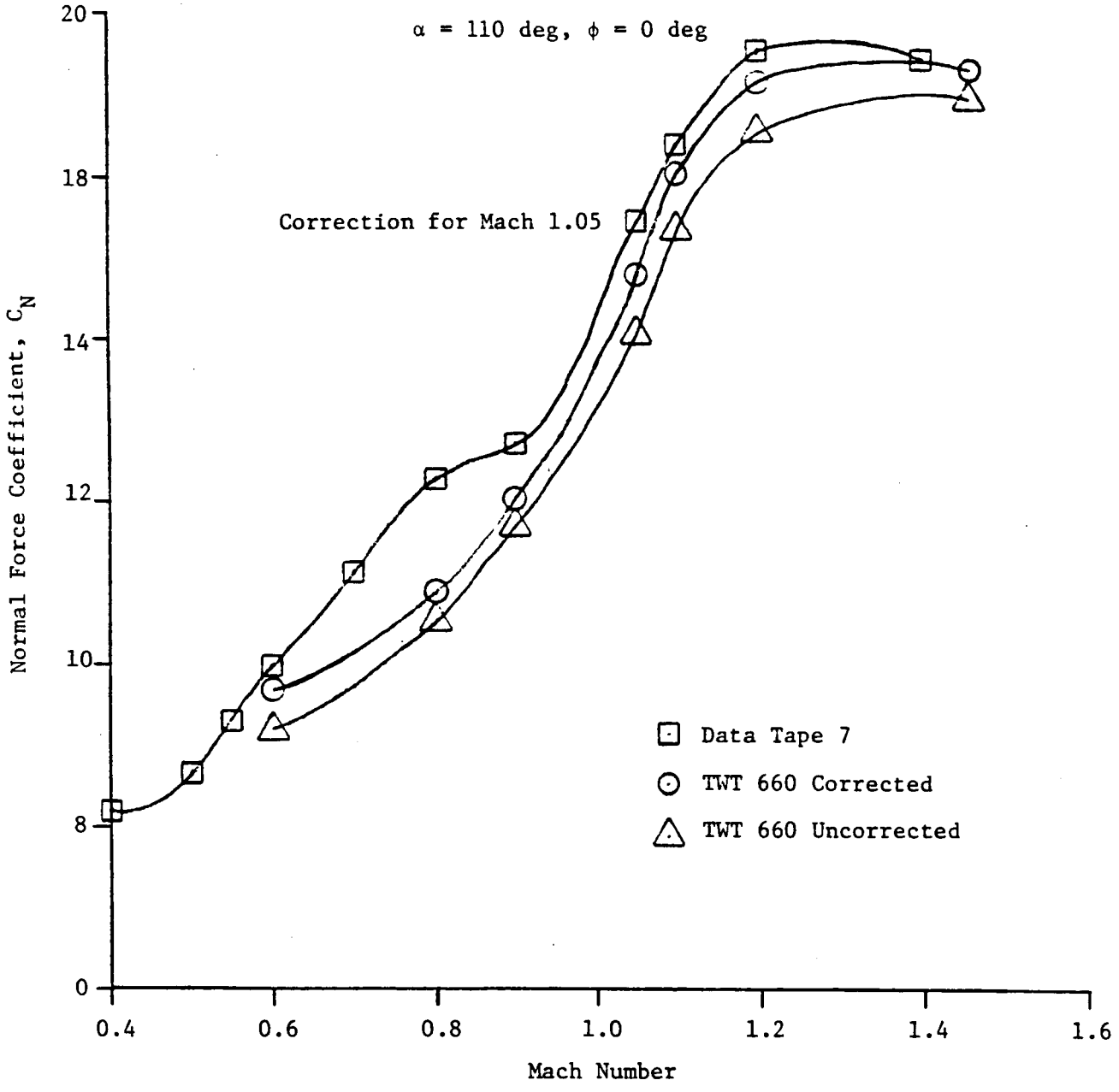

Fig. 4-2 C_N Sting Interference Correction vs Mach Number

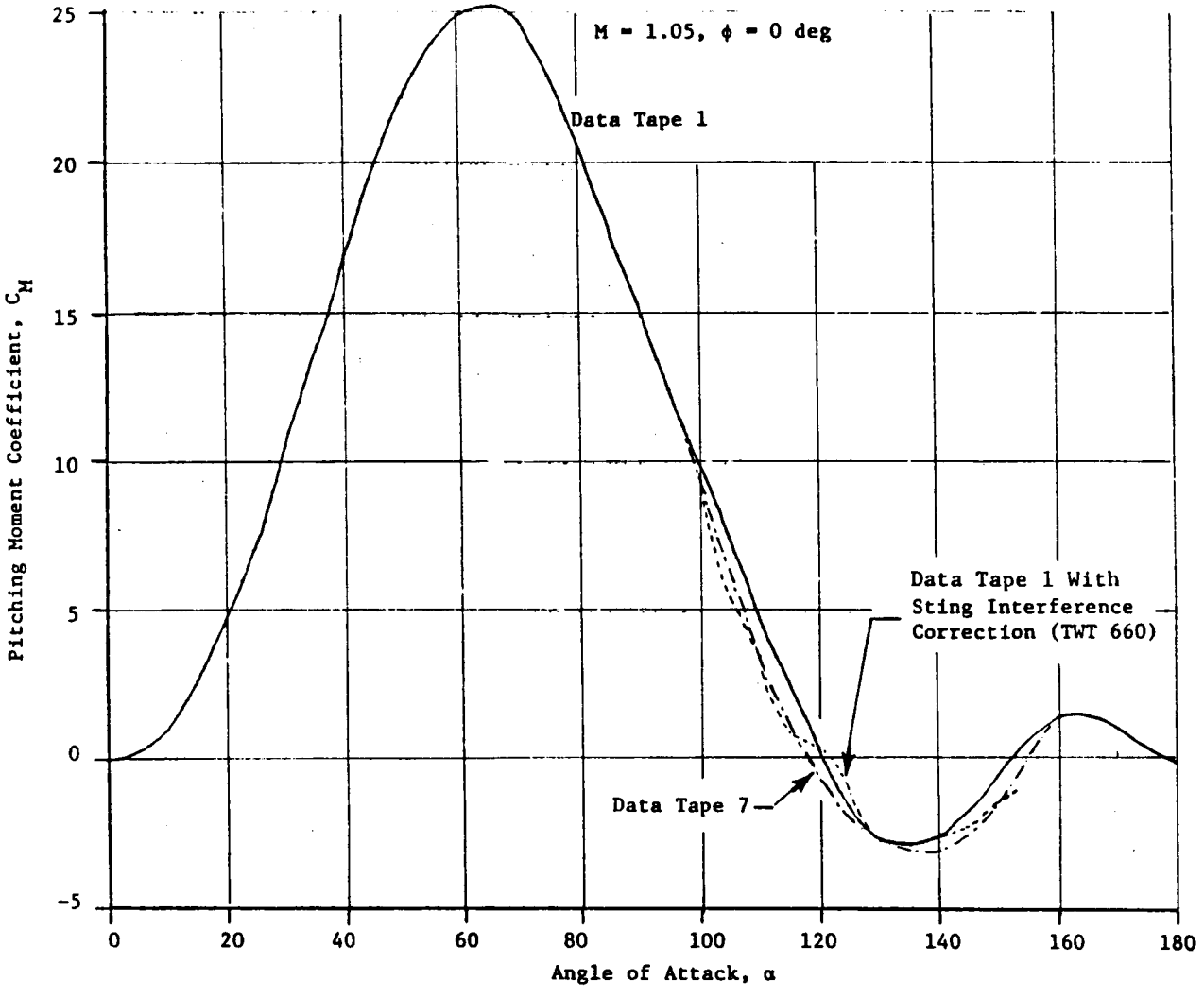

Fig. 4-3 C_M Sting Interference Correction vs α

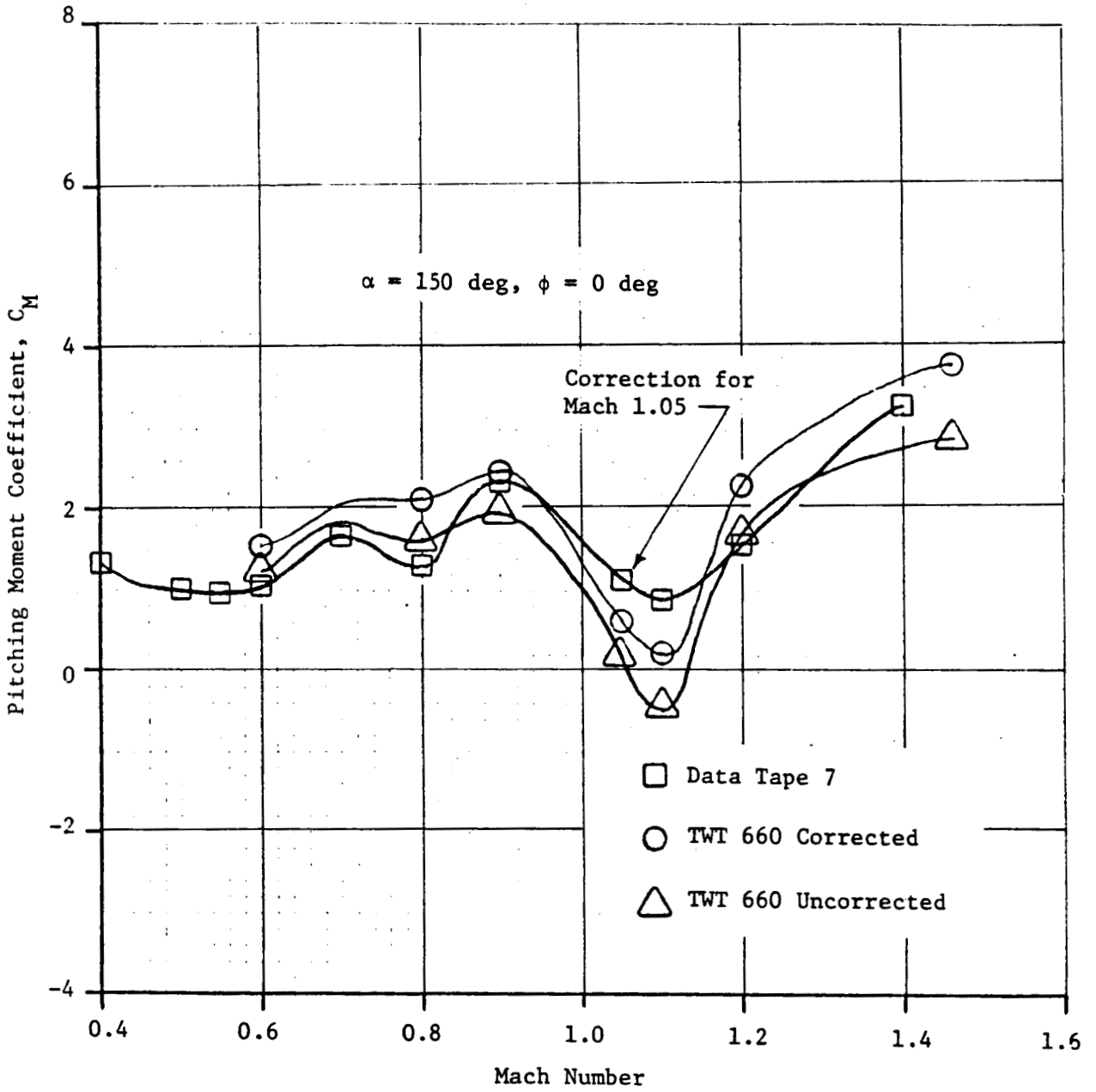

Fig. 4-4 C_M Sting Interference Correction vs Mach Number

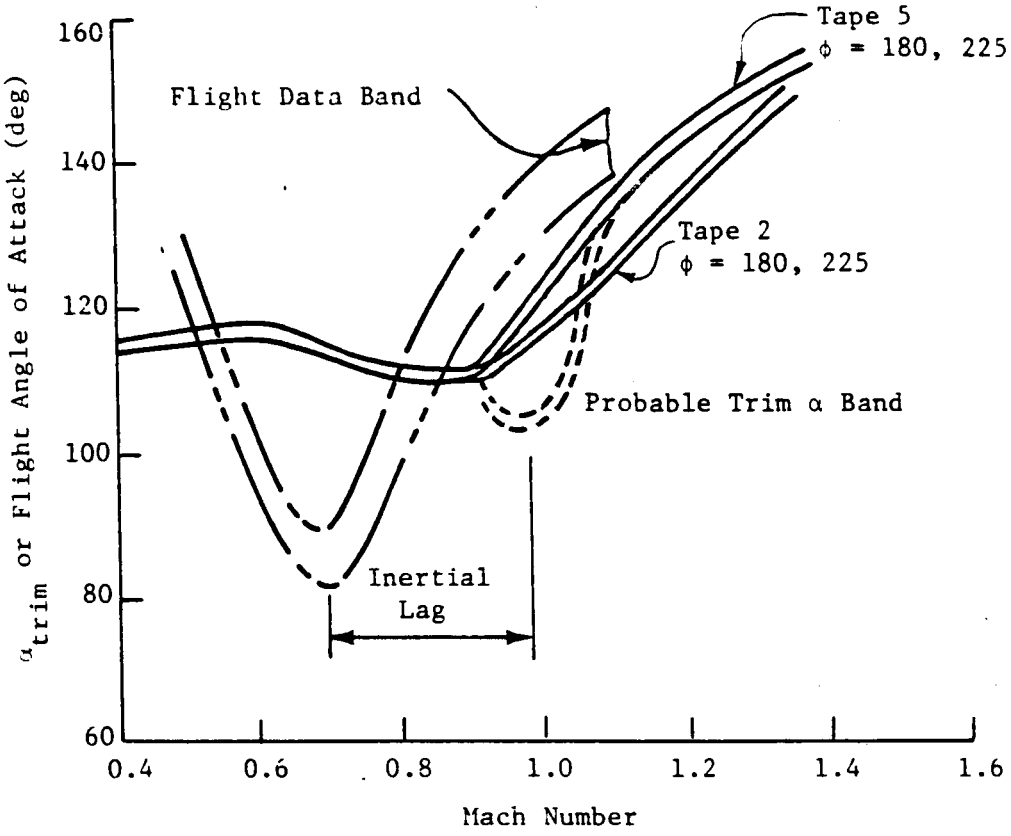

Fig. 4-5 STS-1, -2 Angle of Attack and Trim α Band

near an angle of attack of 125 degrees. The figure shows that Data Tape 5 trim angles are close to the flight data trends for Mach numbers at and above 1.1. Below Mach 1.1 the trim angle of attack is different from the flight angle of attack. This is believed to be due to a large negative pitching moment coefficients near Mach 1.0 which was not represented on Data Tape 5 because of the distribution of the Mach numbers used in making the tape. The addition of data at Mach 1.05 shows that there is a potential for large negative pitching moment coefficients in this regime.

Analysis of the high Reynolds number test program HRWT 042 depicted in Fig. 4-6 shows the need to add not only Mach 1.05 but also Mach 0.55 to the data base. Linear interpolation of Data Tape 5 values between Mach 0.5 and

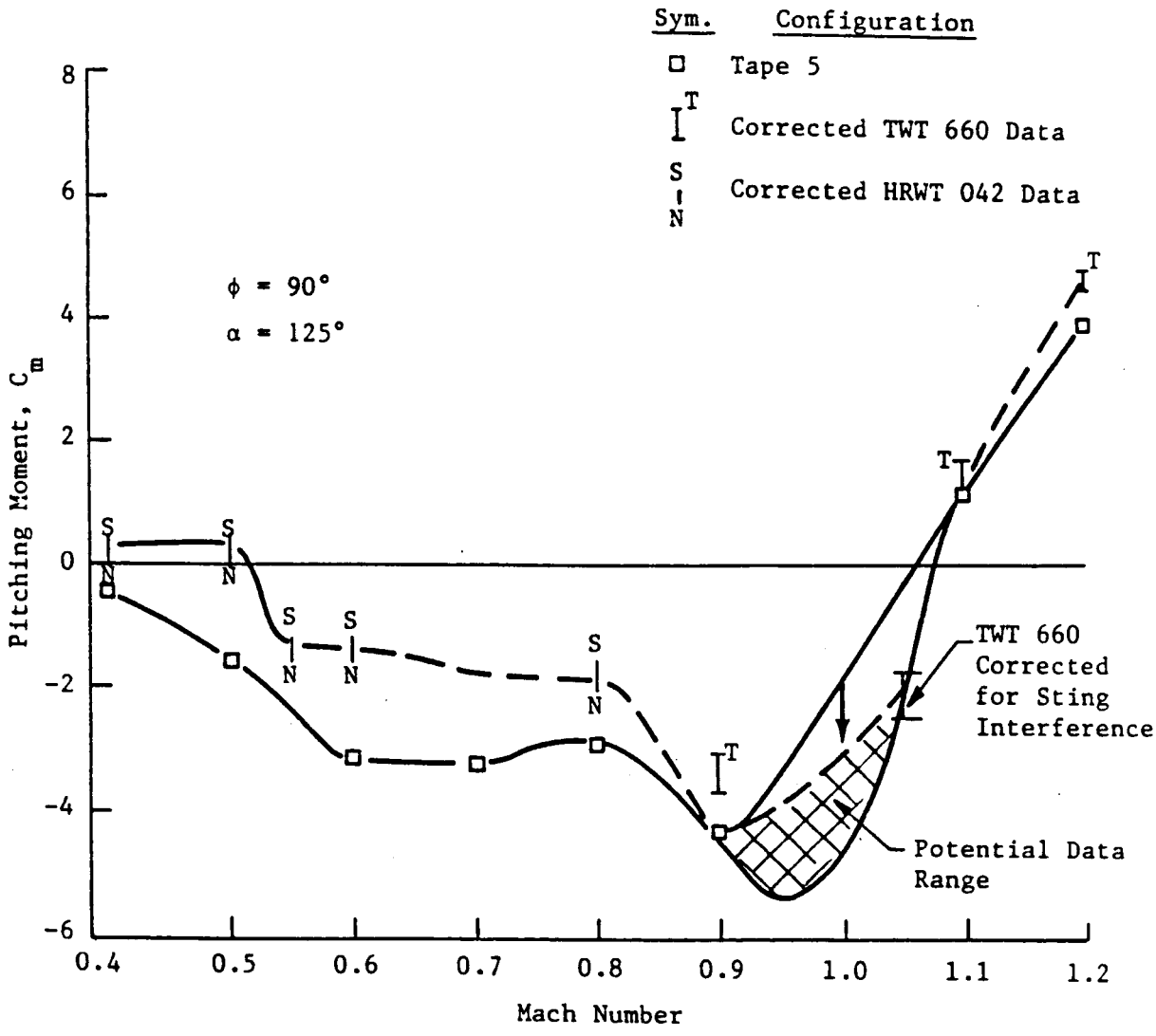

Fig. 4-6 Pitching Moment vs Mach Number, α = 125 deg, ϕ = 90 deg

0.6 would not correctly represent the pitching moment value at Mach 0.55 since Mach 0.55 data are closer in value to Mach 0.6 than Mach 0.5. Figure 4-6 also shows the linear interpolation errors from Mach 0.9 to Mach 1.1. These deficiencies in the existing baseline aerodynamic data tape necessitated the addition of Mach 0.55 and 1.05 to the data base.

4.3 CORRECTION OF ANOMALIES IN THE DATA BASE

Careful analysis of Data Tape 5 resulted in the discovery of several anomalies in the data base which originated during the development of Data Tape 2. The corrections in Data Tape 7 warrant increased confidence in the accuracy of the math model.

Mach 3.0 normal force coefficient was corrected at a roll angle of 225 degrees. This correction was necessary to smooth the normal force versus angle of attack curve so that all roll angles would have the same trends. Plots of normal force versus angle of attack were used to determine the required increments to correct Data Tape 5. Figure 4-7 depicts Data Tape 5 and Data Tape 7 after the corrections were made.

The axial force coefficient for Mach 0.9 also required correcting at 225 degrees roll angle. A significant difference from the other roll angles at high angles of attack was the reason this correction was necessary. Plots of axial force versus angle of attack were used to provide the increments necessary to achieve consistent trends in the data base. Data Tape 5 versus the corrected Data Tape 7 is shown in Fig. 4-8.

For Mach 0.5, only the pitching moment coefficient required correction. This was evident from analyzing the high Reynolds number data at the subsonic regime which showed the pitching moment coefficient at Mach 0.5 was closer to the value at Mach 0.4 than to that of 0.6 (Fig. 4-6). Figure 4-9 shows one roll angle where Data Tape 5 has been corrected in producing Data Tape 7.

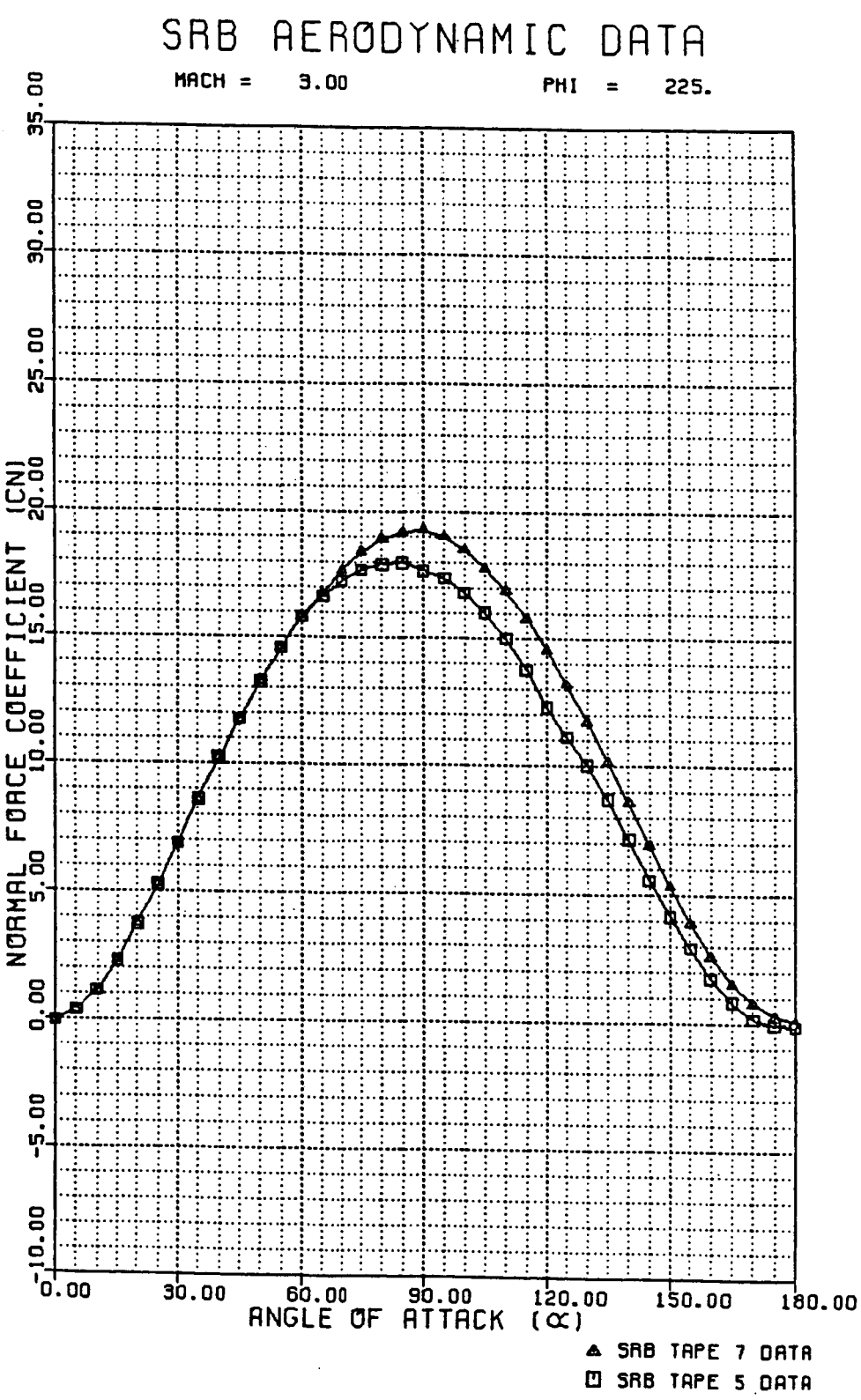

Fig. 4-7 Mach 3.0 Corrections for Normal Force

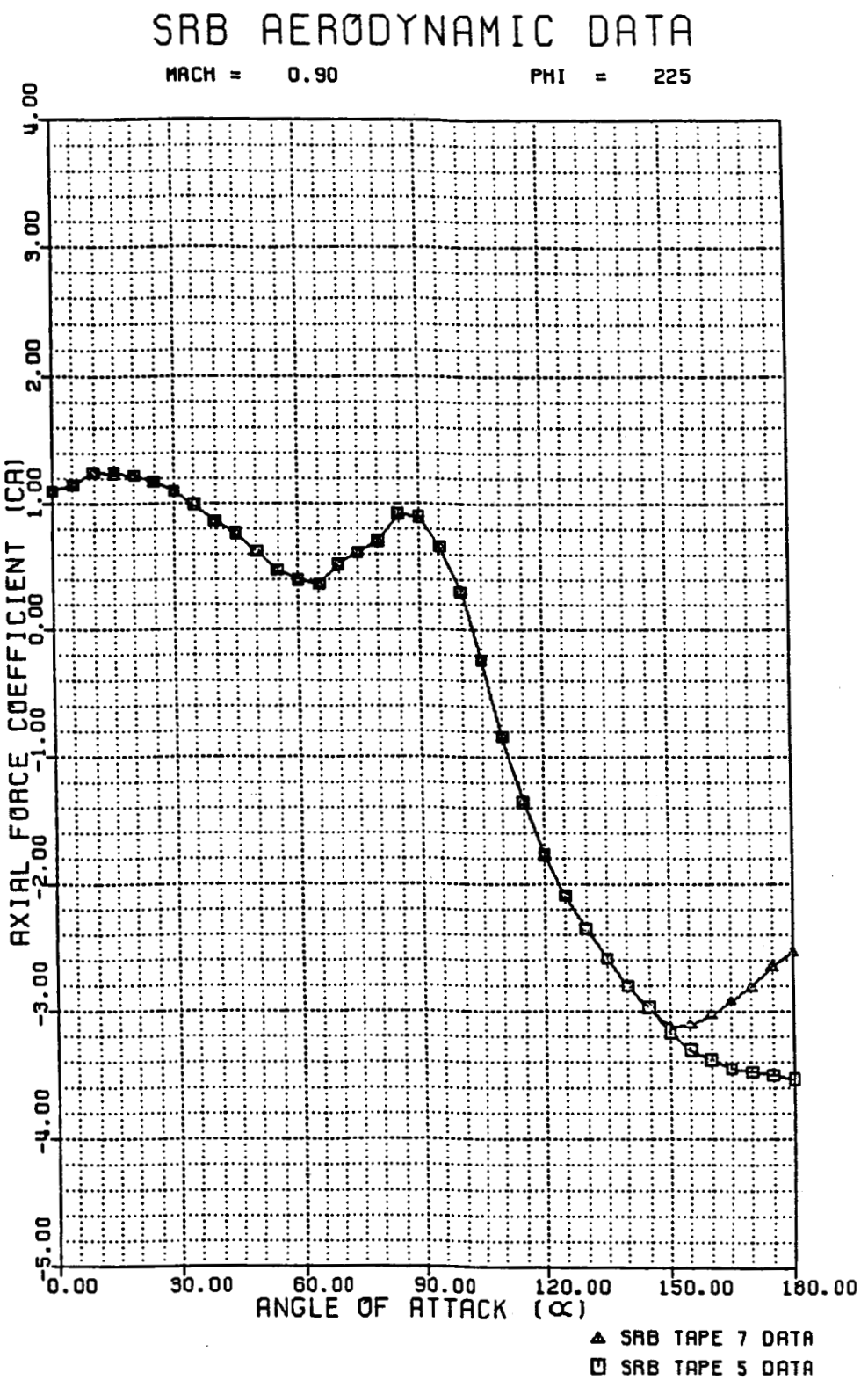

Fig. 4-8 Mach 0.9 Corrections for Axial Force

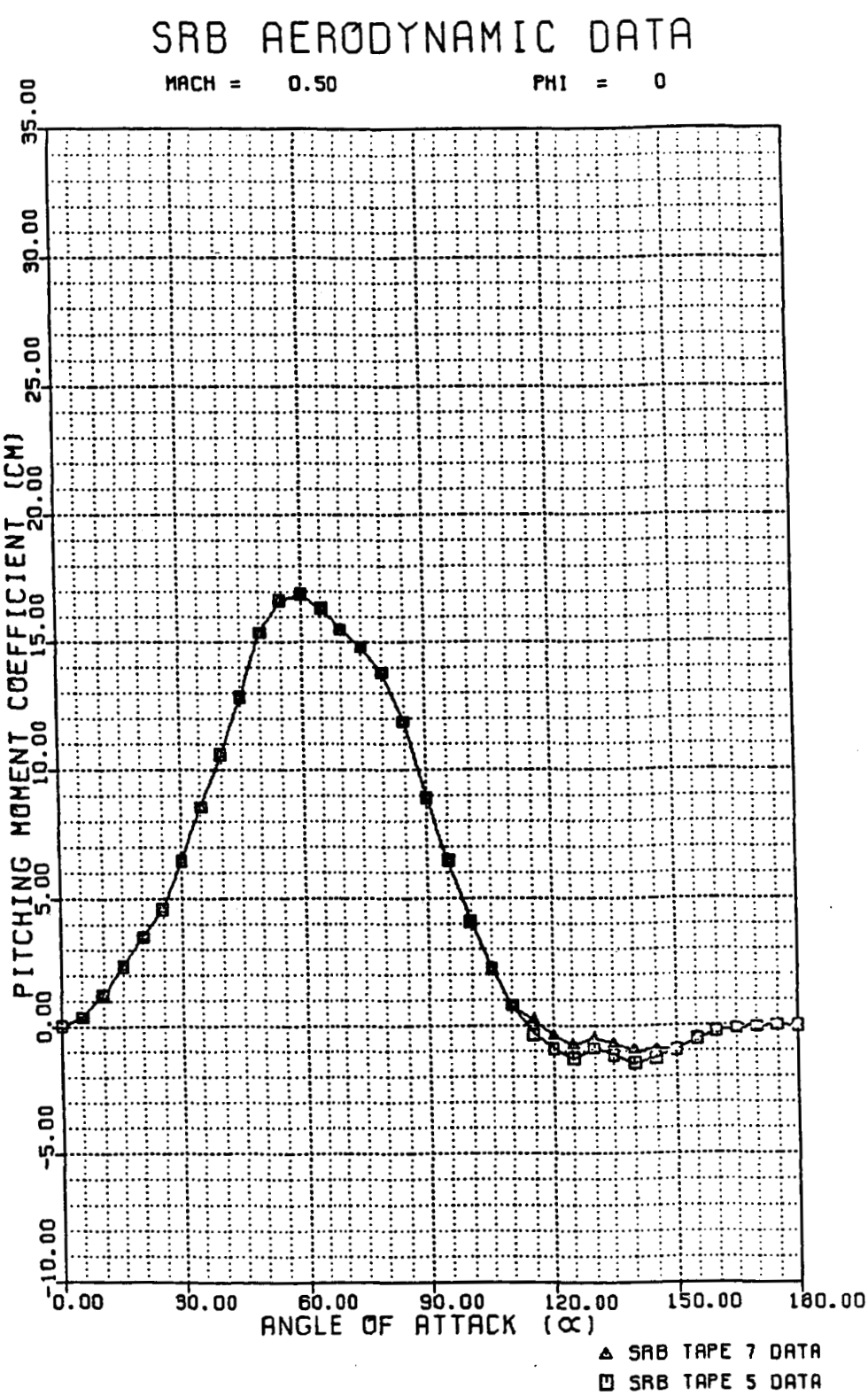

Fig. 4-9 Mach 0.5 Corrections for Pitching Moment

4.4 TABULAR DATA EXAMPLES

Tables 4-1 and 4-2 are examples of the format used to present the new baseline aerodynamic data for the right side steel case SRB without nozzle extension (Data Tape 7). Each table consists of six-component force and moment coefficients as a function of angle of attack from 0 to 180 degrees in 5 degree increments for a specific Mach number and roll angle. A complete tabular listing is available in both Appendix A of Ref. 1 and on tape in the MSFC computer tape library.

4.5 GRAPHICAL DATA EXAMPLES

Figures 4-10 through 4-15 are example plots of Data Tape 7. Each of the six force and moment coefficients (C_N, C_M, C_Y, C_n, C_A, C_ℓ) was plotted as a function of angle of attack for a specific Mach number and roll angle. Appendix B of Ref. 1 presents a complete set of these plots for all Mach numbers and roll angles.

Table 4-1 SAMPLE OF TABULAR DATA FOR DATA TAPE 7

RIGHT SIDE SRB REENTRY STATIC STABILITY COEFFICIENTS

DREF=146 IN
LREF=1789.6 IN
MRP=.59*LREF (STA 1255.9)

MACH= 0.40
PHI= 0.0

ALPHA	CN	CM	CY	CYM	CA	CR
0.	0.07130000	0.04630000	-0.00050000	0.00870000	0.86049992	-0.02020000
5.	0.47679991	0.48509991	-0.05130000	0.01880000	0.90120000	-0.01740000
10.	0.91270000	1.24179995	-0.07179990	0.02290000	0.98829991	0.01340000
15.	1.43090010	2.28000021	0.01210000	0.12509990	1.03520012	0.04690000
20.	2.00449991	3.48880005	0.12080000	-0.25479990	1.01539993	0.06760000
25.	2.65030003	4.90520000	0.18449990	-0.31189990	0.96920002	0.06090000
30.	3.40200019	6.54669952	-0.36899990	0.15349990	0.88239992	0.04640000
35.	4.16660023	8.12019920	-1.89170003	0.39780000	0.76650000	0.03200000
40.	5.12870026	10.05809975	-3.67339993	0.66419983	0.62549990	0.02170000
45.	6.33950043	12.35490036	-5.39649963	1.07789993	0.48040000	0.00970000
50.	7.41199970	14.44510078	-6.22659969	1.53660011	0.33539990	-0.00990000
55.	8.22800064	15.63200092	-6.48270035	3.58100009	0.15759990	-0.01782860
60.	8.84690094	16.15719986	-5.86509991	2.11740017	-0.00025860	-0.02575720
65.	9.22050095	15.70929909	-6.23849583	-1.95948505	-0.17782420	-0.02948110
70.	9.51799965	15.36090088	-7.90787363	-7.73608875	-0.32047570	-0.03129800
75.	9.83970070	15.19639969	-8.30158043	-4.39030266	-0.40720180	-0.03741600
80.	10.05809975	14.11720085	-7.09518242	-1.15729523	-0.35598800	-0.03939800
85.	10.11389828	11.90080166	-6.82890701	-3.58694553	0.34222960	-0.04123000
90.	10.10000038	8.74199963	-6.28835392	-3.44578719	0.27839240	-0.04214840
95.	10.21999836	6.31279993	-5.68286800	-3.59833074	0.07446990	-0.04235000
100.	10.29999924	4.00869989	-5.03343582	-2.54545641	-0.24321990	-0.04564000
105.	10.27349949	2.53700018	-5.15106010	-0.71993601	-0.62536001	-0.04770000
110.	10.20800018	1.29999995	-5.91200018	-2.10223532	-0.98475993	-0.04612000
115.	10.01670170	0.41779980	-6.34852314	-1.18999791	-1.34069991	-0.03802550
120.	9.69639969	-0.15809990	-6.14442158	-1.51999974	-1.60329986	-0.02790000
125.	9.27910042	-0.47470000	-5.25380039	-2.28078938	-1.84644771	-0.03515600
130.	8.39999962	-0.12659980	-4.28353882	-2.11825752	-2.06935978	-0.03135600
135.	7.17119980	-0.39109990	-3.00620222	-1.63847494	-2.20877719	-0.03034610
140.	6.01599979	-0.83230001	-1.94150054	-2.70373678	-2.39303350	-0.02151660
145.	5.10149956	-0.71289992	-1.98653984	-2.41366196	-2.53682852	-0.02672390
150.	4.30430031	-0.65086182	-1.28770995	-2.34250021	-2.60620070	-0.02354000
155.	3.50509977	-0.38669980	-0.79884112	-2.40274858	-2.60762596	-0.01744360
160.	2.54060009	-0.34259990	-0.05254800	-1.41636145	-2.56204128	-0.01172920
165.	1.52550006	-0.22440000	0.06795870	-0.04998570	-2.48485088	-0.00817220
170.	0.81989992	-0.11049990	-0.00334600	0.10370000	-2.37900066	-0.00103330
175.	0.25089991	-0.02310000	0.01699990	0.00650000	-2.24266005	-0.00018540
180.	-0.17440000	-0.00430000	0.01010000	-0.01756000	-2.17856169	0.00000000

Table 4-2 SAMPLE OF TABULAR DATA FOR DATA TAPE 7

RIGHT SIDE SRB REENTRY STATIC STABILITY COEFFICIENTS

DREF=146 IN
LREF=1789.6 IN
MRP=.59*LREF (STA 1255.9)

MACH= 0.40
PHI= 45.0

ALPHA	CN	CM	CY	CYM	CA	CR
0.	0.07130000	0.04630000	-0.00110000	0.00870000	0.86029983	-0.02030000
5.	0.47679991	0.48509991	-0.05130000	0.01880000	0.90450001	-0.01730000
10.	0.83519977	1.09539986	-0.06210000	0.02290000	0.99089992	0.00930000
15.	1.19229984	1.82680011	0.01210000	0.12509990	1.03730011	0.04690000
20.	1.73539984	2.89280009	0.12080000	-0.25290000	1.01729965	0.06760000
25.	2.35150003	4.15040016	0.19470000	-0.31189990	0.97000003	0.06150000
30.	3.07270002	5.64939976	0.36269990	0.06720000	0.88749993	0.04770000
35.	3.93779993	7.33640003	0.53079993	0.60210001	0.78349990	0.02540000
40.	4.65030003	8.66390038	0.65129977	0.75779992	0.62919992	-0.02170000
45.	5.46000004	9.90469933	0.72206593	0.63220000	0.50520003	-0.07400000
50.	6.23719978	10.85589981	0.72079992	0.50909990	0.38909990	-0.13909990
55.	6.96399975	11.09659958	0.63483173	0.21570000	0.26141700	-0.17370000
60.	7.37600040	10.89777565	0.38499051	0.02660000	0.17819600	-0.19992641
65.	7.64550018	10.78979492	-1.22969985	0.14460000	0.00280000	-0.22292240
70.	7.78320026	10.68470001	-1.99342895	1.16677070	-0.11519630	-0.24415420
75.	7.84160042	10.57270050	-1.57531214	0.38246810	-0.17833690	-0.23685651
80.	7.87759972	9.65559959	-0.99470031	-0.54897892	-0.21535440	-0.23978800
85.	7.94040012	7.89139986	-0.32866350	-2.15626907	0.29542580	-0.24341920
90.	7.99040031	6.18050003	0.41043240	-1.89369714	0.31517050	-0.24850141
95.	8.00029945	3.94180012	0.59598023	-0.10021760	0.19759670	-0.24743110
100.	7.96000041	2.29069996	0.65919977	1.47448933	-0.11208290	-0.24970500
105.	7.83460045	1.03569984	0.50267780	2.87648773	-0.46575570	-0.24260750
110.	7.55160046	0.11900000	0.34615570	4.21568584	-0.92185920	-0.22354920
115.	7.26509953	-0.53719980	-0.14424270	4.55431366	-1.22839046	-0.19429870
120.	6.85239983	-1.06770015	-0.67594272	4.81212711	-1.51757574	-0.19281200
125.	6.34720039	-1.41169965	0.62910312	4.16914940	-1.73994780	-0.17236800
130.	5.73229980	-1.64839995	1.47491550	3.47672081	-1.97596383	-0.14929600
135.	5.05630016	-1.99309993	0.22270720	2.66991615	-2.18973589	-0.13466831
140.	4.27149963	-2.15599990	-0.68974853	1.82882476	-2.36929226	-0.11651660
145.	3.40180016	-2.06819987	-0.76687592	1.19303036	-2.55922794	-0.09428400
150.	2.65560007	-1.95299995	-0.97558397	0.63598502	-2.63574028	-0.07619600
155.	1.74880004	-1.45760012	-0.89480102	-0.02673310	-2.61856937	-0.05569480
160.	1.16479993	-0.98509991	-0.42490050	-0.24787650	-2.56692004	-0.03653240
165.	0.68429983	-0.55359977	-0.17961110	-0.12448720	-2.48660707	-0.01758130
170.	0.37519991	-0.27590001	0.00346890	-0.01897670	-2.38558483	-0.00804730
175.	0.09130000	-0.05150000	0.00698000	-0.01736000	-2.24921989	-0.00440000
180.	-0.11790000	0.04050000	0.00490000	-0.02196000	-2.17659983	-0.00001760

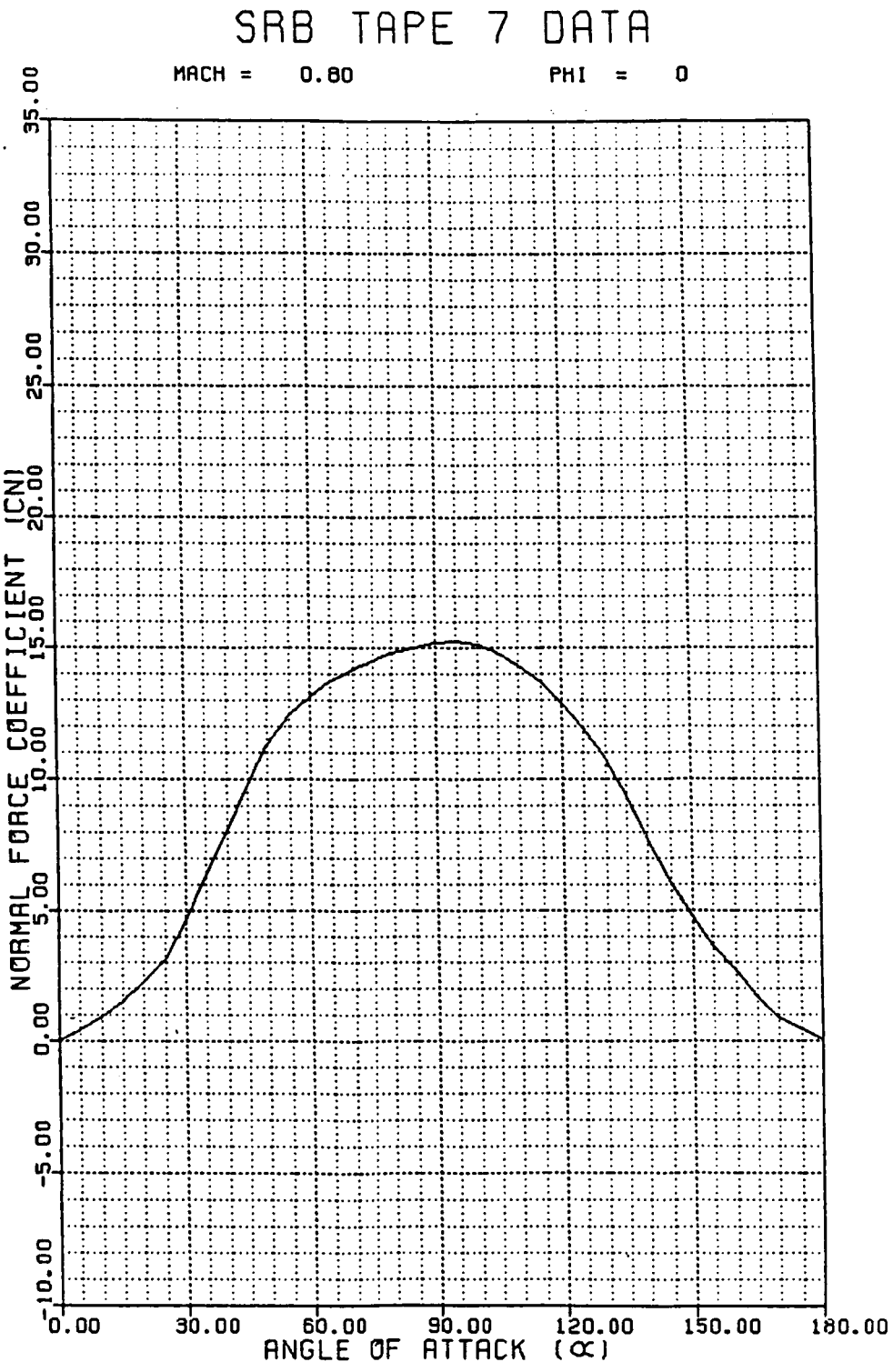

Fig. 4-10 Sample Plot of Normal Force Coefficient for Data Tape 7

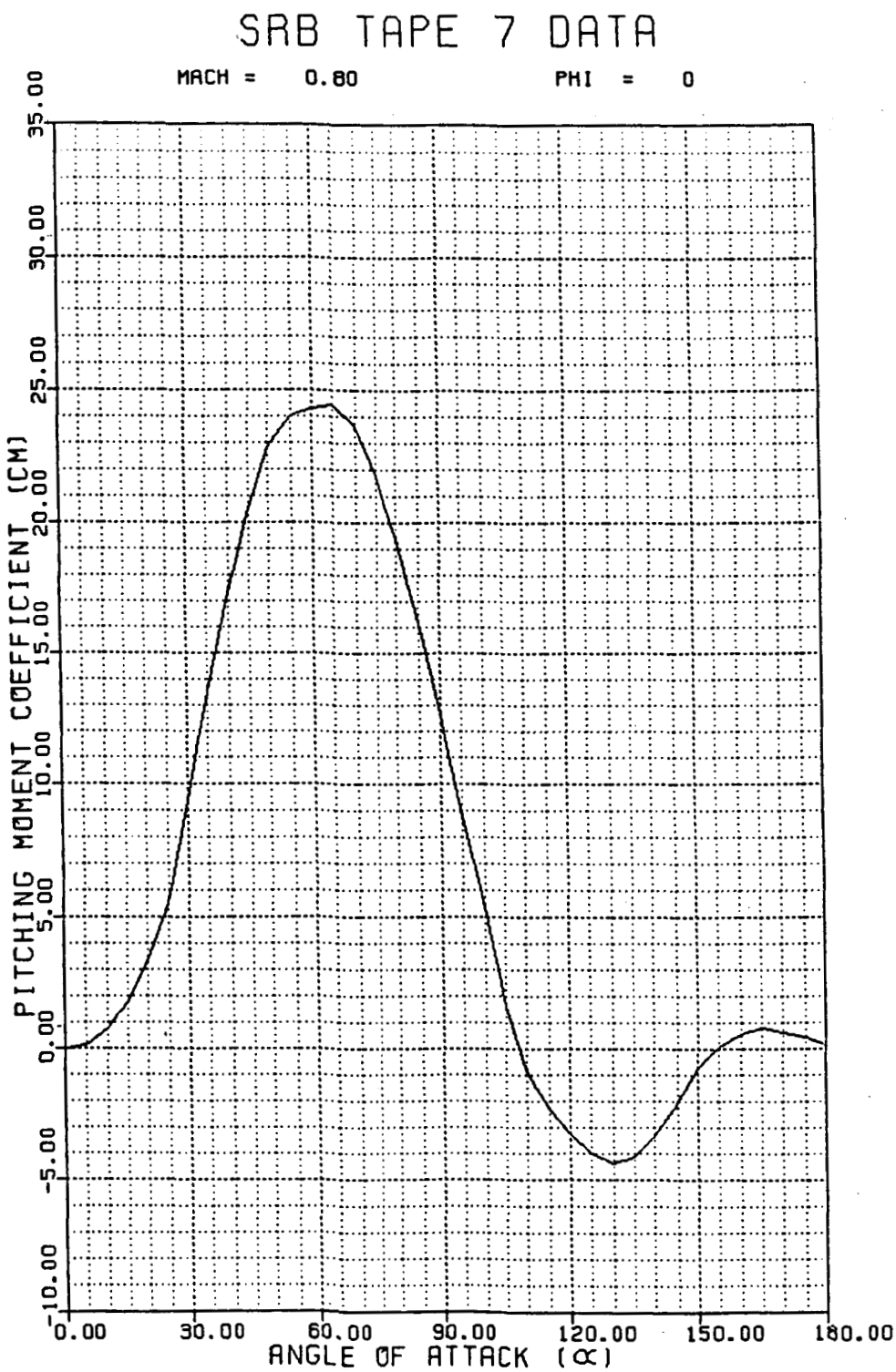

Fig. 4-11 Sample Plot of Pitching Moment Coefficient for Data Tape 7

5. DATA TAPE 8 DEVELOPMENT

Figure 5-1 shows the reentry sequence for the solid rocket boosters. The SRBs are separated from the Space Shuttle Launch Vehicle following burnout of their propellant. Initially, the SRBs enter with a tumbling motion until they are captured in a trim condition. The trim attitude and flight condition (dynamic pressure) existing at initiation of the recovery drogue chute deployment exerts a large influence on the success of the recovery system. A change in trim attitude prior to drogue deployment can change the drag level of the SRB which, in turn, can result in a change in dynamic pressure environment. Thus, an accurate knowledge of the SRB trim condition is required.

Unfortunately, at the large angles of attack where the SRBs "trim," there can be considerable effects on wind tunnel results due to sting interference and changes in the flow characteristics with Reynolds number. The sensitivity of the SRB aerodynamics to Reynolds number effects is felt largely through a change in separation point of the flow about the cylinder-like SRB. The presence of protuberances or changes in configuration can likewise change the flow separation point resulting in changes in the trim conditions. The new FWC SRBs will incorporate several configuration changes to some of the SRB protuberances. These design changes include a lower, wider systems tunnel and a modified external fuel tank (ET) attach ring. Also, the aft segment stiffener rings are lower and wider in profile, fewer in number (two instead of three) and have been relocated. The aerodynamics of the FWC SRB therefore required testing and the data obtained required careful analysis. The results of this analysis has culminated in the creation of an FWC reentry aerodynamics data tape (Data Tape 8). This section outlines the Lockheed rationale used in the Data Tape 8 development.

5.1 WIND TUNNEL TEST PROGRAM

Because of a change in protuberances on the FWC SRB design a wind tunnel test plan was established by MSFC and Lockheed personnel to determine the aerodynamic characteristics of the FWC booster. This plan made maximum use of existing test data to minimize the test requirements for FWC booster. Figure 5-2 presents the SRB reentry angle of attack for STS-1 and STS-2. This figure was used to develop the required test matrix so that data would be obtained in the actual flight regime. The test designated TWT 691, was conducted in the MSFC 14-inch trisonic wind tunnel, an intermittent blowdown tunnel.

Since the current plan is to incorporate the FWC SRB protuberances on the steel case SRB, the test matrix included an investigation of the protuberance effects on the reentry data. Figure 5-3 presents the "full-up" configuration for the FWC SRB model used in the TWT 691 test. A cross section of the FWC and steel case systems tunnels are presented in Fig. 5-4a. Note that the FWC systems tunnel is lower and wider than the steel case version. Figure 5-4b depicts the differences between the steel case and FWC ET attach ring. Figure 5-4c presents the FWC aft segment stiffener rings configuration and the steel case configuration. Note that there are only two rings for the FWC configuration and that they are lower and wider in profile. The nozzle inserts used for this model are presented in Fig. 5-4d. Another difference between the steel case and FWC configurations is that the steel case modeled the heat shield while the FWC did not. The heat shield consists of a round metal screen mounted to the end of the aft skirt with a hole in the center to accommodate the nozzle.

The test matrix for TWT 691 included Mach numbers 0.4, 0.5, 0.55, 0.6, 0.7, 0.8, 0.9, 0.95, 1.05, 1.1, 1.2, 1.3, 1.46, 1.96, and 2.99. The angle of attack range was from 100 to 180 deg while the roll angles tested were 0, 45, and 90 deg. For more information on this test program refer to Ref. 3.

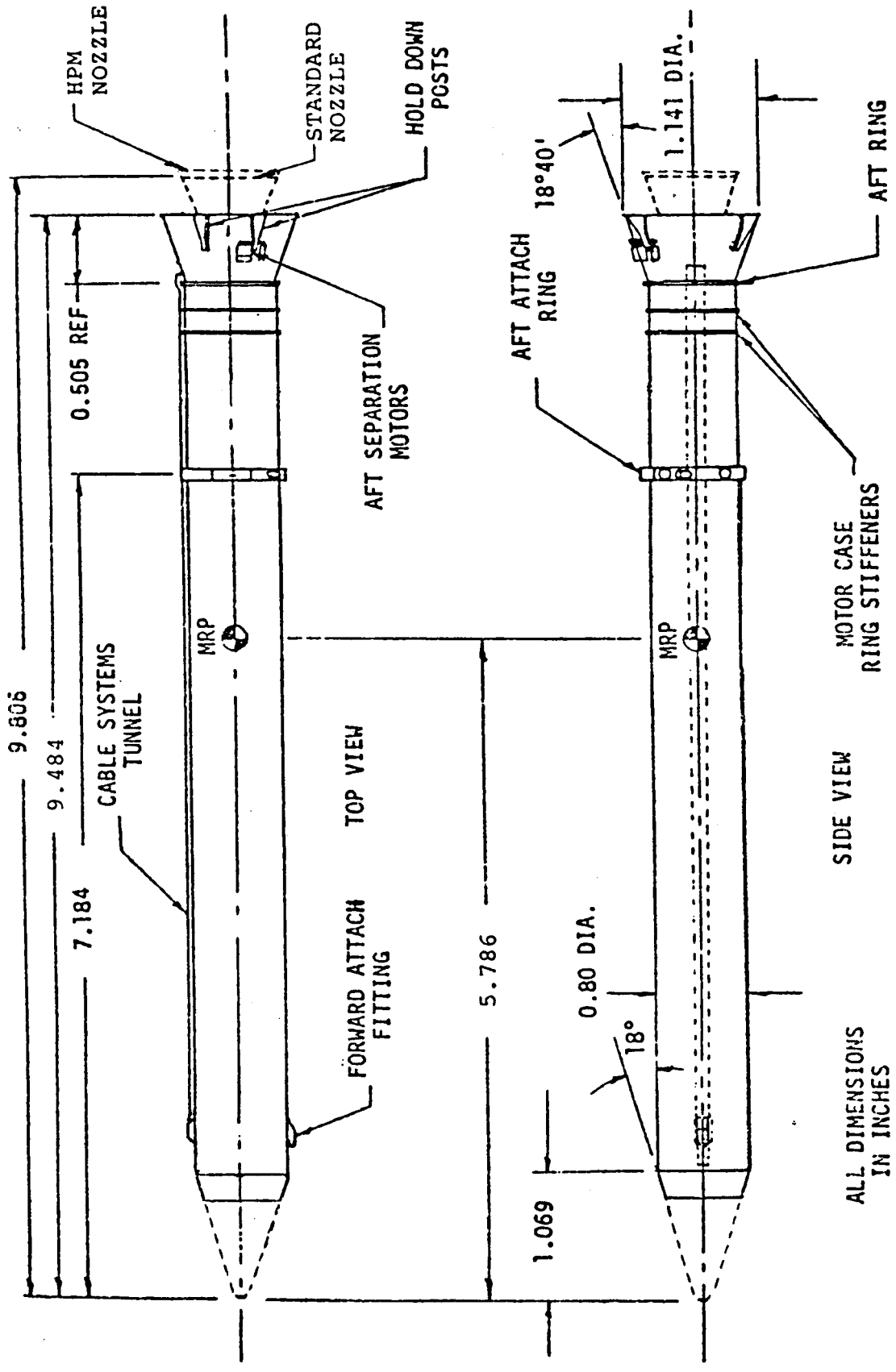

Fig. 5-3 "Full-Up" FWC SRB Scale Model

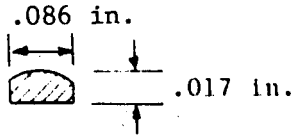

Steel Case SRB Systems Tunnel

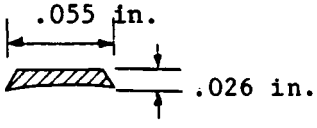

FWC SRB Systems Tunnel

Fig. 5-4a Cross-Section Comparison Steel Case and FWC SRB Systems Tunnels

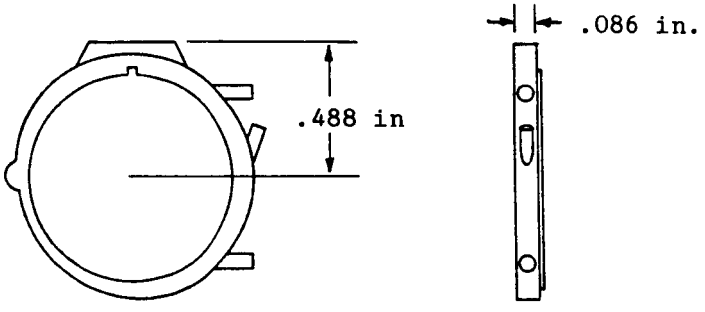

Steel Case SRB ET Attach Ring

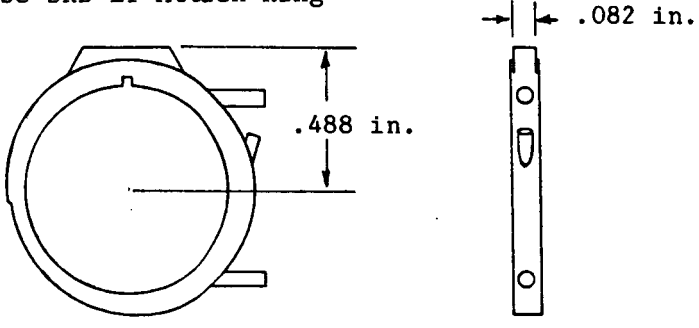

FWC SRB ET Attach Ring

Fig. 5-4b Comparison of Steel Case and FWC SRB ET Attach Rings

Note: All dimensions are in inches.

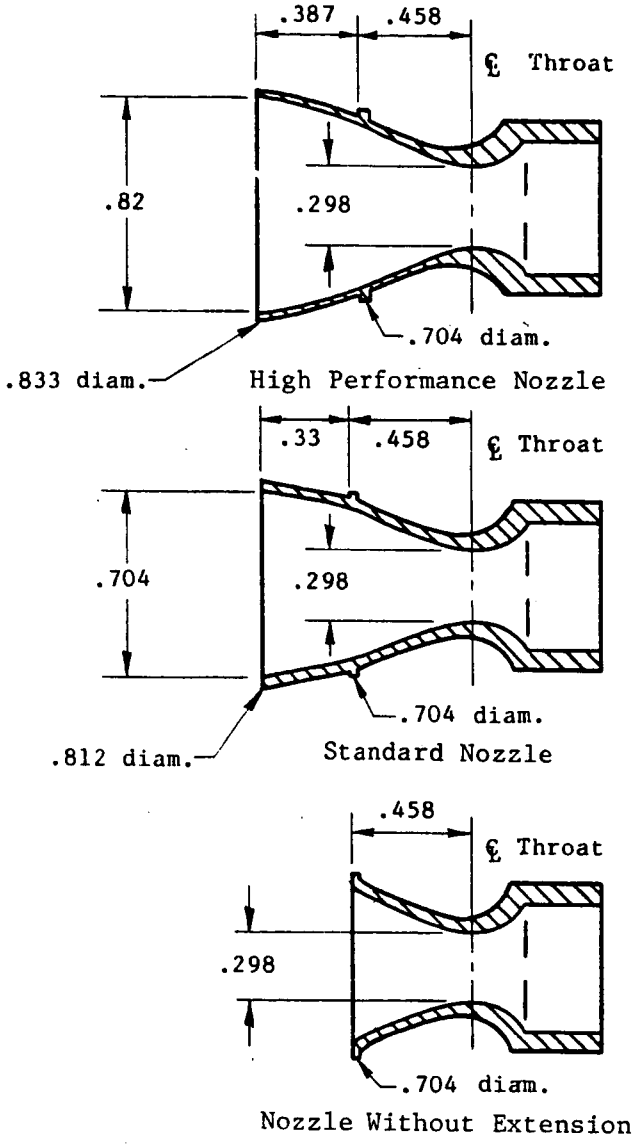

Fig. 5-4d Cross-Section Comparison of Nozzles

5.2 INCREMENT MATRIX DEVELOPMENT

Data Tape 8 was created by developing a set of increments for each of the six aerodynamic coefficients corresponding to the attitudes and Mach numbers for Data Tape 7. These increments were then added to Data Tape 7 resulting in Data Tape 8. Although another method was originally attempted, this method was subsequently chosen to eliminate the need to correct the data for sting interference and Reynolds number effects and to take advantage of the continuous development which has been incorporated into Data Tape 7.

The increment matrix was developed by subtracting the steel case SRB configuration data from the filament wound case SRB configuration data. All the filament wound case data came from wind tunnel tests TWT-691 and TWT-694 while the steel case data also came from various tests with similar sting configurations. Table 5-1 shows the plot schedule which was used to hand plot the data for all coefficients except rolling moment. Figure 5-5 compares TWT-691 rolling moment coefficient data with data from the TWT-694 test which used the sensitive roll balance. Notice the large difference between the TWT-691 and TWT-694 data. For this reason it was decided to use only sensitive roll balance data for the development of the rolling moment coefficient increments even though the available data were very limited. Table 5-2 shows the plot schedule which was used to hand plot the rolling moment coefficient data.

These plots created using the plot schedules described above were used to select the data to develop the increments. Figure 5-6 shows a sample plot where the data to be used has been selected with a curve faired through both the steel case and filament wound case configurations. These data were then cross plotted versus Mach number to ensure data correlation and to develop data for Mach numbers which were not tested. Figures 5-7 and 5-8 show sample Mach cross plots for the pitching moment coefficient and rolling moment coefficient, respectively. Figure 5-7 also shows the method used to develop Mach 0.95 increments. Since Data Tape 7 contained no data for Mach

Table 5-1 PLOT SCHEDULE FOR C_N, C_M, C_y, C_{ym}, C_A

M	Test	$\phi = 0^o$				$\phi = 45^o$				$\phi = 90^o$			
		A	B	C	D	A	B	C	D	A	B	C	D
.4	FWC: TWT-691 SC: TWT-691 TWT-678 TWT-660 TWT-669 TWT-640	453/0	255/0	36/0	478/0	430/0	232/0	37/0	501/0	429/0	231/0	60/0	502/0
.5	FWC: TWT-691 SC: TWT-691 TWT-678 TWT-660 TWT-669 TWT-640	452/0 152/0	254/0	35/0	479/0	431/0 151/0	233/0	38/0	500/0	428/0 116/0	230/0	59/0	503/0
.55	FWC: TWT-691 SC: TWT-691 TWT-678 TWT-660 TWT-669 TWT-640	451/0 153/1	253/0	34/0	480/0	432/0 150/0	234/0	39/0	499/0	427/0 117/0	229/0	58/0	504/0
.6	FWC: TWT-691 SC: TWT-691 TWT-678 TWT-660 TWT-669 TWT-640	45/0 154/0 1/2	252/0 285/0 127/0	33/0 1/3 314/0 (43/1)	481/0 9/0	433/0 149/2 12/0	235/0 216/0 277/0 126/0	40/0 12/0 322/0 (54/0)	498/0	426/0 118/0 13/0	228/0 264/0 115/0	57/0 13/0 335/0 (55/0)	505/0
.7	FWC: TWT-691 SC: TWT-691 TWT-678 TWT-660 TWT-669 TWT-640	449/0 156/0	251/0	32/0	482/0	434/0 147/0	236/0	41/0	497/0	425/0 120/0	227/0	56/0	506/0

A: $\alpha = 100^o$-120^o

B: $\alpha = 120^o$-140^o

C: $\alpha = 140^o$-160^o

D: $\alpha = 160^o$-180^o

Table 5-1 PLOT SCHEDULE FOR C_N, C_M, C_Y, C_{YM}, C_A (Continued)

M	Test	$\Phi = 0^o$				$\Phi = 45^o$				$\Phi = 90^o$			
		A	B	C	D	A	B	C	D	A	B	C	D
.8	FWC: TWT-691	448/0	250/0	31/0	483/0	435/0	237/0	42/0	496/0	424/0	226/0	55/0	507/0
	SC: TWT-691			2/2				11/0				14/1	
	TWT-678	158/0	284/0	315/0		145/0				122/0			
	TWT-660	2/1	128/0	(44/0)		11/0	125/0	(53/0)		14/0	116/0	(56/0)	
	TWT-669												
	TWT-640												
.9	FWC: TWT-691	447/0	249/0	30/0	484/0	436/0	238/0	43/0	495/0	423/0	225/0	54/0	508/0
	SC: TWT-691			3/0			217/0	10/1				15/0	
	TWT-678		283/0	316/0			278/0	321/0			263/0	336/0	
	TWT-660	3/1	129/0	(45/0)		10/0	124/0	(52/0)		15/0	117/1	(57/0)	
	TWT-669				8/0								
	TWT-640												
.95	FWC: TWT-691	446/0	248/0	29/1	485/0	437/0	239/0	44/0	494/0	422/0	224/0	53/0	509/0
	SC: TWT-691												
	TWT-678												
	TWT-660												
	TWT-669												
	TWT-640												
1.05	FWC: TWT-691	445/0	247/0	28/0	486/0	438/0	240/1	45/0	493/0	421/0	223/0	52/0	510/0
	SC: TWT-691												
	TWT-678												
	TWT-660	4/1	130/0	(46/0)		9/1	123/0	(51/0)		16/0	118/0	(58/0)	
	TWT-669												
	TWT-640												
1.1	FWC: TWT-691	444/0	246/0	27/0	487/0	439/0	241/0	46/0	492/0	420/0	222/0	51/0	511/0
	SC: TWT-691			4/0			218/0	9/0				16/0	
	TWT-678		282/0	317/0									
	TWT-660	5/2	131/0	(47/0)		8/1	122/1	(50/0)		17/0	119/2	(59/0)	
	TWT-669												
	TWT-640												

A: $\alpha = 100^o$-120^o

B: $\alpha = 120^o$-140^o

C: $\alpha = 140^o$-160^o

D: $\alpha = 160^o$-180^o

Table 5-1 PLOT SCHEDULE FOR C_N, C_M, C_Y, C_{YM}, C_A (Concluded)

M	Test	$\phi = 0^o$				$\phi = 45^o$				$\phi = 90^o$			
		A	B	C	D	A	B	C	D	A	B	C	D
1.2	FWC: TWT-691	443/0	245/0	26/0	488/0	440/0	242/0	47/0	491/0	419/0	220/0	50/0	512/0
	SC: TWT-691			5/0			219/0	7/0				17/0	
	TWT-678		280/0	318/0			279/0	320/0			262/0	337/0	
	TWT-660	6/2	132/0	(48/0)		7/1	121/0	(49/0)		18/0	120/2	(60/0)	
	TWT-669				7/0								
	TWT-640												
1.3	FWC: TWT-691	442/0	244/0	25/0	489/0	441/0	243/0	48/0	490/0	418/0	221/0	49/0	513/0
	SC: TWT-691			6/0				8/0				18/0	
	TWT-678		281/0	319/0									
	TWT-660												
	TWT-669												
	TWT-640												
1.46	FWC: TWT-691			78/0	650/0			77/0	649/0			76/0	648/0
	SC: TWT-691			74/0				73/0				75/0	
	TWT-678		255/0	344/0			256/0	343/0			261/0	338/0	
	TWT-660	79/0	90/0	(63/0)		80/0	89/0	(62/0)		81/0	88/0	(61/0)	
	TWT-669												
	TWT-640												
1.96	FWC: TWT-691			81/1	645/1			82/0	646/0			83/0	647/0
	SC: TWT-691												
	TWT-678		247/0	352/0			246/0	353/0			241/0	358/0	
	TWT-660												
	TWT-669				6/0								
	TWT-640												
2.99	FWC: TWT-691			86/0	641/0			85/0	640/0			84/0	639/0
	SC: TWT-691												
	TWT-678		234/0	365/0	372/0		235/0	364/0	373/0		240/0	359/0	
	TWT-660												
	TWT-669												
	TWT-640												

A: $\alpha = 100^o$-120^o

B: $\alpha = 120^o$-140^o

C: $\alpha = 140^o$-160^o

D: $\alpha = 160^o$-180^o

- ⊙ TWT-645 SC
- ◈ Data Tape 7
- ⊡ TWT-694 SC
- △ TWT-694 FWC
- ⊙ TWT-691 SC
- ◇ TWT-691 FWC

M = 1.46
α = 155 deg

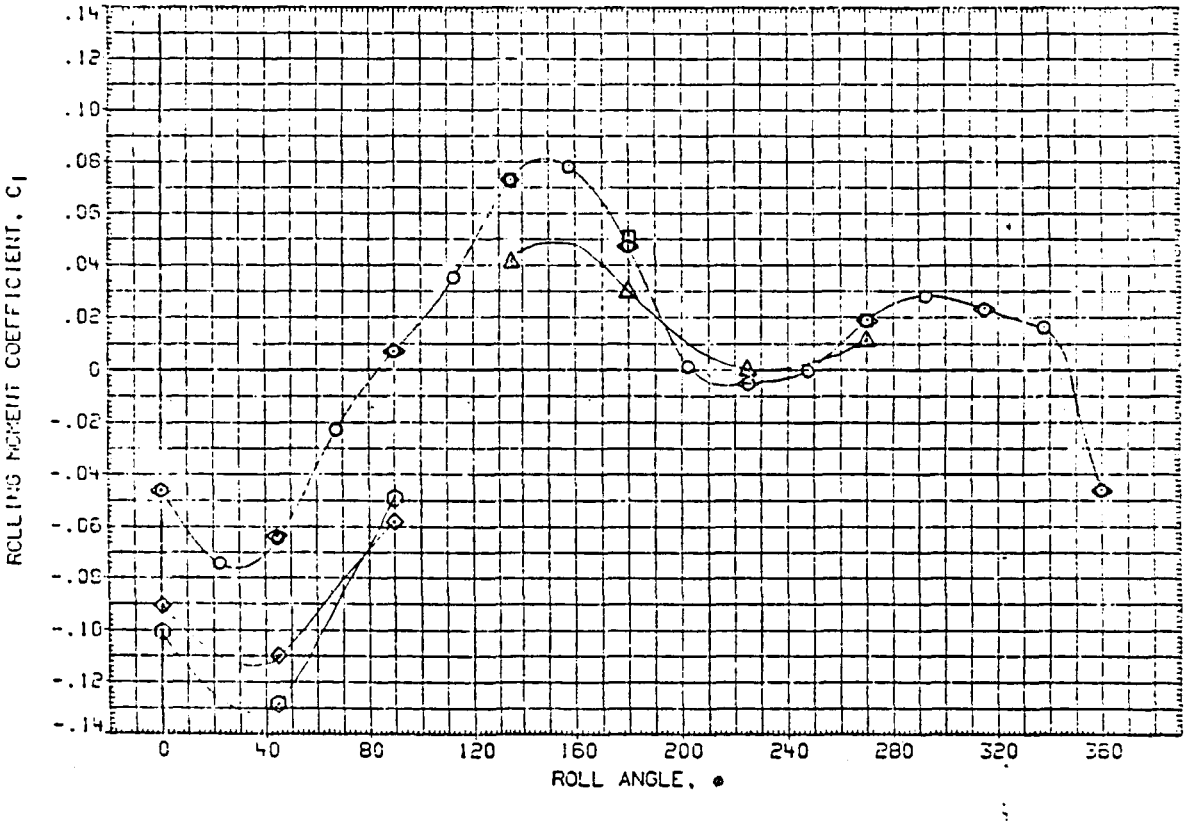

Fig. 5-5 Wind Tunnel Rolling Moment Comparison

Table 5-2 PLOT SCHEDULE FOR ROLLING MOMENT COEFFICIENT

M	Test	$\phi = 0^\circ$		$\phi = 45^\circ$		$\phi = 90^\circ$		$\phi = 135^\circ$		$\phi = 180^\circ$		$\phi = 225^\circ$		$\phi = 270^\circ$		$\phi = 315^\circ$	
		A	B	A	B	A	B	A	B	A	B	A	B	A	B	A	B
2.74	FWC w/o SR (694)	20/0	42/0	19/0		18/0		17/0	33/0	12/1	34/0	11/0	37/0	6/0	38/0	21/0	41/0
	FWC (694)							30/0									
	SC (694)							1/4	44/0	3/0	45/0	4/0		5/0			
	SC w /HS (694)								46/0								
	SC (645)	1/4	4/2	8/0	5/0	9/0	12/0	16/0	13/0	17/0	20/0	24/0	21/1	25/1	28/0	32/0	29/0
3.78	FWC w/o SR (694)		43/0					16/0	32/0	13/0	35/0	10/0	36/0	7/0	39/0		40/0
	FWC (694)							31/0									
	SC (694)							2/1									
	SC w /HS (694)																
	SC (645)	2/1	3/2	7/0	6/2	10/0	11/0	15/0	14/0	18/0	19/0	23/0	22/0	26/0	27/0	31/0	30/0
1.46	FWC w/o SR (694)							50/1		51/0		52/0		53/0			
	FWC (694)																
	SC (694)																
	SC w /HS (694)																
	SC (645)							105/1		104/0		101/0		100/1			

Note:
A: $\alpha = 150^\circ - 170^\circ$
B: $\alpha = 170^\circ - 190^\circ$

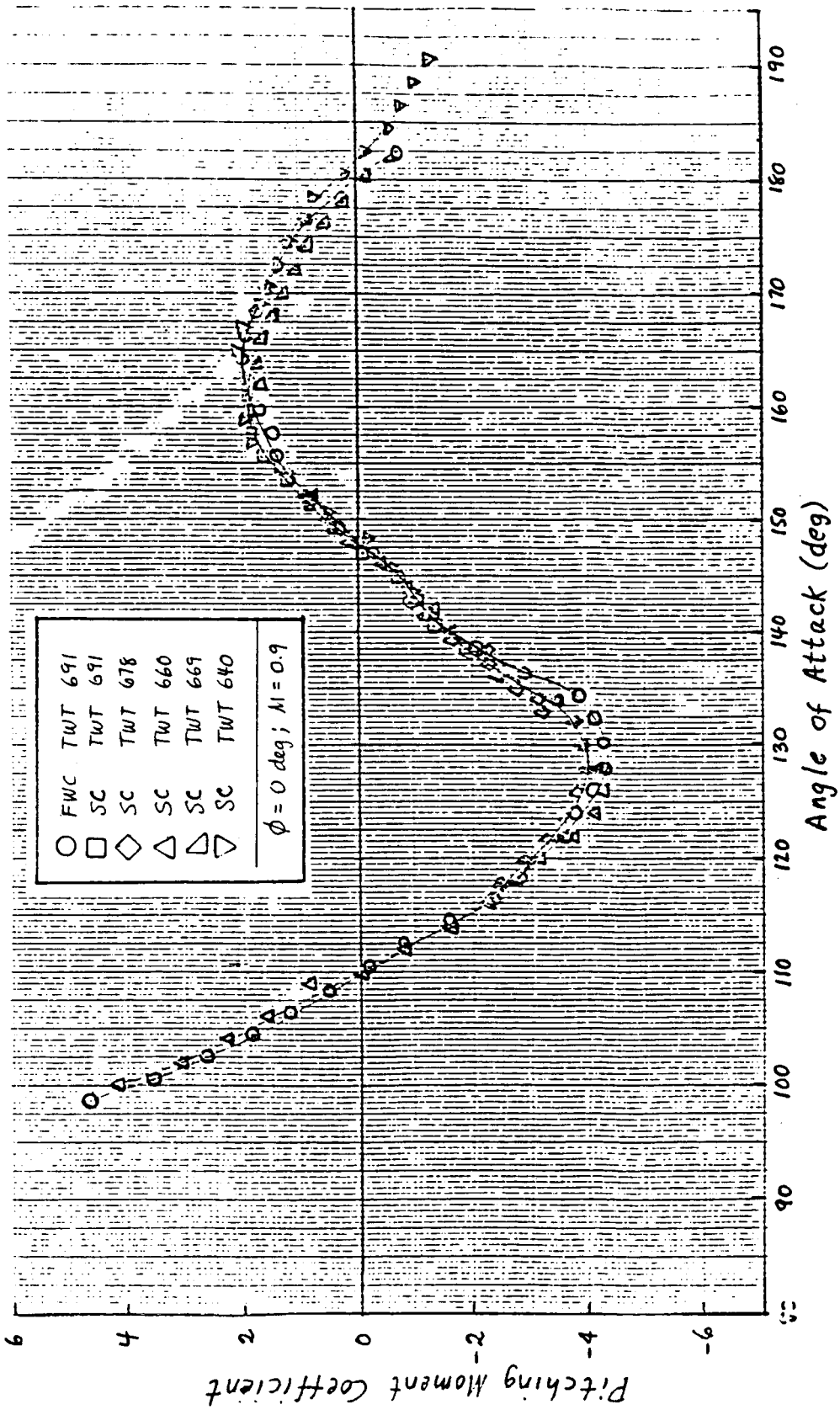

Fig. 5-6 Sample Hand Plot Used for Data Selection

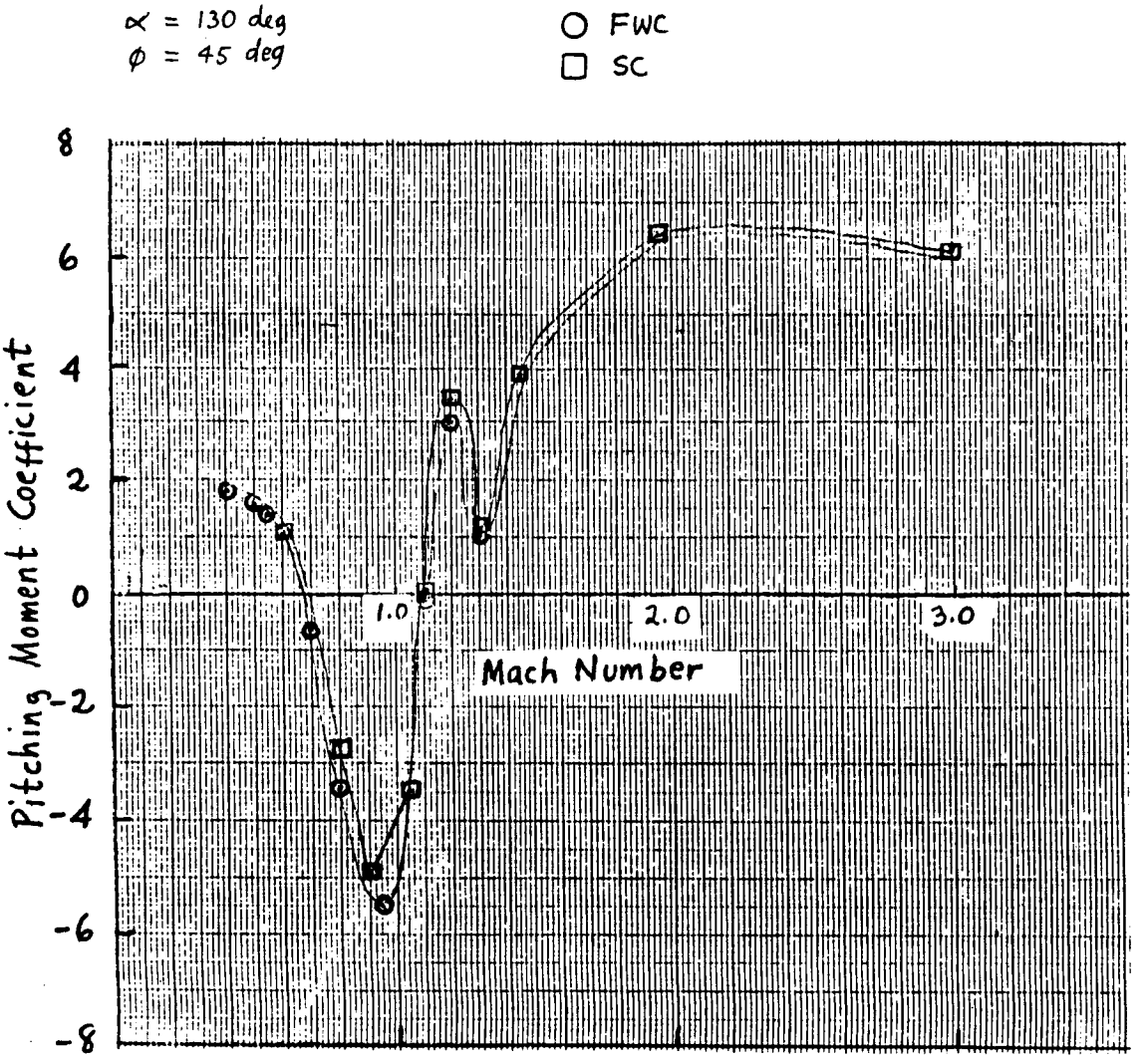

Fig. 5-7 Mach Cross Plot for Pitching Moment

ORIGINAL PAGE IS
OF POOR QUALITY

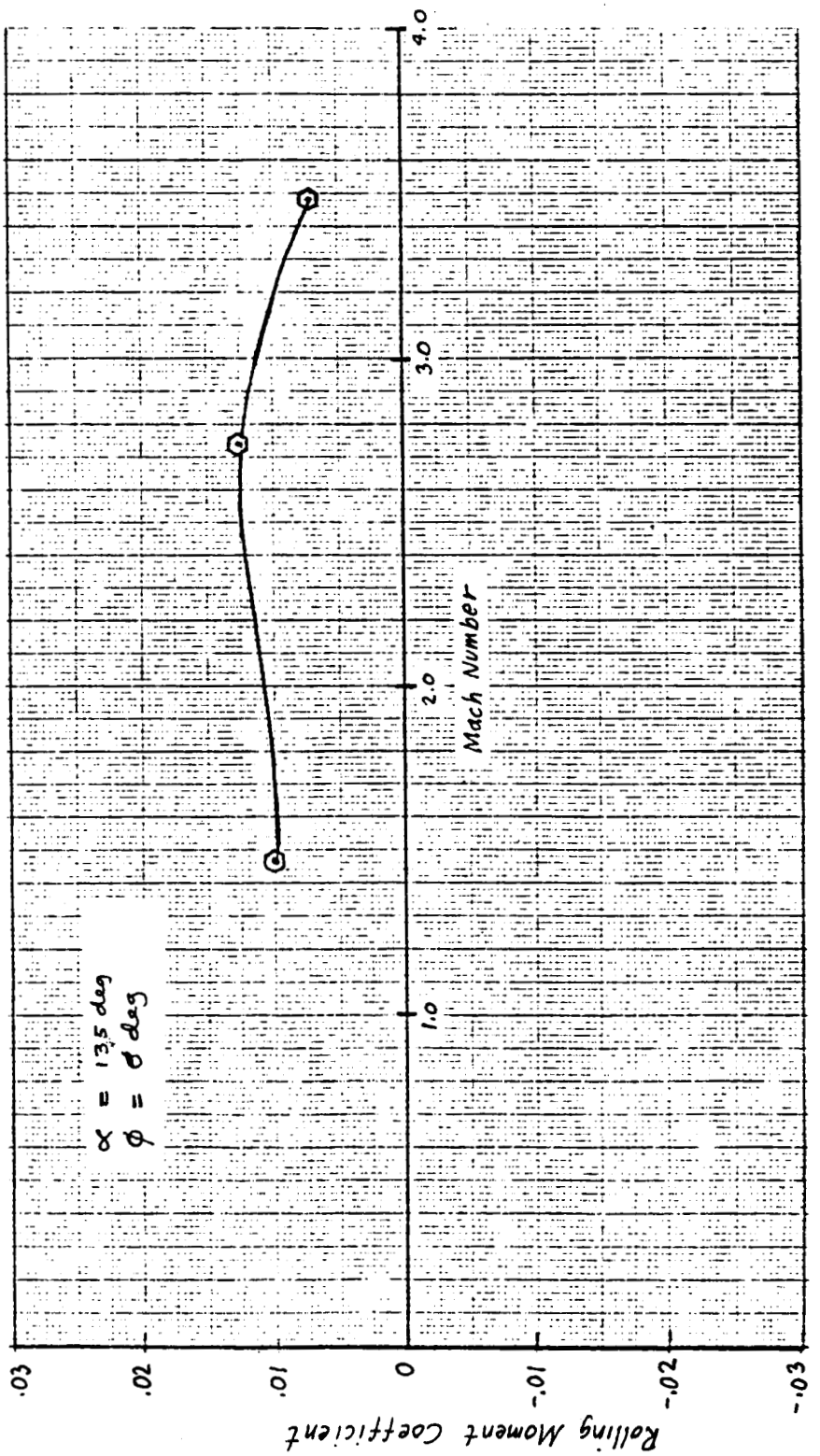

Fig. 5-8 Mach Cross Plot for Rolling Moment

0.95, the data were created by interpolating between Mach 0.9 and 1.05. The increments were then developed by interpolating between Mach 0.9 and 1.05 for the steel case configuration and subtracting it from the filament wound case configuration. Figure 5-8 shows the small amount of data which were available utilizing the sensitive roll balance. Because of this lack of data at the lower Mach numbers, the increments developed for Mach 1.46 were used for the lower Mach matrix. This was felt to be acceptable since the major concern for rolling moment is at maximum dynamic pressure which occurs at high Mach numbers.

The rolling moment data were also cross plotted versus roll angle. Figure 5-9 shows a sample plot versus roll angle. These plots were used to develop rolling moment increments at all roll angles in the Data Tape 7 matrix.

The coefficient difference between the steel case and the filament wound case configurations were determined and plotted versus angle of attack. These plots were smoothed to insure a consistent increment. Figure 5-10 shows an example of these plots. The complete matrix was tabulated for easy entry into a computer data base.

5.3 DATA ANALYSIS

A complete analysis was performed of the resulting increment matrix to determine what effects they would have upon the aerodynamic static stability characteristics of the FWC SRB configuration. The change in center of pressure due to the addition of these increments was investigated using the following formula.

$$\Delta C_p = \frac{\Delta C_M}{\Delta C_N} D_{Ref}$$

Any change which resulted in a ΔC_p which was physically located off the SRB as measured from the moment reference point was corrected by shifting

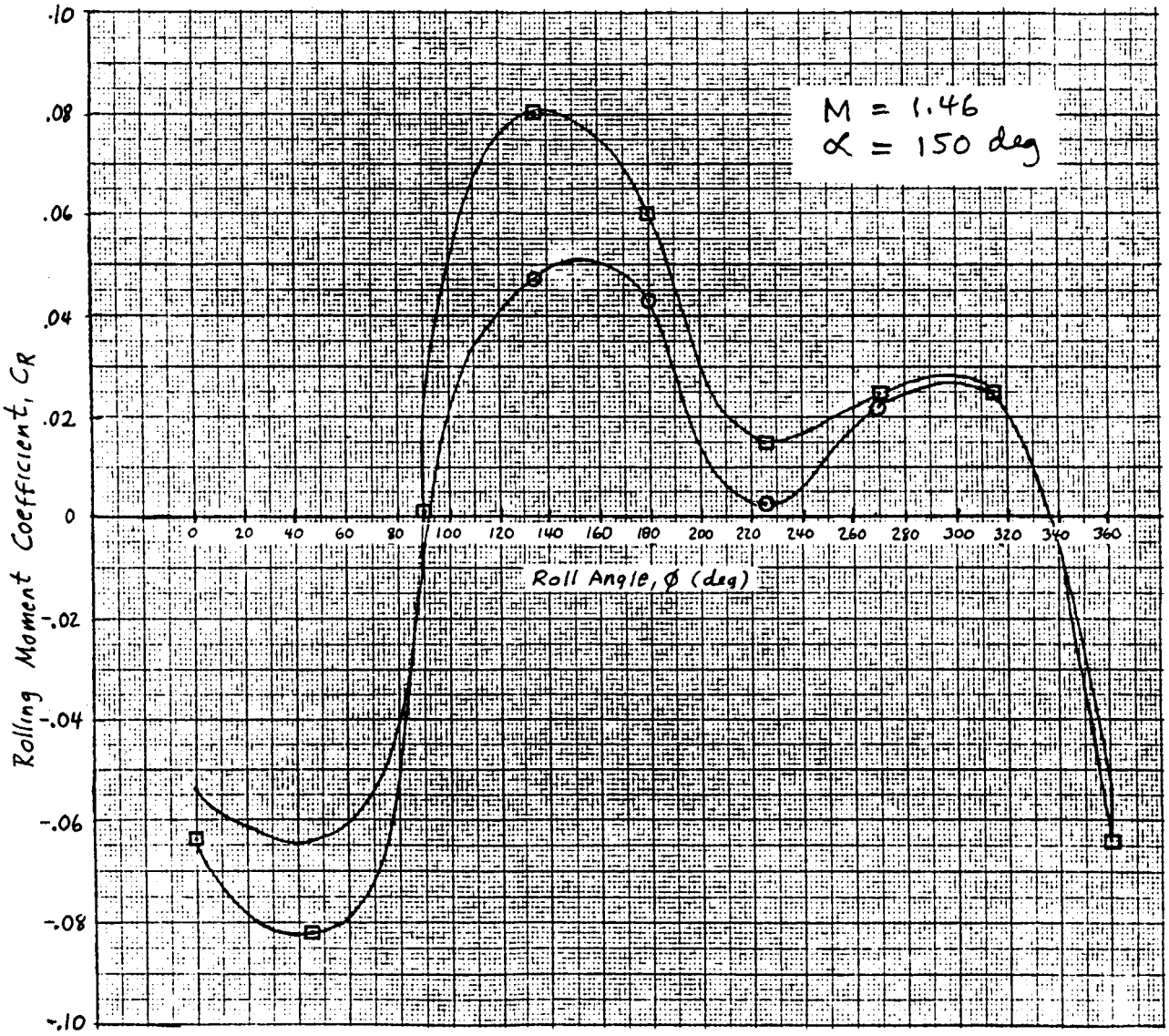

Fig. 5-9 Roll Angle Cross Plot for Rolling Moment

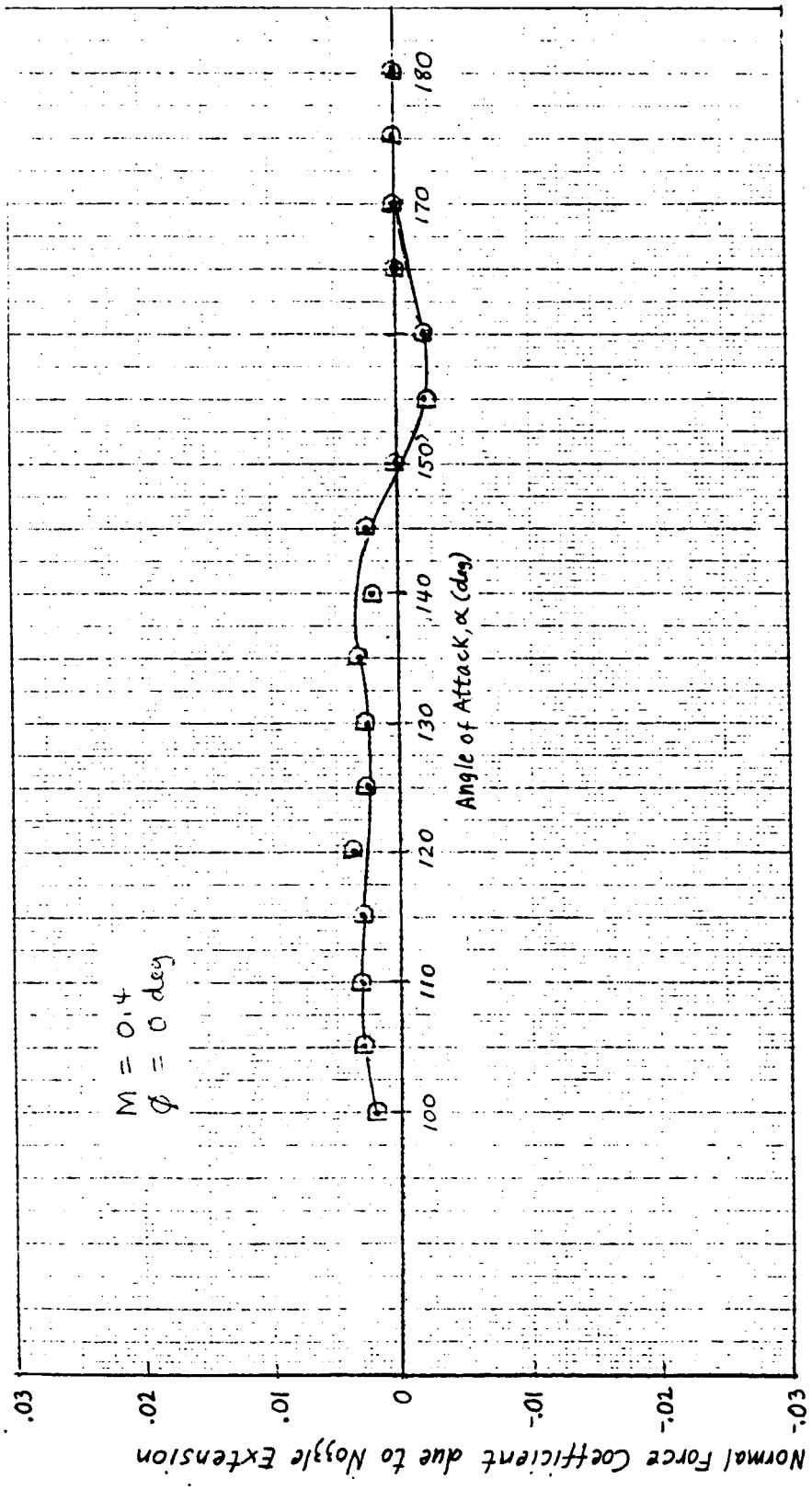

Fig. 5-10 Sample Hand Plot Used for Increment Smoothing

the pitching moment and normal force increments as necessary to ensure real increments. Figure 5-11 shows a plot of axial force data from the TWT-691 test. Due to the extremely small increment between the filament wound case and steel case data without heat shield the axial force increments were set to zero. The difference shown between the triangles and the rest of the data is due to the heat shield.

5.4 COMPUTER ANALYSIS

Five computer codes were developed to assist in the creation of Data Tape 8. These codes were used on the Lockheed in-house Digital Equipment Corporation PDP 11/34 computer. One program enabled tabulated increment matrix to easily be input into a random access file. This program also facilitated easy modification of this increment file. Because the wind tunnel test program TWT-691 tested the SRB model only at roll angles of 0, 45, and 90 deg and at angles of attack of 100 to 180 deg, an analysis was performed to develop a complete increment matrix. The results of this analysis culminated in the development of two computer codes to expand the increment file to the full matrix. The first of these programs developed increments between 0 and 100 deg angle of attack by straight line interpolation back to zero. The other program used the following equations to develop the roll angle matrix for all coefficients except rolling moment which already included the full roll matrix.

1. Increments @ 0 deg as developed from data
2. Increments @ 45 deg as developed from data
3. Increments @ 90 deg as developed from data
4. Increments @ 135 deg = X * (Increments @ 45 deg)
5. Increments @ 180 deg = X * (Increments @ 0 deg)
6. Increments @ 225 deg = X * (Increments @ 90 deg)
7. Increments @ 270 deg = X * (Increments @ 90 deg)

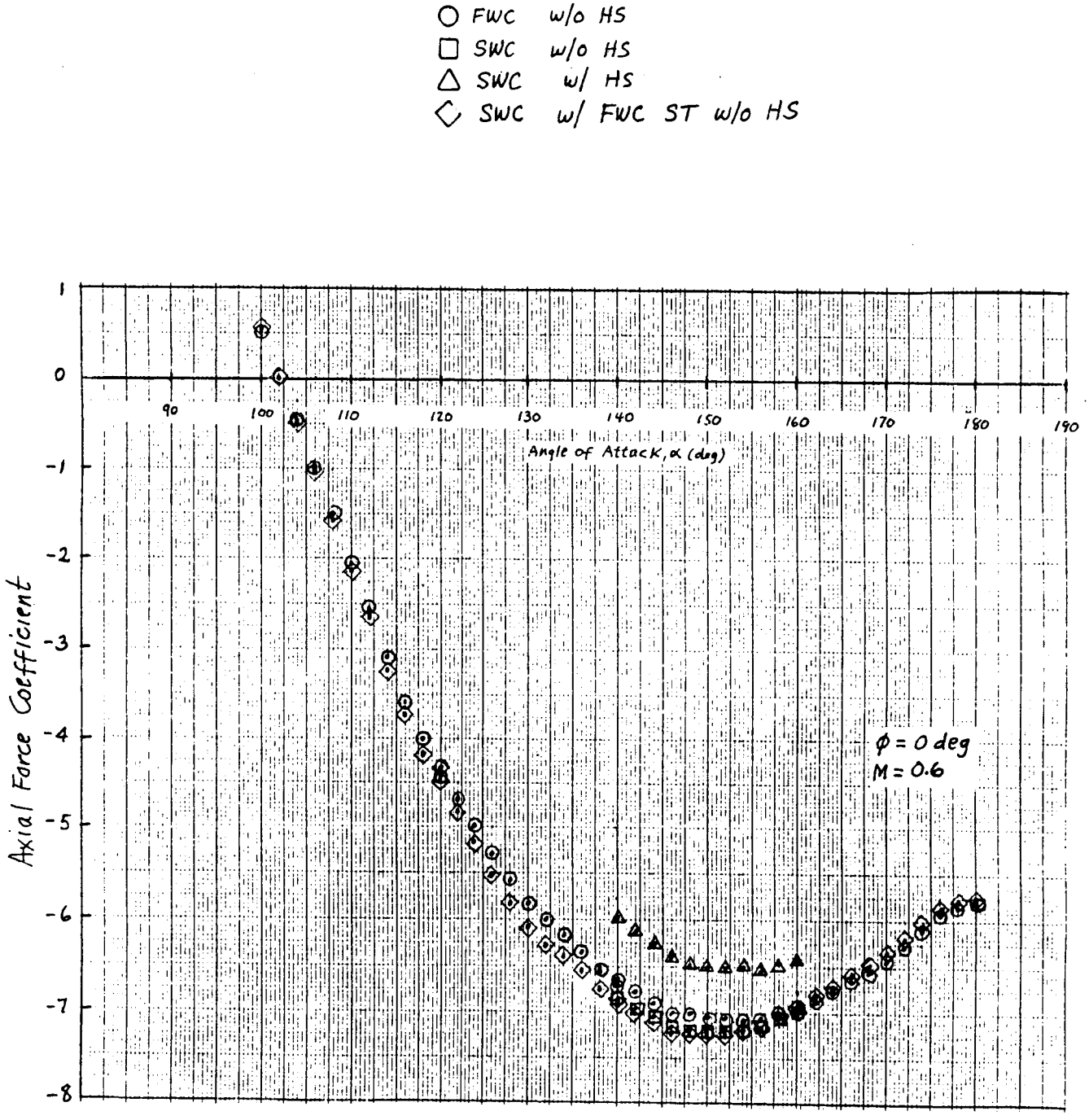

Fig. 5-11 Axial Force Comparison Plot for TWT-691

8. Increments @ 315 deg = X * (Increments @ 90 deg)
9. Increments @ 360 deg = Increments @ 0 deg.

Note: The X factor was necessary to achieve the proper sign for all coefficients. X is equal to 1 for the longitudinal coefficients (C_N, C_M, C_A) and -1 for the lateral coefficients (C_y C_{yM}).

The fourth program was developed to add the increment file to Data Tape 7 to create Data Tape 8. The last program enabled plots to be created of Data Tape 8 versus Data Tape 7. Figures 5-12 through 5-17 show Data Tape 8 compared with Data Tape 7 for a Mach number of 0.5 and a roll angle of 90 deg. Plots like these were analyzed to ensure no anomalies were overlooked.

5.5 TABULAR DATA EXAMPLES

Tables 5-3 through 5-5 are examples of the format of the Data Tape 8 coefficients as presented in Appendix A. Each page consists of six-component force and moment coefficients as a function of angle of attack in 5 deg increments for a specific Mach number and roll angle. Appendix A begins with the coefficients at Mach 0.4 and roll angle of zero, then increments roll angle in 45 deg increments before proceeding to the next Mach number. The Mach number range is 0.4 to 3.48.

5.6 GRAPHICAL DATA EXAMPLES

Figures 5-18 through 5-23 are examples of the plots of the Data Tape 8 coefficients as presented in Appendix B. Each coefficient is plotted as a function of angle of attack for a specific Mach number and roll angle. Appendix B begins with Mach 0.4 and increments roll angle in 45 degree increments before proceeding to the next Mach number. After all Mach numbers and roll angles have been plotted for a specific coefficient, a new coefficient is begun. The order of the coefficients is normal force coefficient, C_N, pitching moment coefficient, C_m, side force coefficient, C_Y, yawing moment coefficient, C_n, axial force coefficient, C_A, and rolling moment coefficient, C_ℓ.

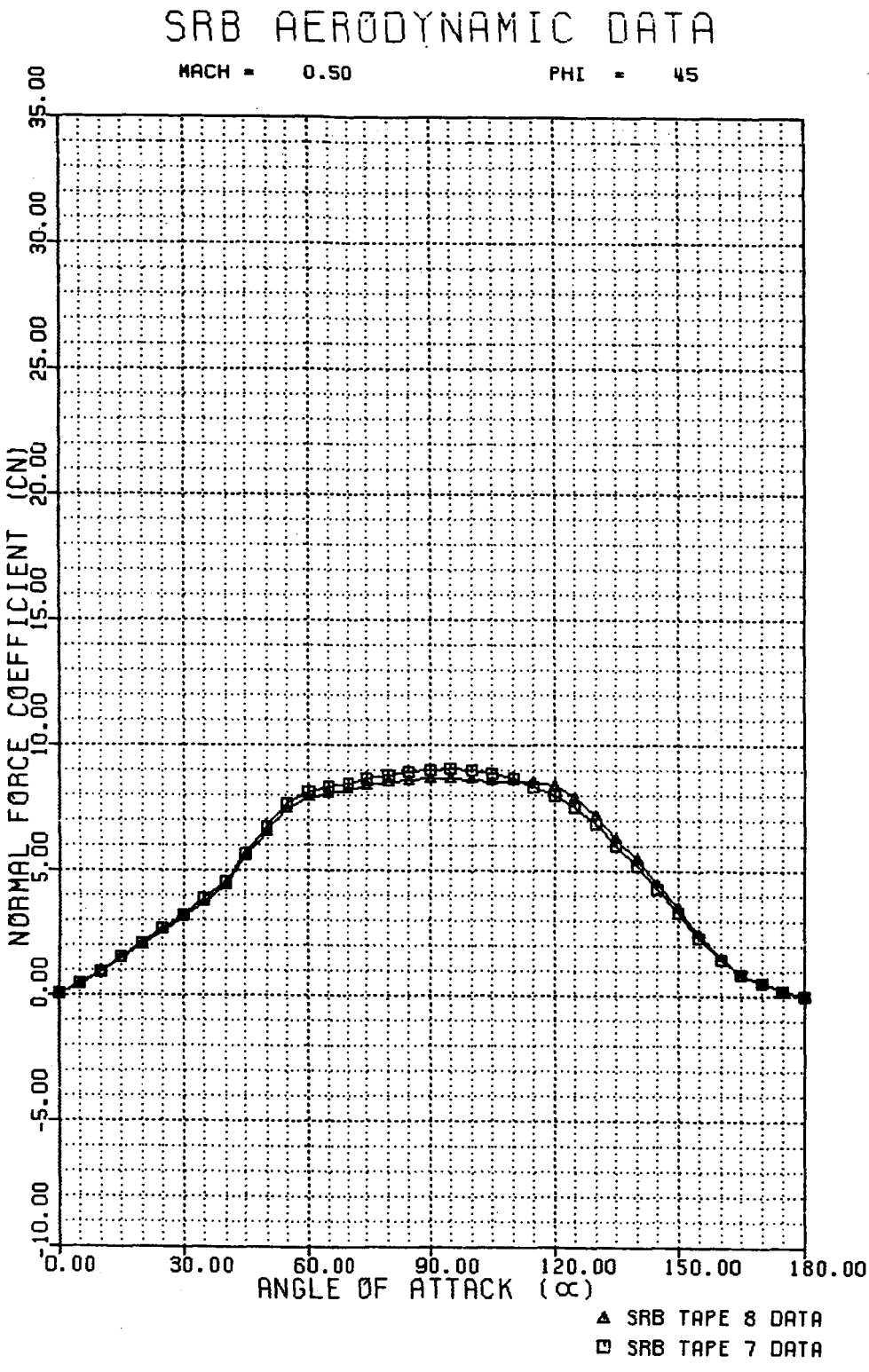

Fig. 5-12 Data Tape 8 vs Data Tape 7 for Normal Force

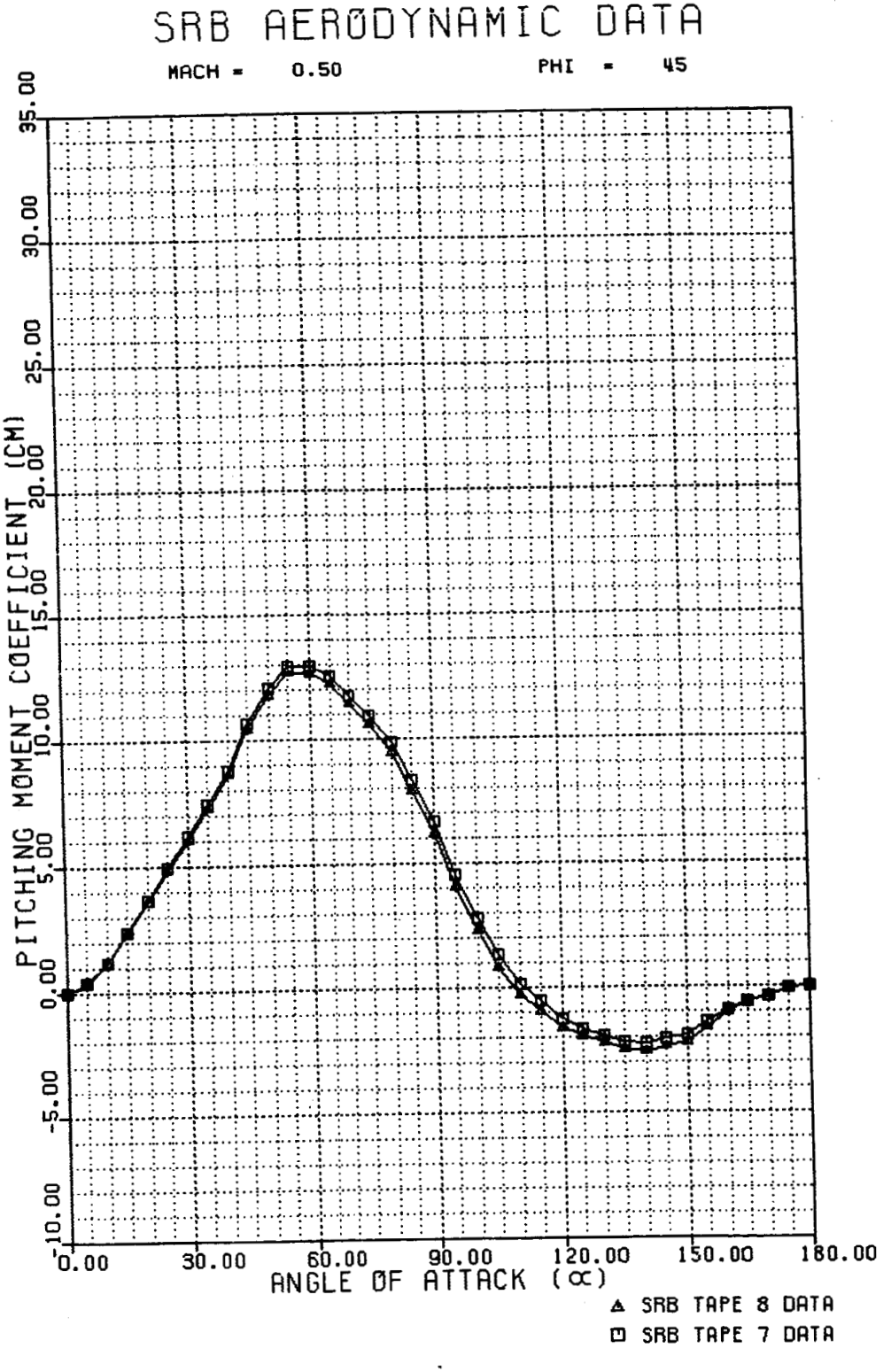

Fig. 5-13 Data Tape 8 vs Data Tape 7 for Pitching Moment

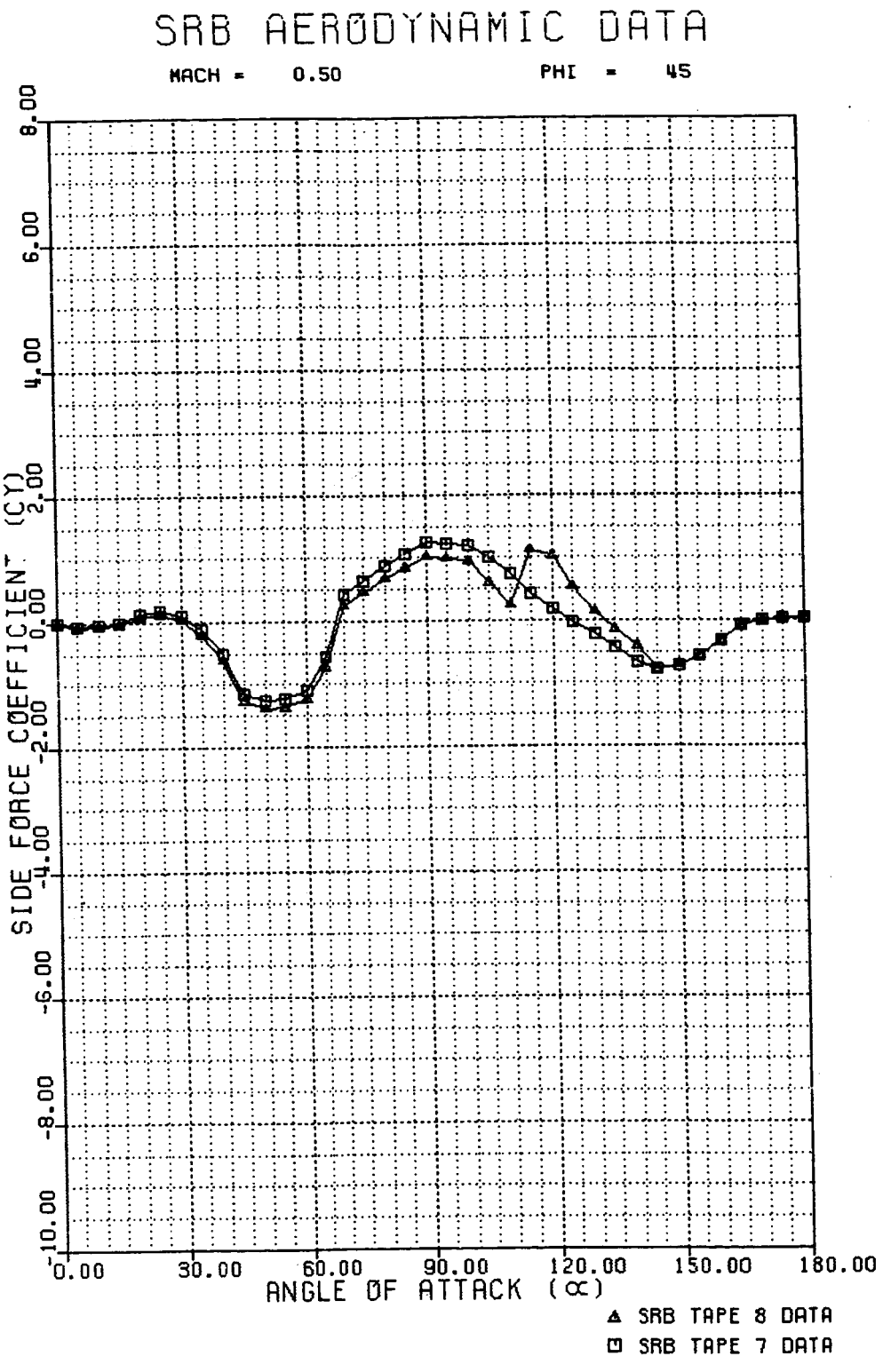

Fig. 5-14 Data Tape 8 vs Data Tape 7 for Side Force

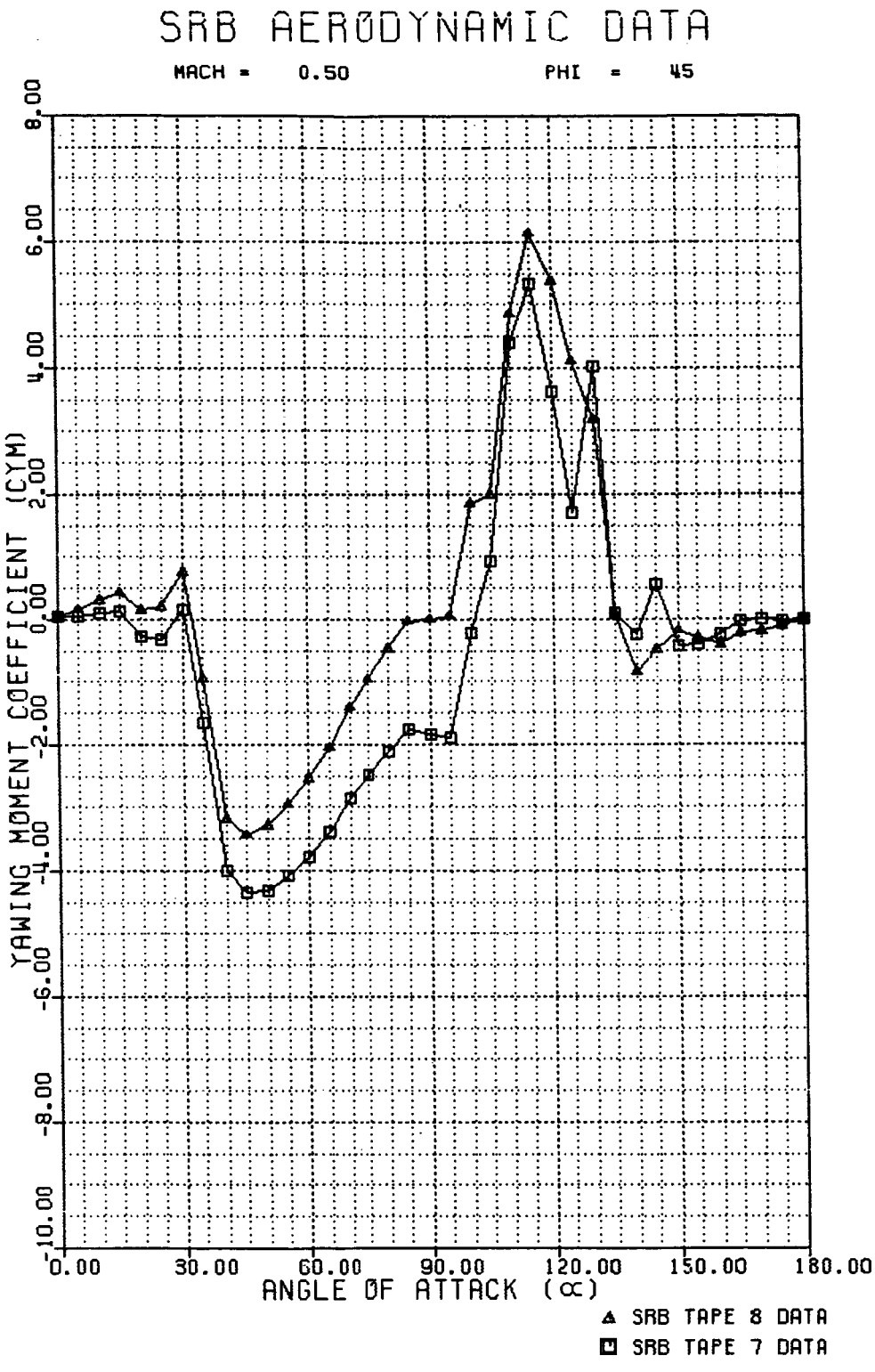

Fig. 5-15 **Data Tape 8 vs Data Tape 7 for Yawing Moment**

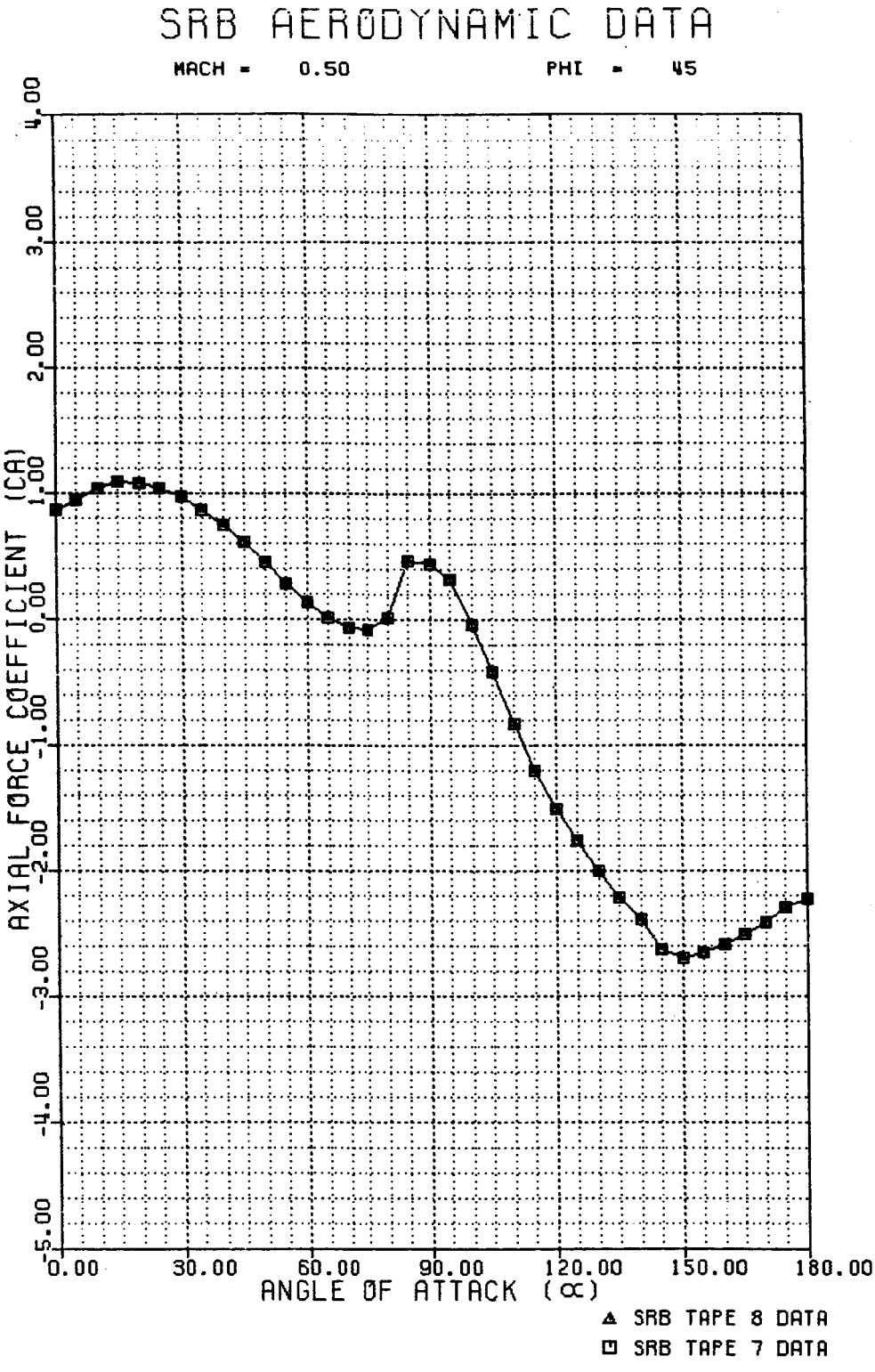

Fig. 5-16 Data Tape 8 vs Data Tape 7 for Axial Force

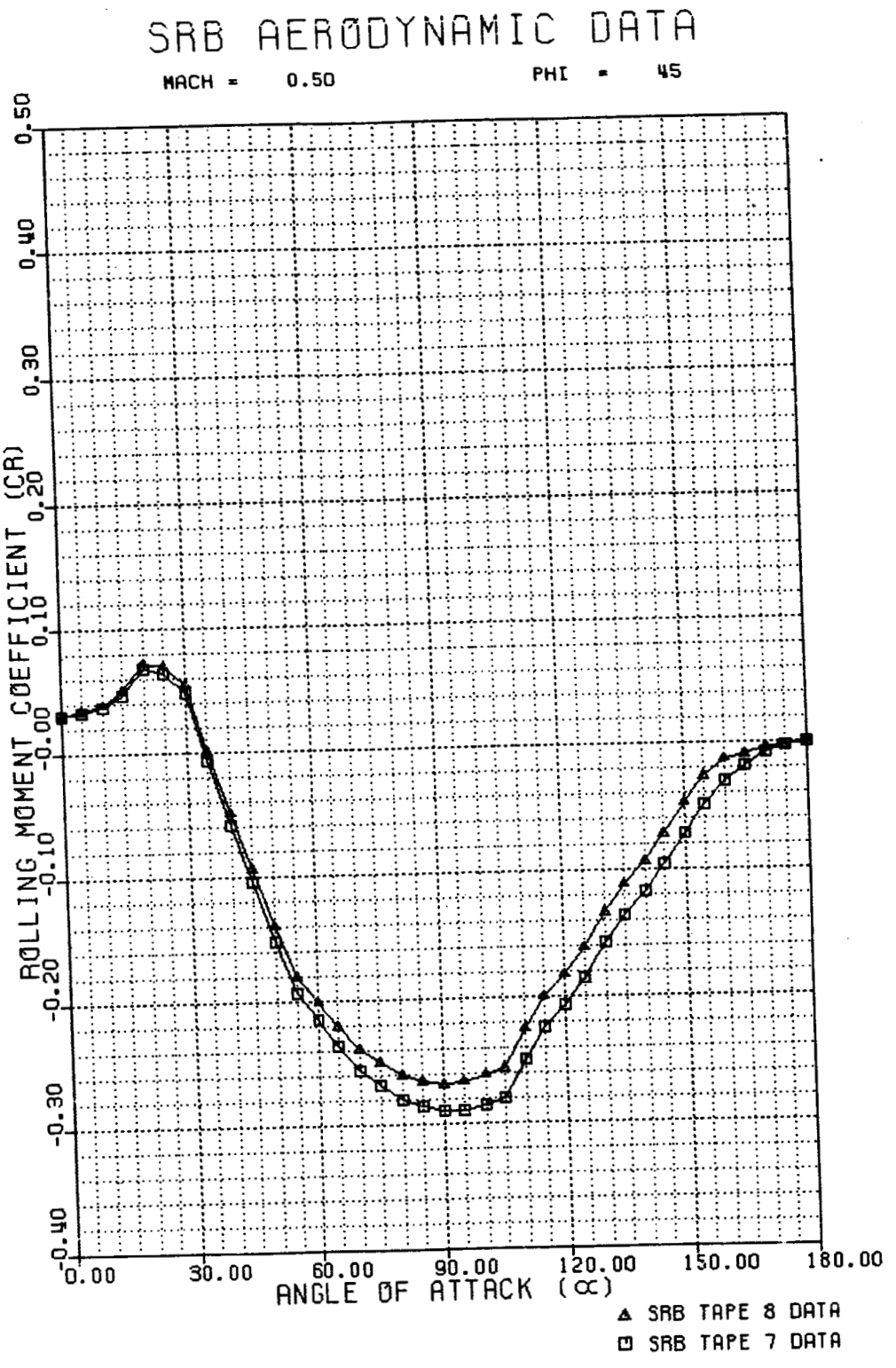

Fig. 5-17 Data Tape 8 vs Data Tape 7 for Rolling Moment

Table 5-3 SAMPLE OF TABULAR DATA IN APPENDIX A FOR M = 0.4, ϕ = 0 DEG

FILAMENT WOUND CASE RIGHT SIDE SRB STATIC STABILITY COEFFICIENTS

DREF=146 IN
LREF=1789.6 IN
MRP=.59*LREF (STA 1255.9)

MACH= 0.40
PHI= 0.

ALPHA	CN	CM	CY	CYM	CA	CR
0.	0.07130000	0.04630000	-0.00050000	0.00870000	0.86049992	-0.02020000
5.	0.48679990	0.50009990	-0.02880000	0.07630000	0.90120000	-0.01690000
10.	0.93269998	1.27179992	-0.02679989	0.13789999	0.98829991	0.01440000
15.	1.46090007	2.32500029	0.07960001	0.29759991	1.03520012	0.04840000
20.	2.04449987	3.54879999	0.21080001	-0.02479991	1.01539993	0.06959999
25.	2.70029998	4.98019981	0.29699998	-0.02439991	0.96920002	0.06340000
30.	3.46200013	6.63669968	-0.23399991	0.49849990	0.88239992	0.04940000
35.	4.23660040	8.22519875	-1.73420000	0.80030000	0.76650000	0.03550000
40.	5.20870018	10.17809963	-3.49339996	1.12419987	0.62549998	0.02570000
45.	6.42950058	12.48990059	-5.19399977	1.59539998	0.48040000	0.01420000
50.	7.51199961	14.59510040	-6.00159979	2.11160016	0.33539990	-0.00490000
55.	8.33800030	15.79700089	-6.23520041	4.21350002	0.15759998	-0.01232660
60.	8.96690083	16.33720016	-5.59589993	2.80740023	-0.00025860	-0.01975720
65.	9.35050106	15.90429878	-5.94599581	-1.21198511	-0.17782420	-0.02298110
70.	9.65799999	15.57090092	-7.59287357	-6.93108892	-0.32047570	-0.02429800
75.	9.98970032	15.42140007	-7.96403033	-3.52780271	-0.40720180	-0.02991560
80.	10.21809959	14.35720062	-6.73518229	-0.23729527	-0.35598800	-0.03139860
85.	10.28389835	12.15580177	-6.44640684	-2.60944557	0.34222960	-0.03273000
90.	10.28000069	9.01200008	-5.88335419	-2.41078734	0.27639240	-0.03314940
95.	10.40999794	6.59779978	-5.25536823	-2.50583076	0.07446990	-0.03285000
100.	10.49999905	4.30870008	-4.58343601	-1.39545643	-0.24321990	-0.03564000
105.	10.57349968	2.83700013	-4.70106030	1.78006399	-0.62536001	-0.03770000
110.	10.50800037	1.60000002	-5.61199999	1.44776464	-0.98475993	-0.03612000
115.	10.31670189	0.71779984	-5.34852314	3.06000209	-1.34069991	-0.02802550
120.	9.94639969	0.19190009	-3.89442158	3.78000045	-1.60329986	-0.01790000
125.	9.52910042	-0.02470002	-2.80380034	4.41921043	-1.84644771	-0.02515500
130.	8.64999962	0.42340022	-1.83353877	5.63174248	-2.06935978	-0.02135600
135.	7.47119999	0.20890012	-0.85620213	6.01152515	-2.20877719	-0.02034510
140.	6.36539970	-0.28230000	-1.44150054	2.79626322	-2.39303350	-0.01151660
145.	5.30149937	-0.31289992	-3.33653998	-3.41366196	-2.53682852	-0.01672390
150.	4.30430031	-0.65386182	-2.83770990	-4.19250011	-2.60620070	-0.01359900
155.	3.30509973	-0.63669980	-1.34884119	-4.15274858	-2.60762596	-0.00844360
160.	2.34080005	-0.64259994	0.19745201	-1.66636145	-2.56204128	-0.00572220
165.	1.42550004	-0.32440001	-0.03204130	-0.14998570	-2.48495088	-0.00517260
170.	0.81999992	-0.11049990	-0.15334600	-0.04630001	-2.37900066	-0.00003330
175.	0.25089991	-0.02310000	-0.03300010	-0.09350000	-2.24266005	-0.00018540
180.	-0.17440000	-0.00430000	0.01010000	-0.01756200	-2.17856169	0.00000000

Table 5-4 SAMPLE OF TABULAR DATA IN APPENDIX A FOR M = 0.4, ϕ = 45 DEG

FILAMENT WOUND CASE RIGHT SIDE SRB STATIC STABILITY COEFFICIENTS

DREF=146 IN
LREF=1789.6 IN
MRP=.59*LREF (STA 1255.9)

MACH= 0.40
PHI= 45.

ALPHA	CN	CM	CY	CYM	CA	CR
0.	0.07130000	0.04630000	-0.00110000	0.00870000	0.86029983	-0.02030000
5.	0.45679989	0.46009991	-0.06630000	0.01880000	0.90450001	-0.01610000
10.	0.79519975	1.04539990	-0.09210000	0.02290000	0.99089992	0.01170000
15.	1.13229990	1.75180006	-0.03290000	0.12509990	1.03730011	0.05050000
20.	1.65539980	2.79280019	0.06080000	-0.25290000	1.01729965	0.07240000
25.	2.25150013	4.02540016	0.11970000	-0.31189990	0.97000003	0.06750000
30.	2.95270014	5.49939966	0.27269989	0.06720000	0.88749993	0.05490000
35.	3.79779983	7.16139984	0.42579994	0.60210001	0.78349990	0.03380000
40.	4.49030018	8.46390057	0.53129977	0.75779992	0.62919992	-0.01210000
45.	5.28000021	9.67969894	0.58706594	0.63220000	0.50520003	-0.06320000
50.	6.03719997	10.60589981	0.57079995	0.50909990	0.38909990	-0.12709990
55.	6.74399996	10.82159996	0.46983173	0.21570000	0.26141700	-0.16050000
60.	7.13600063	10.59777546	0.20499051	0.02660000	0.17819600	-0.18552640
65.	7.38550043	10.46479511	-1.42469990	0.14460000	0.00280000	-0.20732240
70.	7.50320005	10.33469963	-2.20342898	1.16677070	-0.11519630	-0.22735420
75.	7.54160023	10.19770050	-1.80031216	0.38246810	-0.17833690	-0.21885691
80.	7.55759954	9.25559998	-1.23470032	-0.54897892	-0.21535440	-0.22058800
85.	7.60039997	7.46639967	-0.58366352	-2.15626907	0.29542580	-0.22301970
90.	7.63040018	5.73050022	0.14043239	-1.89369714	0.31517050	-0.22690141
95.	7.62029934	3.46680021	0.31090020	-0.10021760	0.19759670	-0.22463119
100.	7.56800032	1.79069996	0.35919976	1.47448933	-0.11208290	-0.22570500
105.	7.53460026	0.53569984	0.10267779	3.92648768	-0.46575570	-0.21860750
110.	7.45160055	-0.33100000	0.34615570	4.99568605	-0.92185920	-0.19954920
115.	7.51509953	-0.93719983	1.10575736	5.35431385	-1.22839046	-0.17029870
120.	7.25239992	-1.41770017	0.62405723	5.41212702	-1.51757574	-0.16981199
125.	6.74720049	-1.71169972	0.27910313	5.16914940	-1.73994780	-0.14836800
130.	6.03230000	-1.94840002	0.02491546	3.97672081	-1.97596383	-0.12529600
135.	5.30630016	-2.29309988	-0.37729284	2.36991620	-2.18973589	-0.11066831
140.	4.52149963	-2.45599985	-0.93974853	1.42882478	-2.36929226	-0.09251660
145.	3.60180020	-2.36819983	-1.51687598	1.19303036	-2.55922794	-0.07028400
150.	2.65560012	-2.25300002	-1.22558403	0.63598502	-2.63574028	-0.05219600
155.	1.89880002	-1.70760012	-0.99480104	-0.12673311	-2.61856937	-0.03369480
160.	1.26479995	-1.08509994	-0.42490050	-0.39787650	-2.56692004	-0.01853240
165.	0.68429983	-0.55359977	-0.17961110	-0.32448721	-2.48660707	-0.00858130
170.	0.37519991	-0.27590001	0.00346890	-0.21897671	-2.38558483	-0.00504730
175.	0.09130000	-0.05150000	0.00698000	-0.06736000	-2.24921989	-0.00440000
180.	-0.11790000	0.04050000	0.00490000	-0.02196000	-2.17859983	-0.00001760

Table 5-5 SAMPLE OF TABULAR DATA IN APPENDIX A FOR M = 0.4, ϕ = 90 DEG

FILAMENT WOUND CASE RIGHT SIDE SRB STATIC STABILITY COEFFICIENTS

DREF=146 IN
LREF=1739.6 IN
MRP=.59*LREF (STA 1255.9)

MACH= 0.40
PHI= 90.

ALPHA	CN	CM	CY	CYM	CA	CR
0.	0.07130000	0.03670000	-0.00050000	0.00870000	0.86029983	-0.02110000
5.	0.44509989	0.39619979	-0.07880000	-0.05620001	0.92820001	-0.01735000
10.	0.73899990	0.85749990	-0.12679990	-0.12710001	1.00979996	0.01320000
15.	1.13229990	1.56220007	-0.07040001	-0.09990011	1.05130005	0.04585000
20.	1.68649995	2.60489988	0.01000000	-0.55290002	1.02390003	0.06140000
25.	2.25150013	3.79099989	0.05839990	-0.68689996	0.97430003	0.05895000
30.	2.91090012	5.08100033	0.23919989	-0.53299999	0.88779992	0.04030000
35.	3.68009973	6.55569983	0.40250003	-0.36600015	0.78349990	0.02285000
40.	4.45760059	7.93359947	0.43919978	0.01809990	0.61080003	0.01267340
45.	5.26610041	9.16550064	0.08899990	0.47900003	0.42100000	0.00591320
50.	6.15330029	10.23499966	-0.22760001	0.97149986	0.29409990	0.00028430
55.	6.98390055	11.08229923	-0.45110002	0.88419986	0.18269990	-0.00393500
60.	7.76970100	11.73740005	-0.59139985	0.34219986	0.04329730	-0.00699320
65.	8.13579941	11.47150040	-0.73339993	-0.88511914	-0.11666000	-0.01433490
70.	8.33190060	10.48680019	-0.76950002	-2.06891203	-0.22759990	-0.02184170
75.	8.32560062	9.36410713	-0.64600003	-2.89136100	-0.21349980	-0.02422320
80.	8.30560112	8.21321487	-0.54769999	-3.58375621	-0.13043401	-0.01756430
85.	8.14539909	7.12839985	-0.45280001	-3.15661645	0.16189770	-0.01408590
90.	8.04119968	5.69759989	-0.40030000	-2.98360014	0.44470420	-0.01749130
95.	7.99380016	4.42549992	-0.32889998	-2.86351204	0.34746760	-0.01975000
100.	7.95400000	3.05509996	-0.32130003	-2.70016551	-0.04370020	-0.01676040
105.	7.94599962	2.01349998	-0.36528069	-2.13511300	-0.44540390	-0.01268720
110.	7.82940006	1.00209987	-0.66447961	-1.88520002	-0.87223452	-0.00801920
115.	7.78589964	0.14340010	-0.33950162	-1.51628566	-1.21940756	-0.01527140
120.	7.51749945	-0.57279992	-0.52200007	-0.79629099	-1.56158376	-0.02874790
125.	6.71970034	-0.82899982	-2.63049077	-2.07808328	-1.83761156	-0.03064800
130.	5.73120022	-0.88899982	-2.16509986	-2.39212704	-2.09552002	-0.02246000
135.	4.43459988	-1.01809990	-1.72880459	-0.52905810	-2.24686813	-0.00916920
140.	3.89830017	-1.37850010	-1.20103562	0.59127533	-2.36710215	-0.00904520
145.	3.57060051	-1.84600008	-0.76333612	0.39078161	-2.53267527	-0.00765800
150.	2.97420025	-1.79619992	-0.47239611	0.25709200	-2.65547895	-0.00355600
155.	2.38450003	-1.46459973	-0.61472714	0.08723661	-2.67252827	-0.00225460
160.	1.74600005	-1.16020012	-0.65382820	-0.41758901	-2.58793783	-0.00468790
165.	0.88529992	-0.54259992	-0.20968680	-0.27292222	-2.49937773	-0.00228380
170.	0.44859990	-0.24739990	-0.04717700	-0.13039240	-2.40162373	-0.00342820
175.	0.21470000	-0.01840000	-0.04614000	-0.15206000	-2.25050020	-0.00233070
180.	0.06690000	0.00570000	0.00878000	-0.00456000	-2.17829561	0.00000000

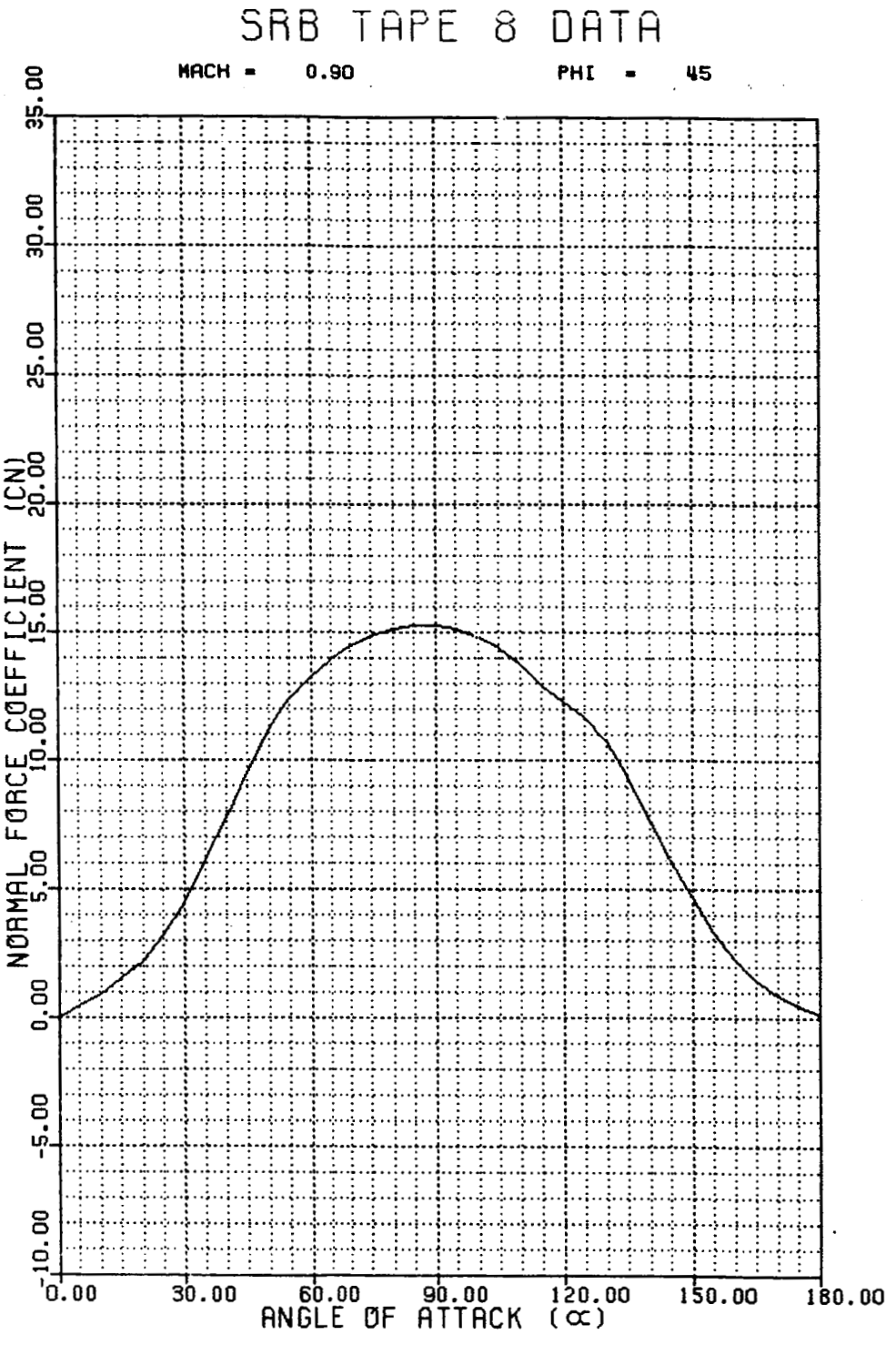

Fig. 5-18 Sample Plot of Normal Force in Appendix B

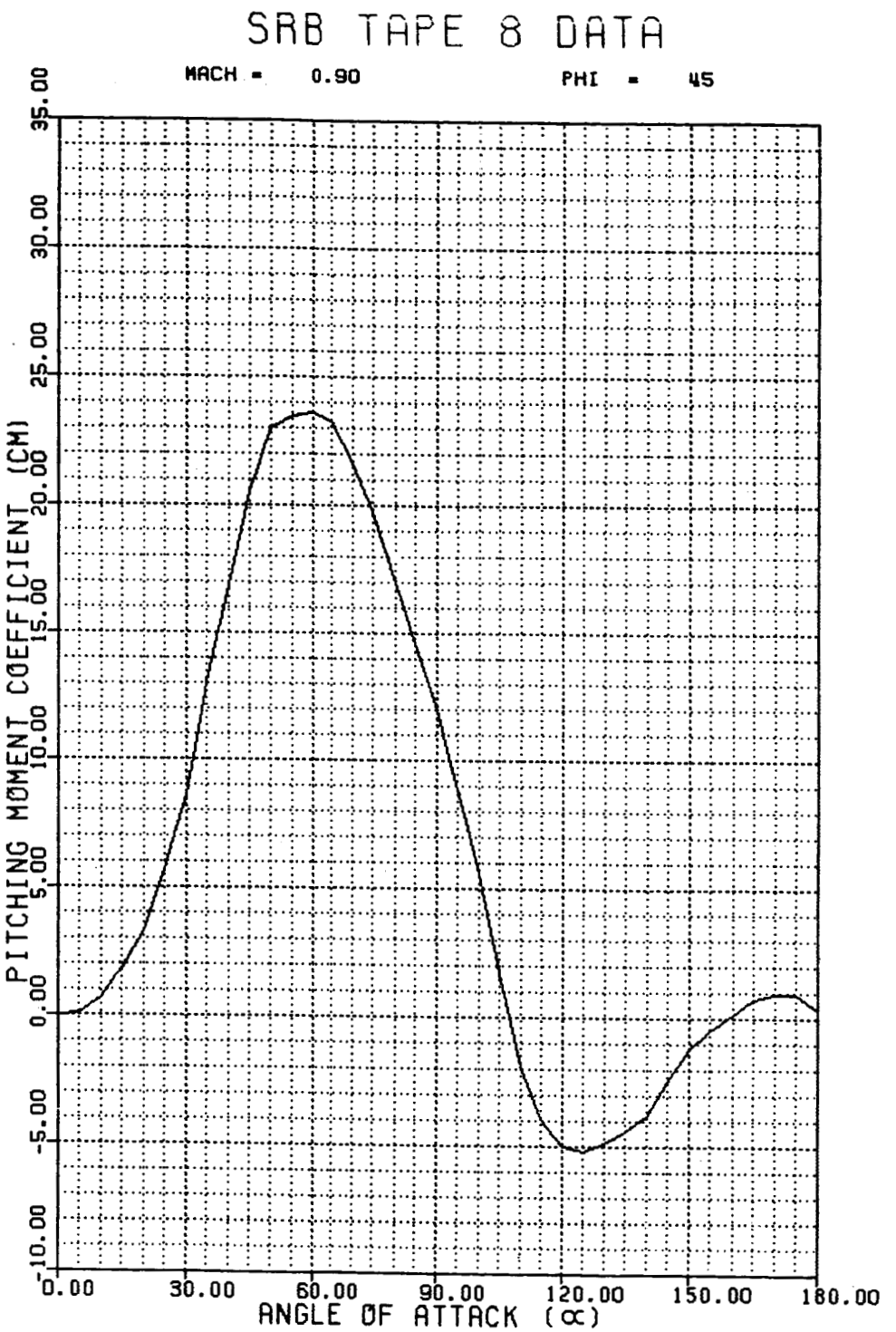

Fig. 5-19 Sample Plot of Pitching Moment in Appendix B

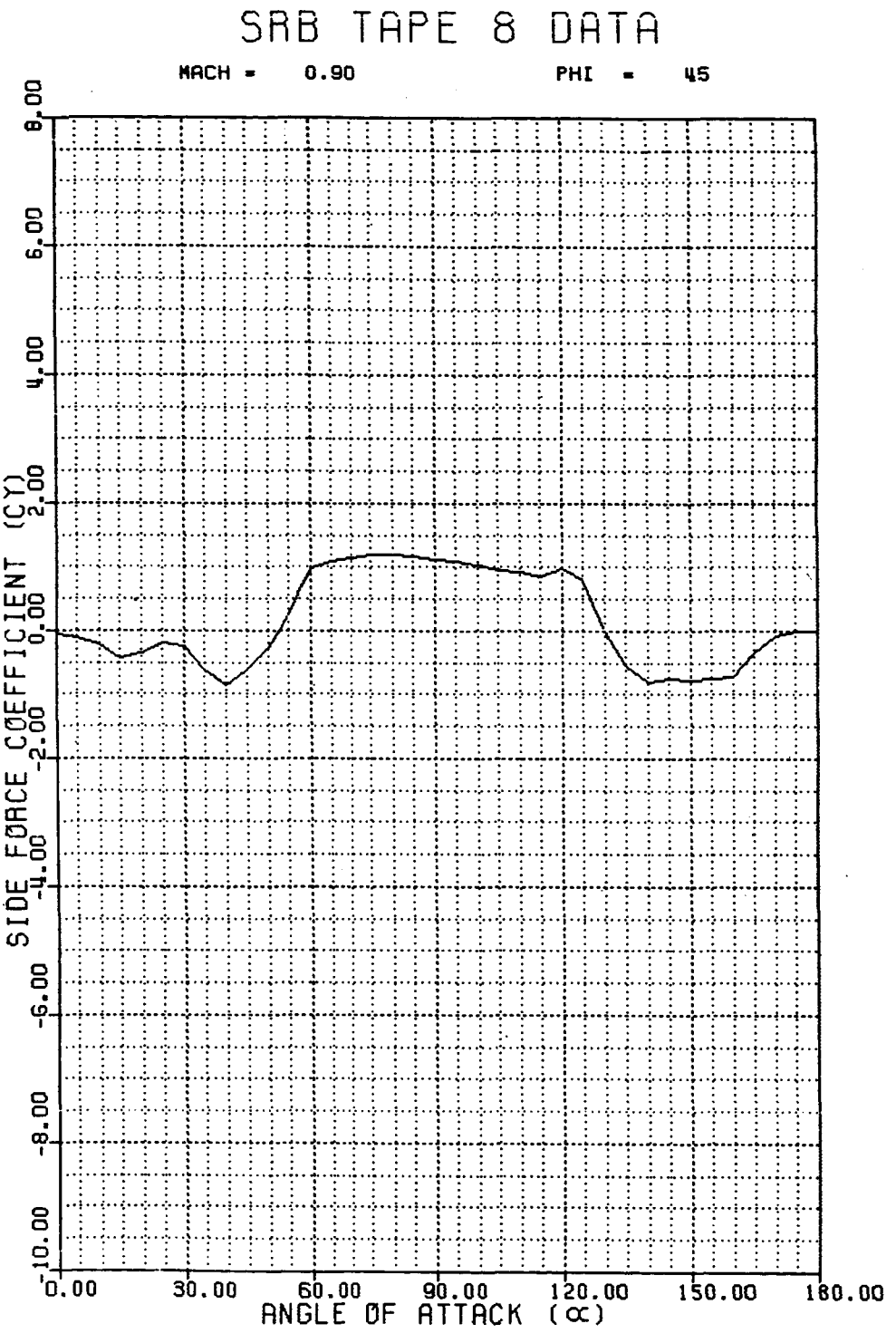

Fig. 5-20 Sample Plot of Side Force in Appendix B

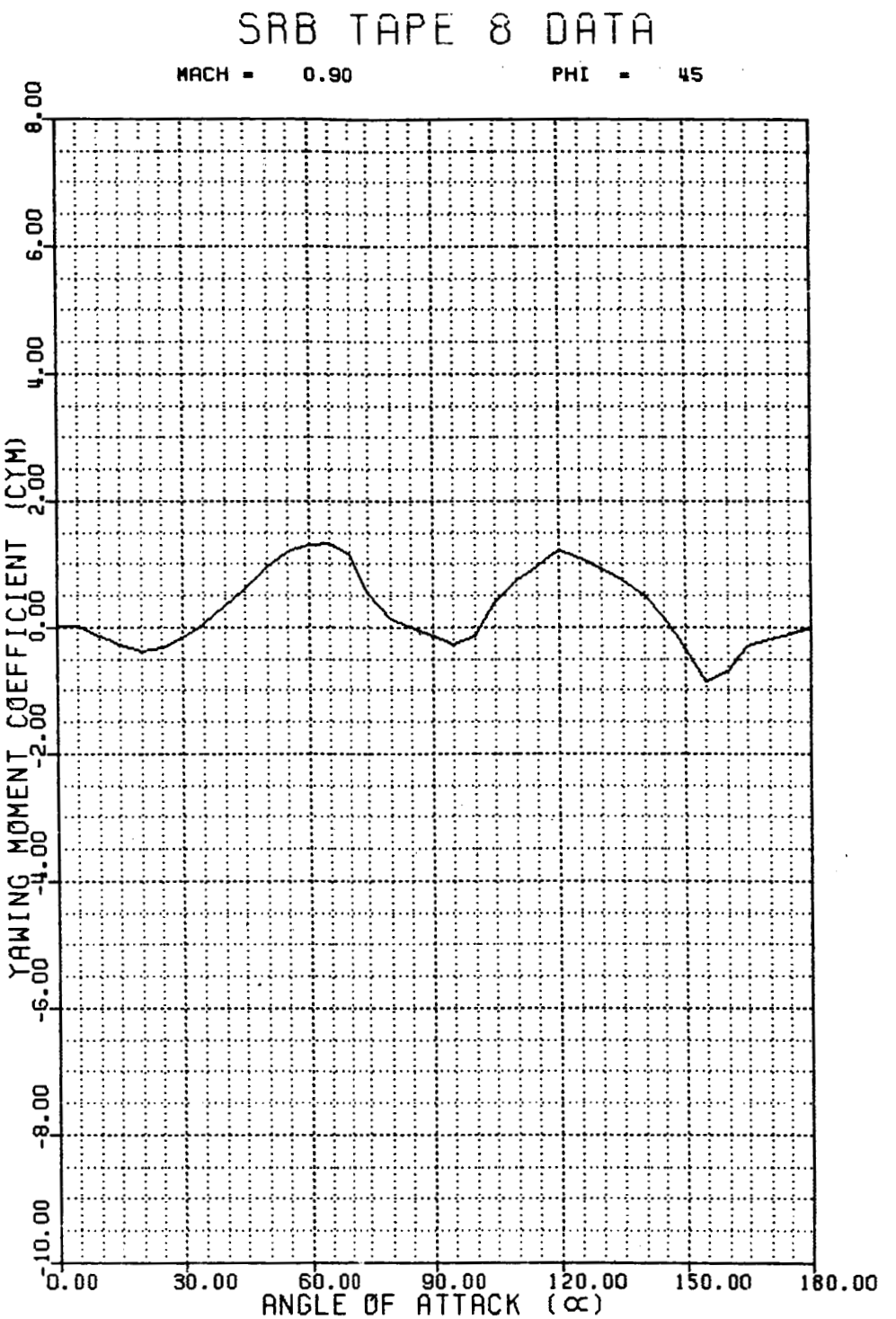

Fig. 5-21 Sample Plot of Yawing Moment in Appendix B

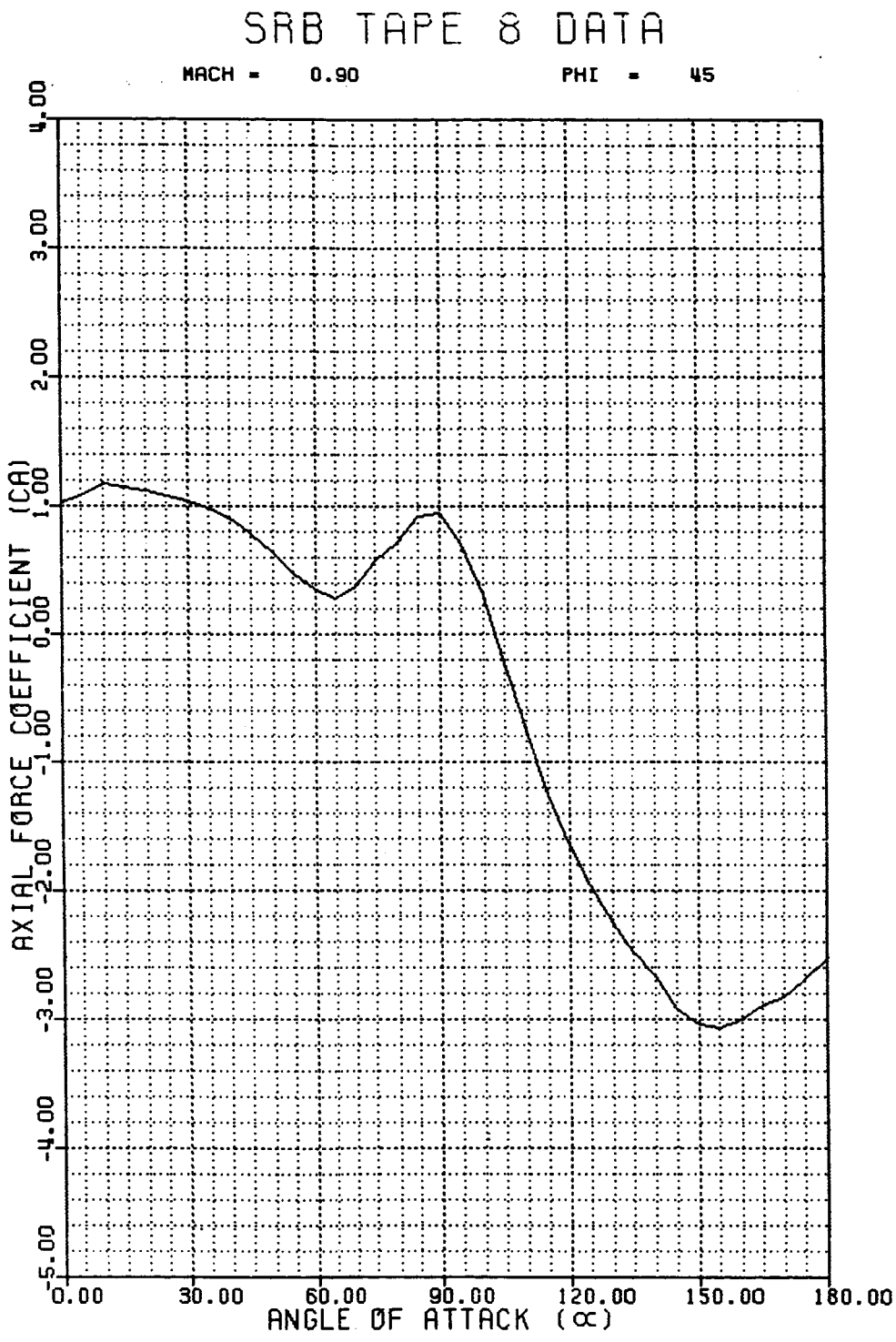

Fig. 5-22 Sample Plot of Axial Force in Appendix B

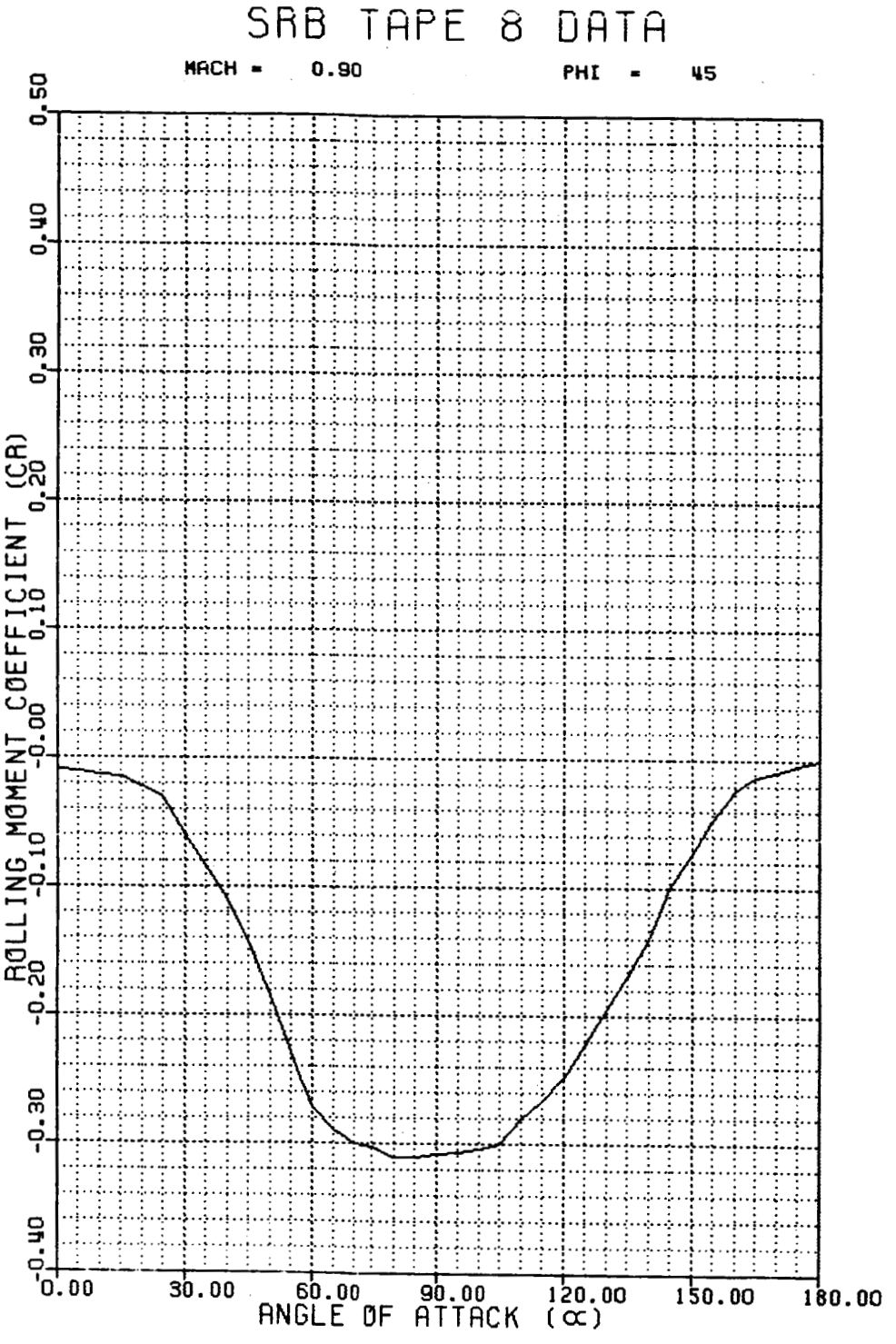

Fig. 5-23 Sample Plot of Rolling Moment in Appendix B

6. PROTUBERANCE INCREMENTS

The new FWC SRBs will incorporate several configuration changes which will affect the SRB aerodynamic characteristics. These protuberances, which include a redesigned systems tunnel and ET attach ring along will fewer and modified aft segment motor case stiffener rings, are described in Section 5.1. Presence of these protuberances will modify the basic SRB aerodynamic data. It is reasonable to expect changes in the normal force, and axial force, and pitching moment coefficients due to the addition of the protuberances. In addition, however, the coefficient increments will also be a function of SRB roll angle. Since the protuberances in effect create a non-symmetrical body, it is reasonable to expect a change in the lateral force coefficients (C_y, C_n, C_ℓ) over the angle of attack and roll angle ranges.

NASA is trying to integrate the FWC systems tunnel and ET attach ring designs on the steel case SRBs before flying on the FWC SRBs. As a result, the TWT 691 wind tunnel test matrix was developed to allow an investigation to determine protuberance effects on the reentry aerodynamic data. Configurations were tested for the FWC and steel case systems tunnels, ET attach rings, and stiffener rings along with configurations without these protuberances. These configurations allowed coefficient increments to be developed for each of the individual protuberances. In addition, configurations were tested to enable increments to be developed for the high performance motor nozzle extension.

The data from the TWT 691 wind tunnel test was transferred to the Lockheed in-house PDP computer by magnetic tape from the MSFC Univac 1108. This enabled easy analysis of the data. Due to sting deflections all data were not obtained at the same angles of attack. To alleviate this problem a computer code was developed to interpolate the data to even angles of attack. Table 6-1 shows three runs from the wind tunnel test after they

Table 6-1 EXAMPLE RUNS FROM TWT 691 INTERPOLATED TO EVEN ANGLES OF ATTACK

TWT-691 RUN= 10/0 MACH= 0.901 PHI= 45
PO= 22.015 PSTAT= 12.988 Q= 7.397 RN= 6.184

ALPHA	CN	CM	CY	CYM	CR	CAT	XCP/LB
140.0000	7.3412	5.6182	-0.5148	-0.3115	-0.1711	-2.9708	0.5278
142.0000	6.6327	4.4836	-0.6965	-0.3759	-0.1589	-3.0010	0.5355
144.0000	6.0019	3.3856	-0.7246	-0.1385	-0.1462	-3.0454	0.5443
146.0000	5.2965	2.3515	-0.7155	0.0321	-0.1425	-3.0842	0.5542
148.0000	4.5569	1.4133	-0.6389	-0.0799	-0.1342	-3.1150	0.5653
150.0000	4.0201	0.6509	-0.7151	-0.1365	-0.1234	-3.1273	0.5773
152.0000	3.4659	0.0610	-0.8232	-0.4679	-0.1171	-3.1059	0.5888
154.0000	2.9981	-0.0991	-0.8987	-0.6126	-0.1019	-3.0791	0.5927
156.0000	2.5576	0.0548	-0.7820	-0.4732	-0.0920	-3.0500	0.5881
158.0000	2.2040	0.2637	-0.5896	-0.0529	-0.0831	-3.0232	0.5801
160.0000	1.9404	0.5010	-0.4452	0.2203	-0.0710	-2.9906	0.5692

TWT-691 RUN= 11/0 MACH= 0.802 PHI= 45
PO= 22.013 PSTAT= 14.411 Q= 6.489 RN= 5.864

ALPHA	CN	CM	CY	CYM	CR	CAT	XCP/LB
140.0000	6.2391	-1.8408	-1.4096	-1.0688	-0.1923	-2.5289	0.6140
142.0000	5.6533	-1.3105	-1.3033	-0.6036	-0.1782	-2.6247	0.6082
144.0000	5.3210	-0.9408	-1.2070	-0.1016	-0.1628	-2.7139	0.6044
146.0000	4.6922	-0.7343	-1.1517	0.0301	-0.1516	-2.7874	0.6029
148.0000	4.0705	-0.6719	-1.1434	-0.2368	-0.1384	-2.8438	0.6035
150.0000	3.6091	-0.5902	-1.1272	-0.4410	-0.1248	-2.8752	0.6034
152.0000	3.1511	-0.5654	-1.0491	-0.5944	-0.1091	-2.8881	0.6047
154.0000	2.7435	-0.5252	-0.9377	-0.6343	-0.0971	-2.8809	0.6056
156.0000	2.3799	-0.3359	-0.9532	-0.5154	-0.0824	-2.8589	0.6031
158.0000	2.0842	-0.1644	-0.8979	-0.2301	-0.0721	-2.8401	0.5964
160.0000	1.8334	0.0945	-0.8243	-0.0787	-0.0574	-2.8234	0.5859

TWT-691 RUN= 12/0 MACH= 0.600 PHI= 45
PO= 22.013 PSTAT= 17.246 Q= 4.358 RN= 4.913

ALPHA	CN	CM	CY	CYM	CR	CAT	XCP/LB
140.0000	5.1764	-1.0876	-2.0351	-2.3927	-0.1651	-2.3938	0.6072
142.0000	4.9445	-0.6053	-1.7651	-1.0522	-0.1571	-2.4610	0.6000
144.0000	4.5697	-0.3604	-1.4909	-0.3569	-0.1442	-2.5282	0.5965
146.0000	4.1615	-0.2587	-1.3711	-0.3373	-0.1389	-2.5891	0.5952
148.0000	3.6806	-0.3436	-1.4350	-0.6934	-0.1201	-2.6302	0.5977
150.0000	3.2673	-0.4793	-1.3879	-0.8414	-0.1090	-2.6484	0.6021
152.0000	2.8913	-0.5298	-1.3029	-1.0822	-0.0934	-2.6504	0.6051
154.0000	2.5391	-0.6266	-1.2359	-1.3099	-0.0796	-2.6328	0.6103
156.0000	2.1749	-0.7032	-1.1179	-1.1309	-0.0650	-2.6041	0.6165
158.0000	1.8731	-0.7572	-0.9729	-0.9610	-0.0505	-2.5975	0.6231
160.0000	1.5746	-0.7109	-0.8622	-0.6665	-0.0380	-2.5821	0.6272

were interpolated to even ables of attack by this computer program. The interpolated coefficients for the configuration without the protuberances were then subtracted from those of the configuration with the protuberances to develop the individual aerodynamic contributions of each protuberance. The data were then arranged into individual computer files for each protuberance increment. Plots were made of each increment by a computer code developed by Lockheed. These plots were analyzed and data anomalies were smoothed by hand and reentered in the computer file. The data were then interpolated to angles of attack in 5 deg increments. Because of the limited angle-of-attack range that was tested, data had to be independently developed for angles of attack from 0 to 100 deg. This was accomplished by hand fairing the data back to zero. The data were then picked off at angles of attack of 5 deg increments from 0 to 100 deg.

Since the wind tunnel test program TWT 691 included roll angles of only 0, 45, and 90 deg, Lockheed has developed a rationale which may be used to develop the complete roll angle matrix for each of the protuberance increments. Table 6-2 shows the definition of the roll angle matrix development for the stiffener rings and systems tunnel increments. These two were judged to be compatible because any variation in stiffener ring coefficients with roll angle variation would probably be due to interference from the systems tunnel. Notice that the lateral directional data require a change of sign for roll angles 135 to 315 deg. Table 6-3 depicts the roll angle matrix definition for the ET attach ring increments. The development of the ET attach ring increments over the complete roll angle matrix requires a sign change in the lateral directional data for roll angles 135 to 270 deg.

Each of the protuberances will be discussed in detail in the following subsections. The analyses performed on each protuberance along with sample plots and tables will be presented.

6.1 HIGH PERFORMANCE NOZZLE INCREMENTS

Figure 5-1 depicts the SRB nozzle extension being separated at apogee. All previous and current SRB reentry data tapes are for SRB configurations

Table 6-2 DEFINITION OF STIFFENER RINGS AND SYSTEMS TUNNEL INCREMENT FOR ALL ROLL ANGLES

Configuration	Roll Angle	Data Used
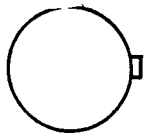	0°	0°
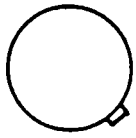	45°	45°
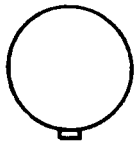	90°	90°
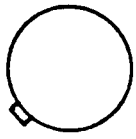	135°	45° (Change sign of the lateral directional data)
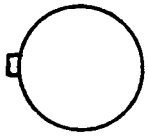	180°	0° (Change sign of the lateral directional data)
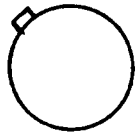	225°	90° (Change sign of the lateral directional data)
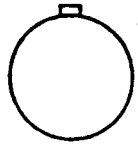	270°	90° (Change sign of the lateral directional data)
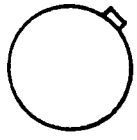	315°	90° (Change sign of the lateral directional data)
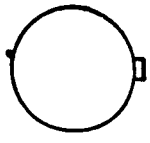	360°	0°

Table 6-3 DEFINITION OF ET ATTACH RING INCREMENTS FOR ALL ROLL ANGLES

Configuration	Roll Angle	Data Used
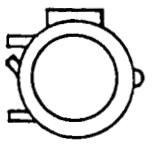	0°	0°
	45°	45°
	90°	90°
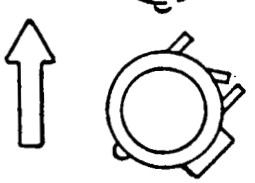 Windward Side	135°	45° (Change sign of the lateral directional data)
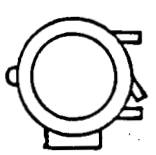	180°	0° (Change sign of the lateral directional data)
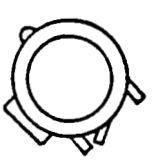	225°	45° (Change sign of the lateral directional data)
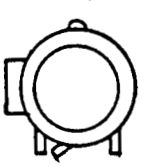	270°	90° (Change sign of the lateral directional data)
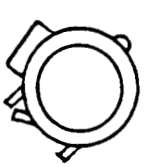	315°	0° (Change sign of the lateral directional data)
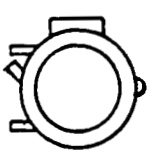	360°	0°

without the nozzle extension and thus the aerodynamic data base does not consider the influence of the nozzle extension. The STS-1 flight was the only flight where the nozzle extension was separated at apogee. Post flight reconstruction theorized that the separation of the nozzle extension resulted in an unforeseen incidence of aerodynamic flutter that tore the thermal curtain. On the second flight (STS-2) the integrated electronics assembly was programmed to delay the nozzle extension severance from apogee, which was 270,000 ft in the first flight, until approximately 20 sec after deployment of the main recovery parachute. Thus, starting from STS-2 the nozzle extension has been present during reentry until after deployment of the main parachutes.

At this time, no decision has been made on whether the FWC SRBs will reenter with or without the nozzle extension. Therefore, the aerodynamic effects the addition of the nozzle extension has upon the SRBs is of interest. Lockheed has analyzed data from the wind tunnel test program TWT 691 and previous nozzle increments (see Ref. 6). Figure 5-4d shows the nozzle configurations which were tested in the TWT 691 test program. This analysis has culminated in the development of a model data base reflecting the aerodynamic characteristic increments for the high performance nozzle extension.

Figure 6-1 presents a comparison of Data Tape 8 and Data Tape 7 axial force with and without nozzle extensions for a 180 deg angle of attack. Notice that the addition of the high performance nozzle produces a significant reduction in negative axial force coefficient which translates into a decrease in drag at this angle of attack. This is important to the recovery since the SRBs must decelerate to a velocity which will allow safe deployment of the recovery parachutes.

Figure 6-2 shows a comparison of the center of pressure increment location of both the previous and the new high performance nozzle increments. These were calculated by the following equation:

$$\Delta C_{p_{noz}} = \frac{\Delta C_{M_{noz}}}{\Delta C_{N_{noz}}} \times D_{Ref}$$

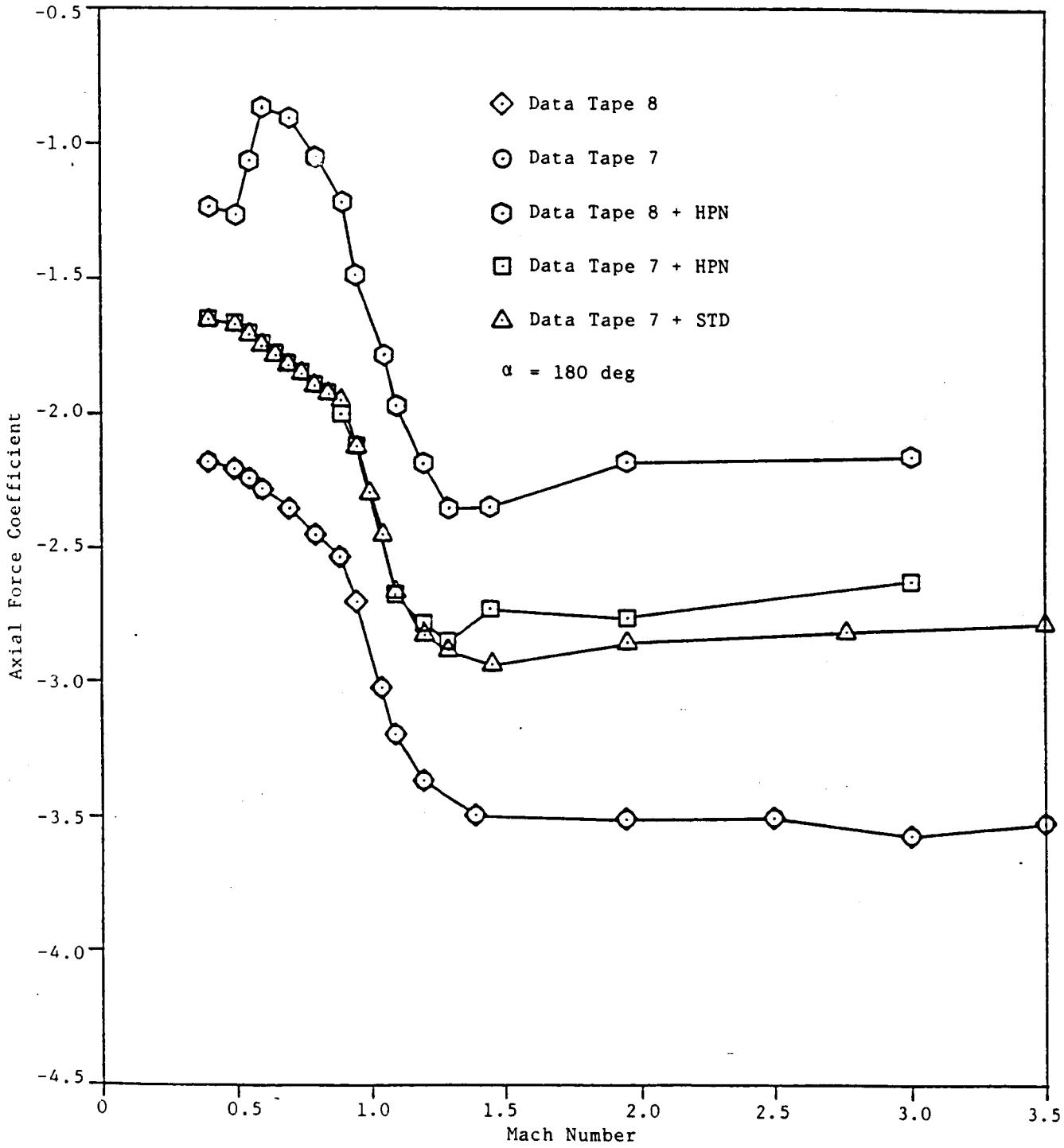

Fig. 6-1 Comparison of Drag Due to Addition of High Performance Nozzle and Standard Nozzle

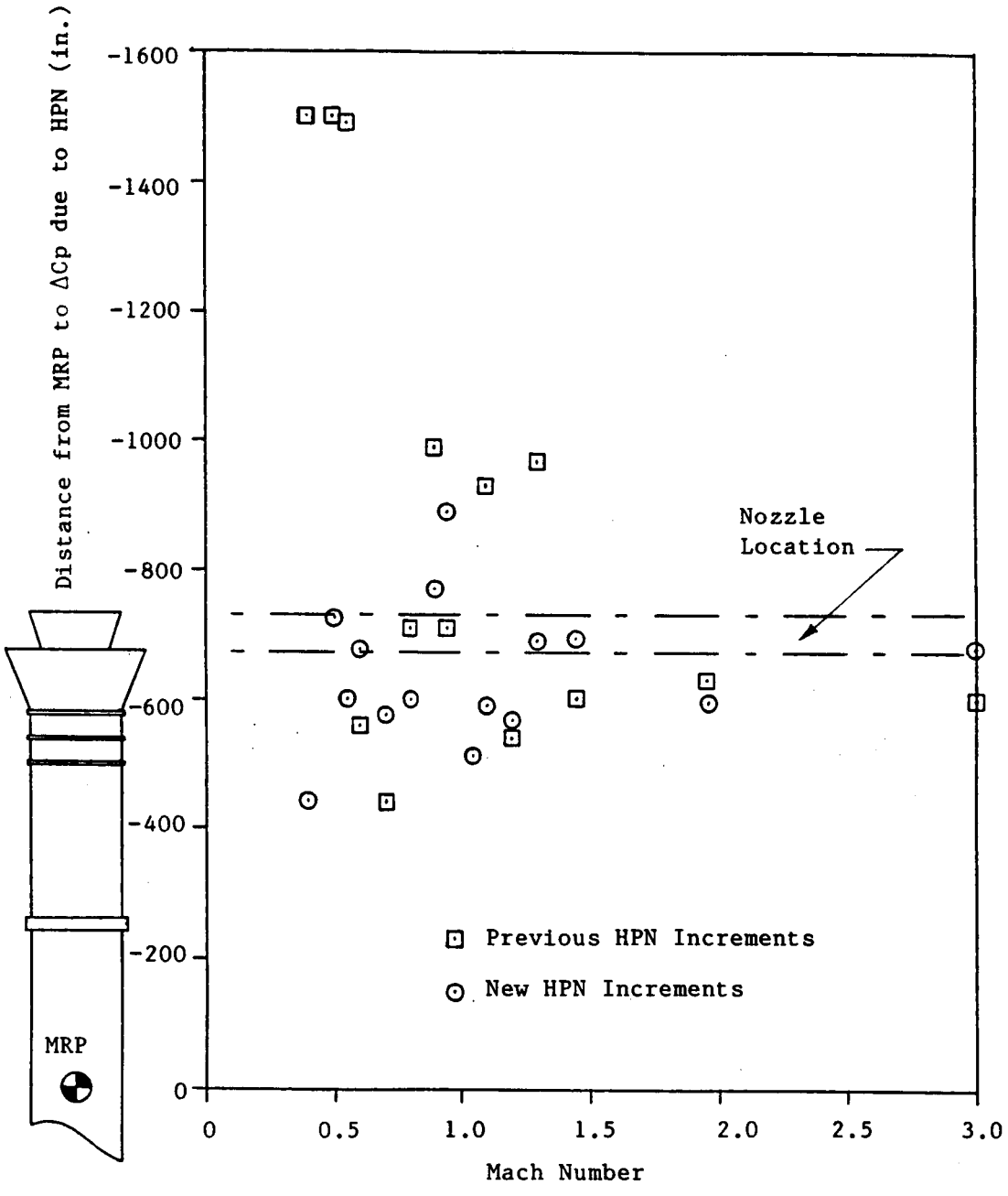

Fig. 6-2 Comparison of Center of Pressure Resulting from Old and New High Performance Nozzle Increments

In theory, the center of pressure should fall within the nozzle location band. Notice that the new increments are closer to the nozzle band than the previous increments. This is believed to be due to an increase in accuracy since the new increments are presented in angle of attack increments of 5 deg while the previous increments are presented every 10 deg.

Figures 6-3 through 6-5 show comparisons between nozzle increments from TWT 691, TWT 679 and those presently in use for normal force, pitching moment, and axial force. These plots were analyzed to develop the nozzle increments. The lateral directional increments for the new high performance nozzle were zero due to the symmetry of the nozzle extension.

Table 6-4 is an example of the tabular data presented in Appendix A for the high performance nozzle increments. Only a roll angle of zero degree is presented since the aerodynamic characteristics of the nozzle do not vary with roll angle. The Mach numbers presented are 0.4, 0.5, 0.55, 0.6, 0.7, 0.8, 0.9, 0.95, 1.05, 1.1, 1.2, 1.3, 1.46, 1.96, and 2.99. Figures 6-6 through 6-8 show examples of the plots of high performance nozzle increments that are presented in Appendix A. In the appendix, all the longitudinal coefficient increment plots for one Mach number are grouped together.

6.2 SYSTEMS TUNNEL INCREMENTS

Lockheed has developed increments for both the steel case and FWC systems tunnel configurations. These increments were developed using data from the TWT 691 test program. The configurations tested are presented in Fig. 5-4a.

Figures 6-9 and 6-10 show cross plots of rolling moment coefficients versus roll angle for the FWC and steel case systems tunnel configurations. Notice that the greatest rolling moment increment is developed at a roll angle of 45 deg. The rolling moment increment is the one most affected by the systems tunnel. Figures 6-11 and 6-12 show sample plots of the systems

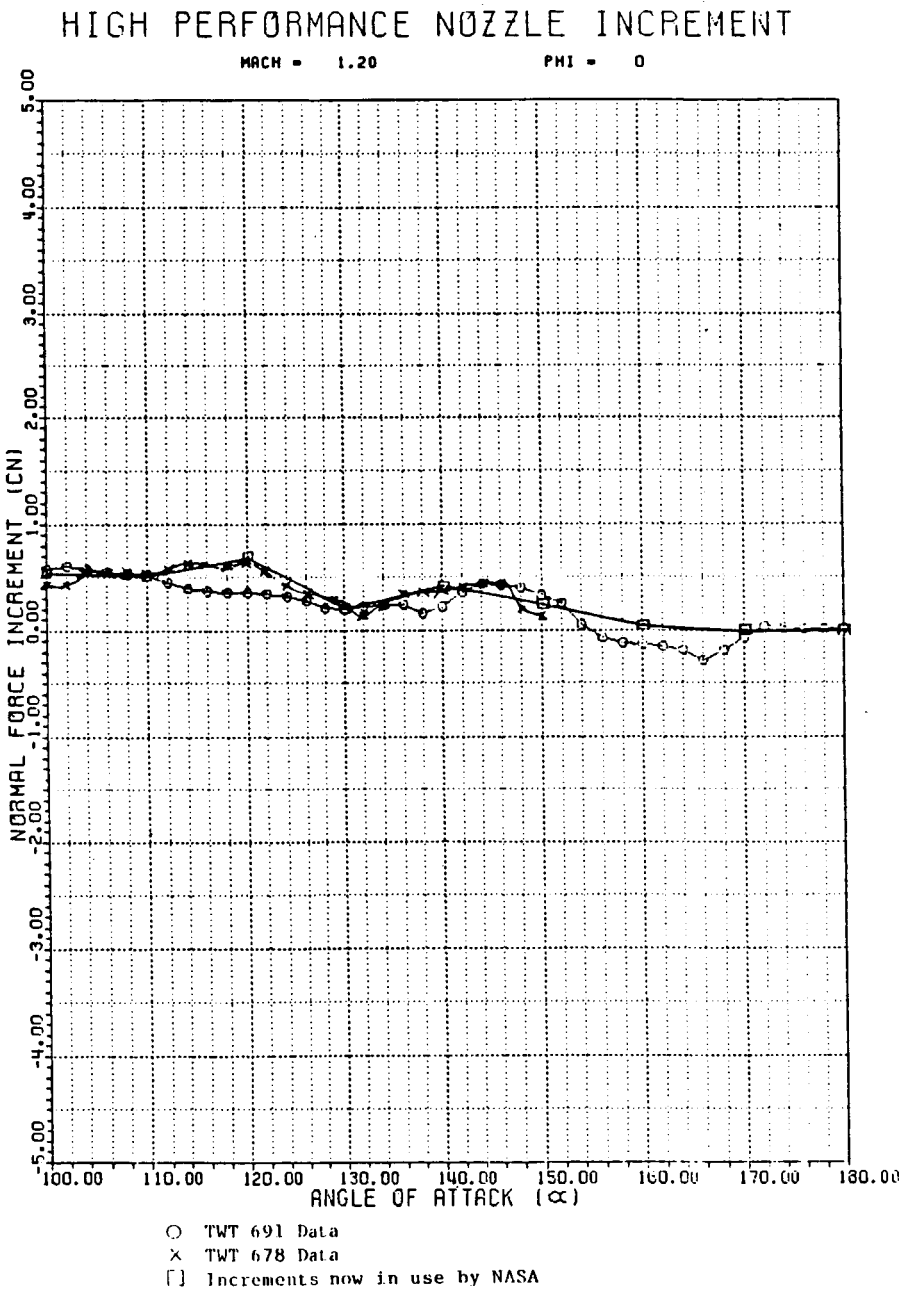

Fig. 6-3 Comparison of Data Used to Develop the Normal Force Increment for the High Performance Nozzle

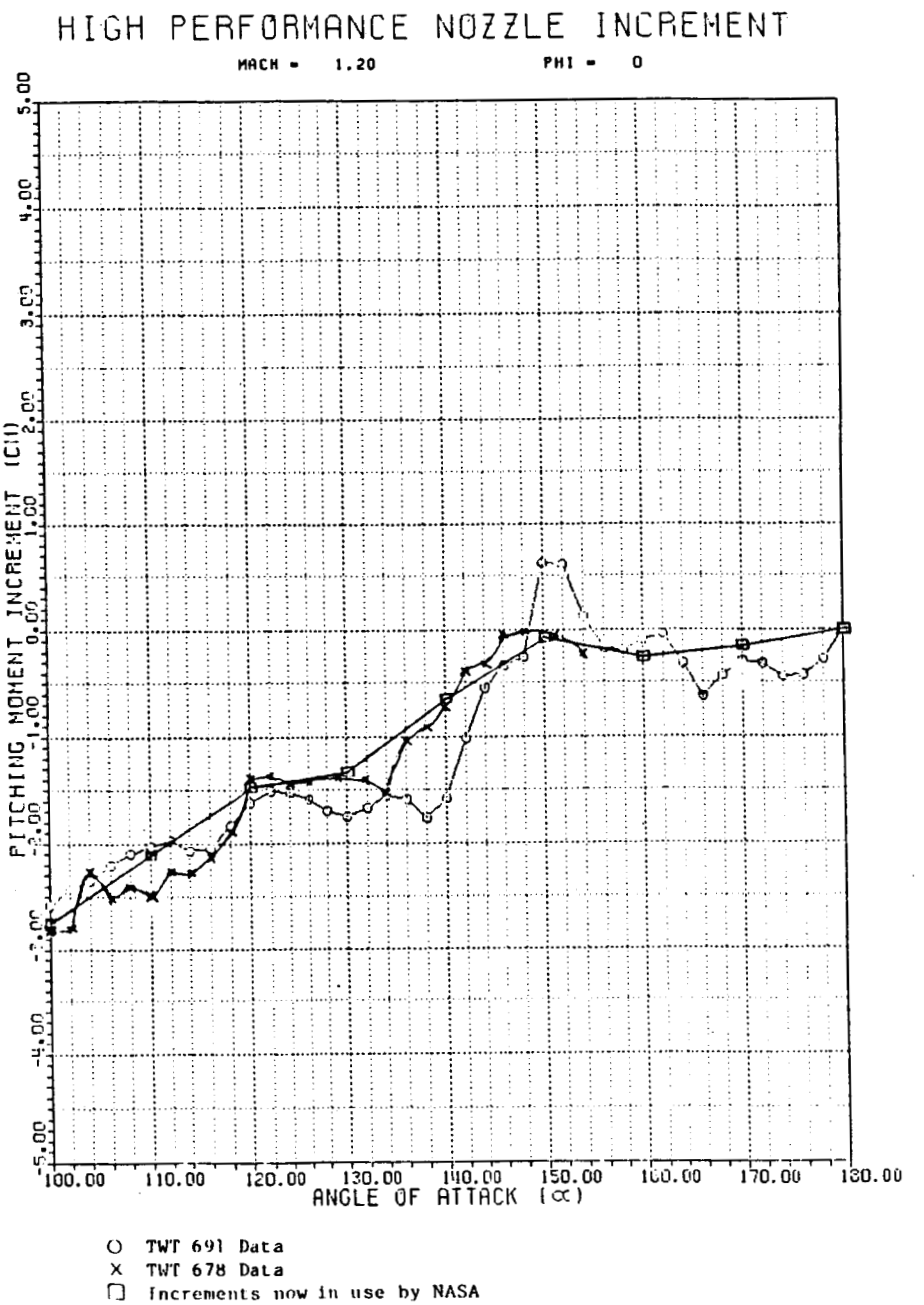

Fig. 6-4 Comparison of Data Used to Develop the Pitching Moment Increment for the High Performance Nozzle

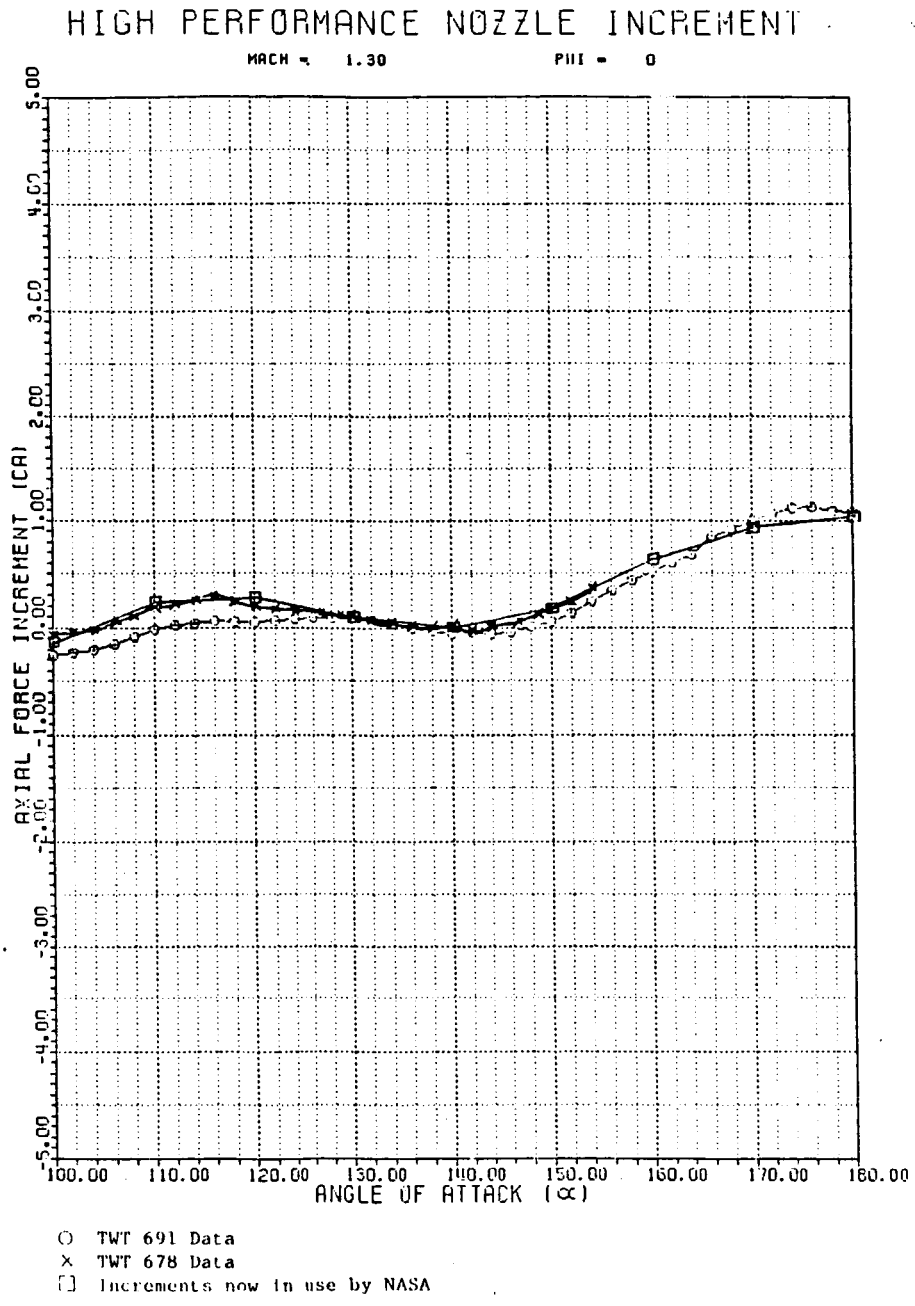

Fig. 6-5 Comparison of Data Used to Develop the Axial Force Increments for the High Performance Nozzle

Table 6-3 Sample of Tabular Data in Appendix A for High Performance Nozzle Increments

HIGH PERFORMANCE NOZZLE INCREMENT

DREF=146 IN
LREF=1789.6 IN
MRP=.59*LREF (STA 1255.9)

MACH= 0.40
PHI= 0.

ALPHA	CN	CM	CY	CYM	CA	CR
0.	0.00000000	0.00000000	0.00000000	0.00000000	0.00000000	0.00000000
5.	0.00000000	0.00000000	0.00000000	0.00000000	0.00000000	0.00000000
10.	0.00000000	0.00000000	0.00000000	0.00000000	0.00000000	0.00000000
15.	0.00000000	0.00000000	0.00000000	0.00000000	0.00000000	0.00000000
20.	0.00000000	0.00000000	0.00000000	0.00000000	0.00000000	0.00000000
25.	0.00000000	0.00000000	0.00000000	0.00000000	0.00000000	0.00000000
30.	0.00000000	0.00000000	0.00000000	0.00000000	0.00000000	0.00000000
35.	0.00000000	0.00000000	0.00000000	0.00000000	0.00000000	0.00000000
40.	0.00000000	0.00000000	0.00000000	0.00000000	0.00000000	0.00000000
45.	0.00000000	0.00000000	0.00000000	0.00000000	0.00000000	0.00000000
50.	0.00000000	0.00000000	0.00000000	0.00000000	0.00000000	0.00000000
55.	0.00000000	-0.04500000	0.00000000	0.00000000	0.00000000	0.00000000
60.	0.00000000	-0.13000000	0.00000000	0.00000000	0.00000000	0.00000000
65.	0.00000000	-0.20050000	0.00000000	0.00000000	0.00000000	0.00000000
70.	0.00000000	-0.30500001	0.00000000	0.00000000	0.00000000	0.00000000
75.	0.04500000	-0.44499999	0.00000000	0.00000000	-0.02500000	0.00000000
80.	0.10500000	-0.60049999	0.00000000	0.00000000	-0.04500000	0.00000000
85.	0.23000000	-0.73000002	0.00000000	0.00000000	-0.08500000	0.00000000
90.	0.34500000	-0.89109999	0.00000000	0.00000000	-0.12690000	0.00000000
95.	0.44499999	-1.07000005	0.00000000	0.00000000	-0.16670001	0.00000000
100.	0.50449997	-1.22459996	0.00000000	0.00000000	-0.20330000	0.00000000
105.	0.55049998	-1.34000003	0.00000000	0.00000000	-0.09470000	0.00000000
110.	0.48500001	-1.45879996	0.00000000	0.00000000	0.00790000	0.00000000
115.	0.40050000	-1.55050004	0.00000000	0.00000000	-0.00460000	0.00000000
120.	0.36970001	-1.57809997	0.00000000	0.00000000	-0.07930000	0.00000000
125.	0.42490001	-1.48150003	0.00000000	0.00000000	-0.05130000	0.00000000
130.	0.57139999	-1.21879995	0.00000000	0.00000000	-0.12650000	0.00000000
135.	0.55500001	-0.80500001	0.00000000	0.00000000	-0.15030000	0.00000000
140.	0.42660001	-0.46790001	0.00000000	0.00000000	-0.19550000	0.00000000
145.	0.17919999	-0.19000000	0.00000000	0.00000000	-0.16520000	0.00000000
150.	-0.10790000	-0.22229999	0.00000000	0.00000000	-0.07920000	0.00000000
155.	-0.06450000	-0.35820001	0.00000000	0.00000000	0.17919999	0.00000000
160.	-0.03350000	-0.55599999	0.00000000	0.00000000	0.61030000	0.00000000
165.	-0.16170000	-0.63249999	0.00000000	0.00000000	0.85900003	0.00000000
170.	-0.08900000	-0.56330001	0.00000000	0.00000000	0.96900002	0.00000000
175.	0.06540000	-0.34500000	0.00000000	0.00000000	1.06690001	0.00000000
180.	0.00000000	0.00000000	0.00000000	0.00000000	0.95980000	0.00000000

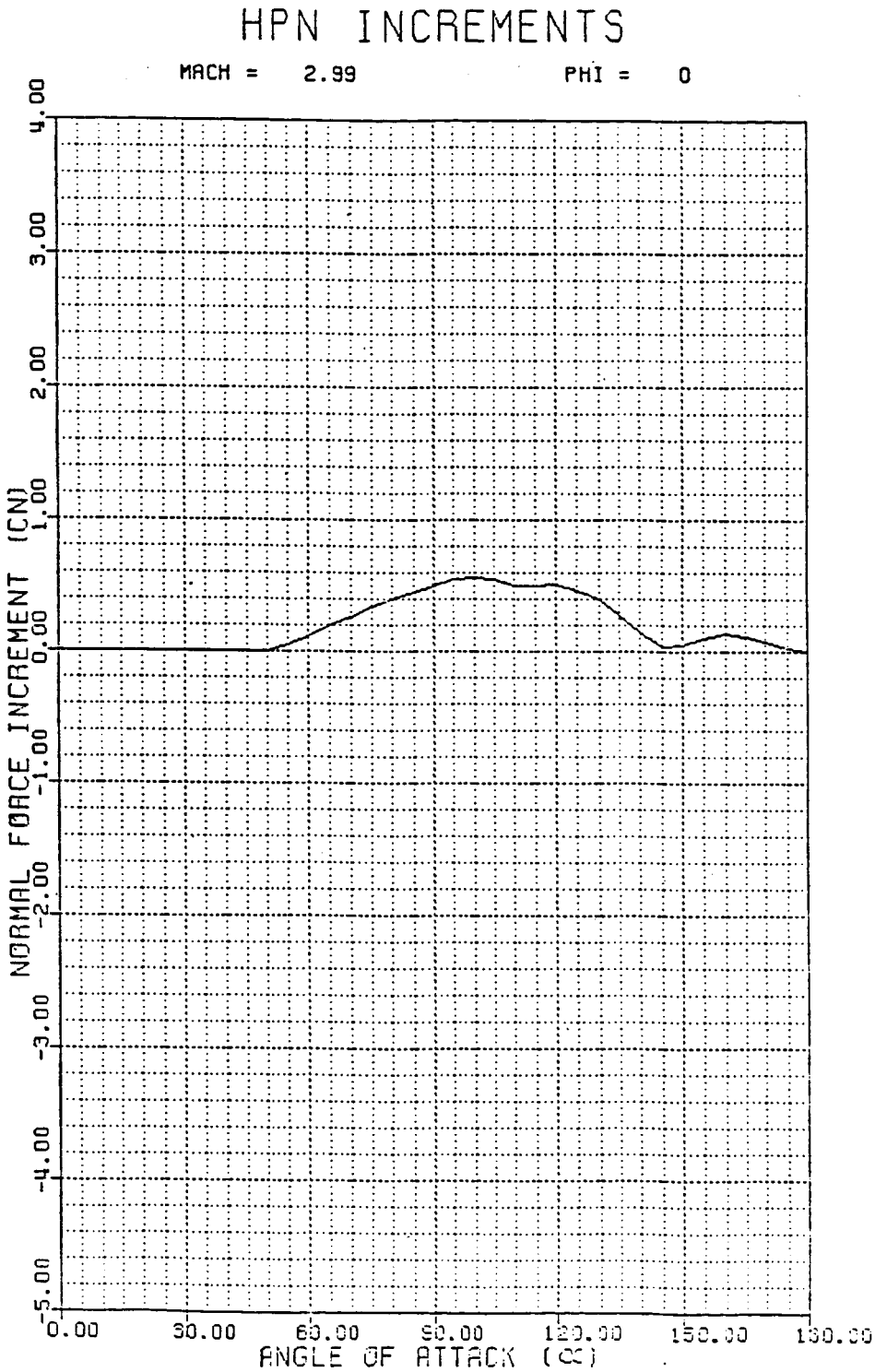

Fig. 6-6 Sample Plot from Appendix A of High Performance Nozzle Normal Force Increment

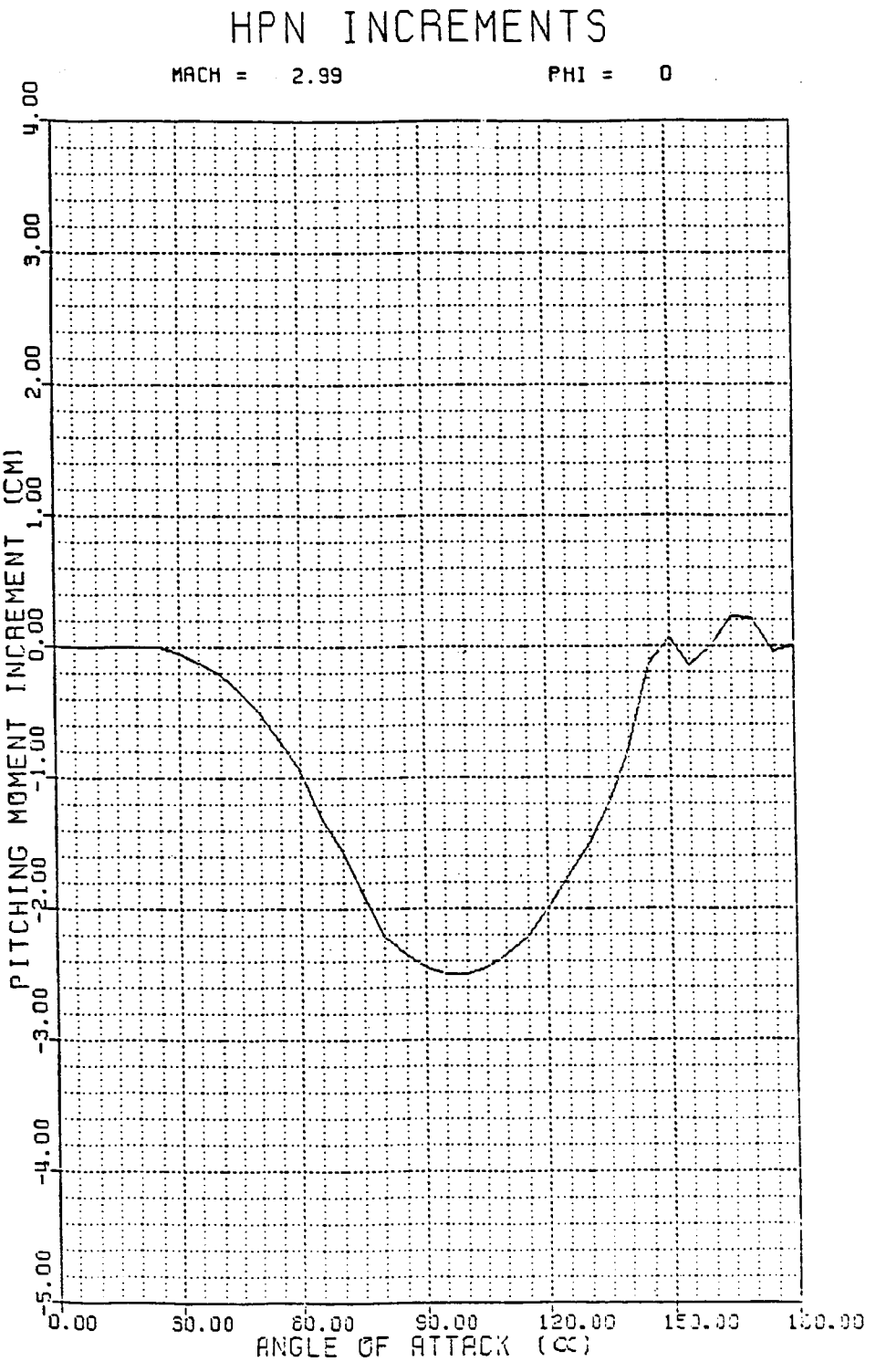

Fig. 6-7 Sample Plot from Appendix A of High Performance Nozzle Pitching Moment Increment

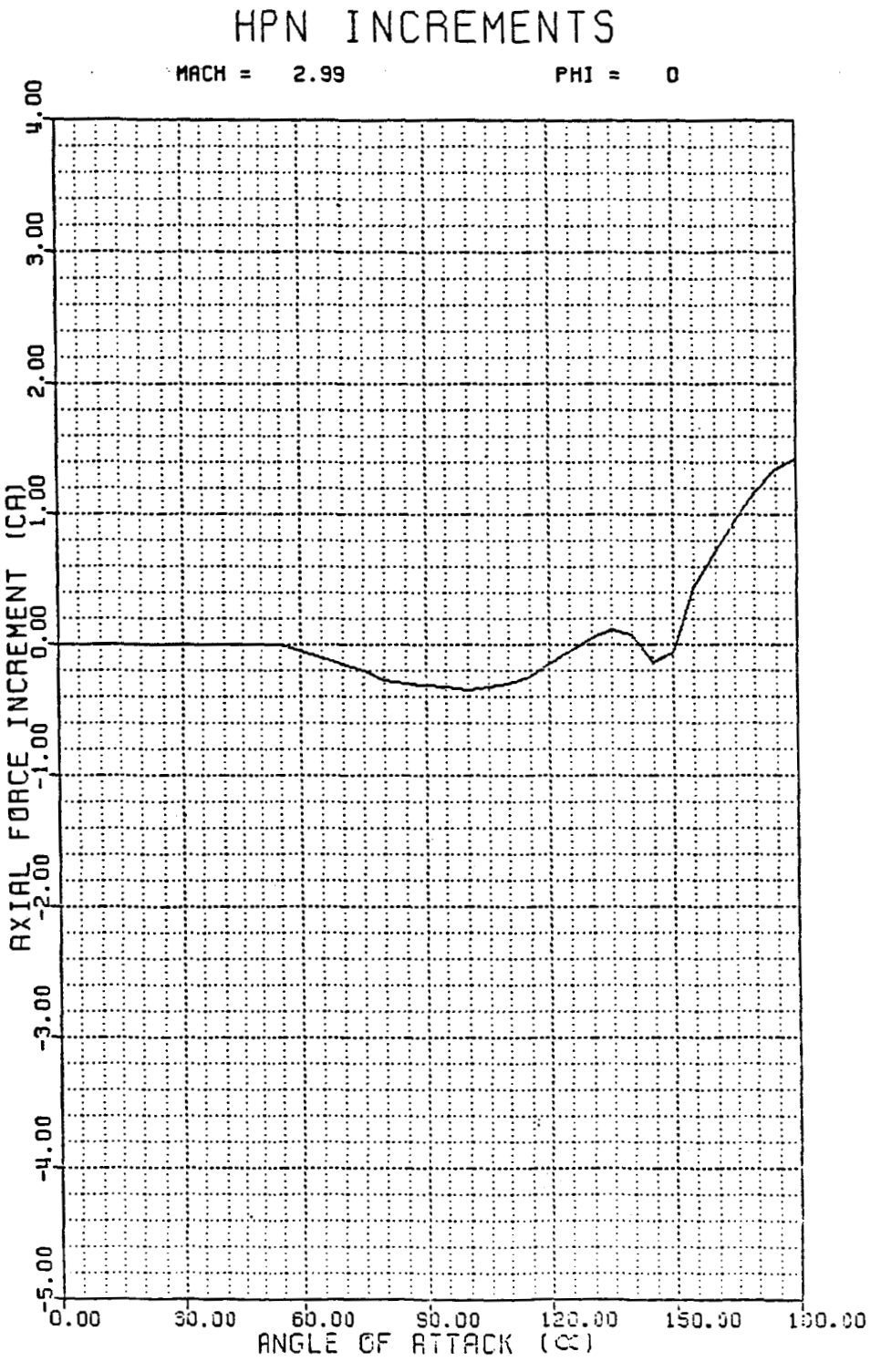

Fig. 6-8 Sample Plot from Appendix A of High Performance Nozzle Axial Force Increment

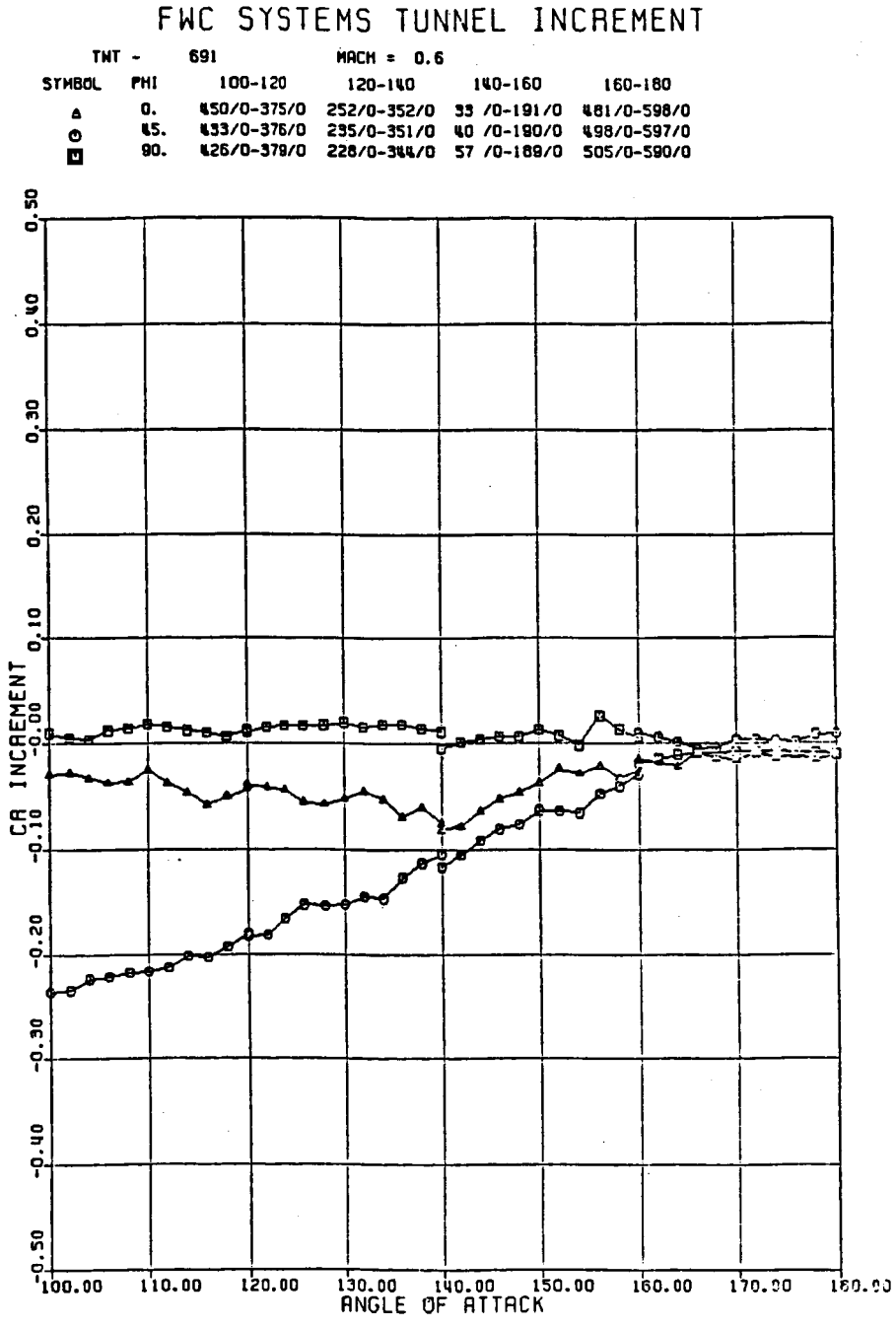

Fig. 6-9 Cross Plot of Rolling Moment Increments for FWC Systems Tunnel

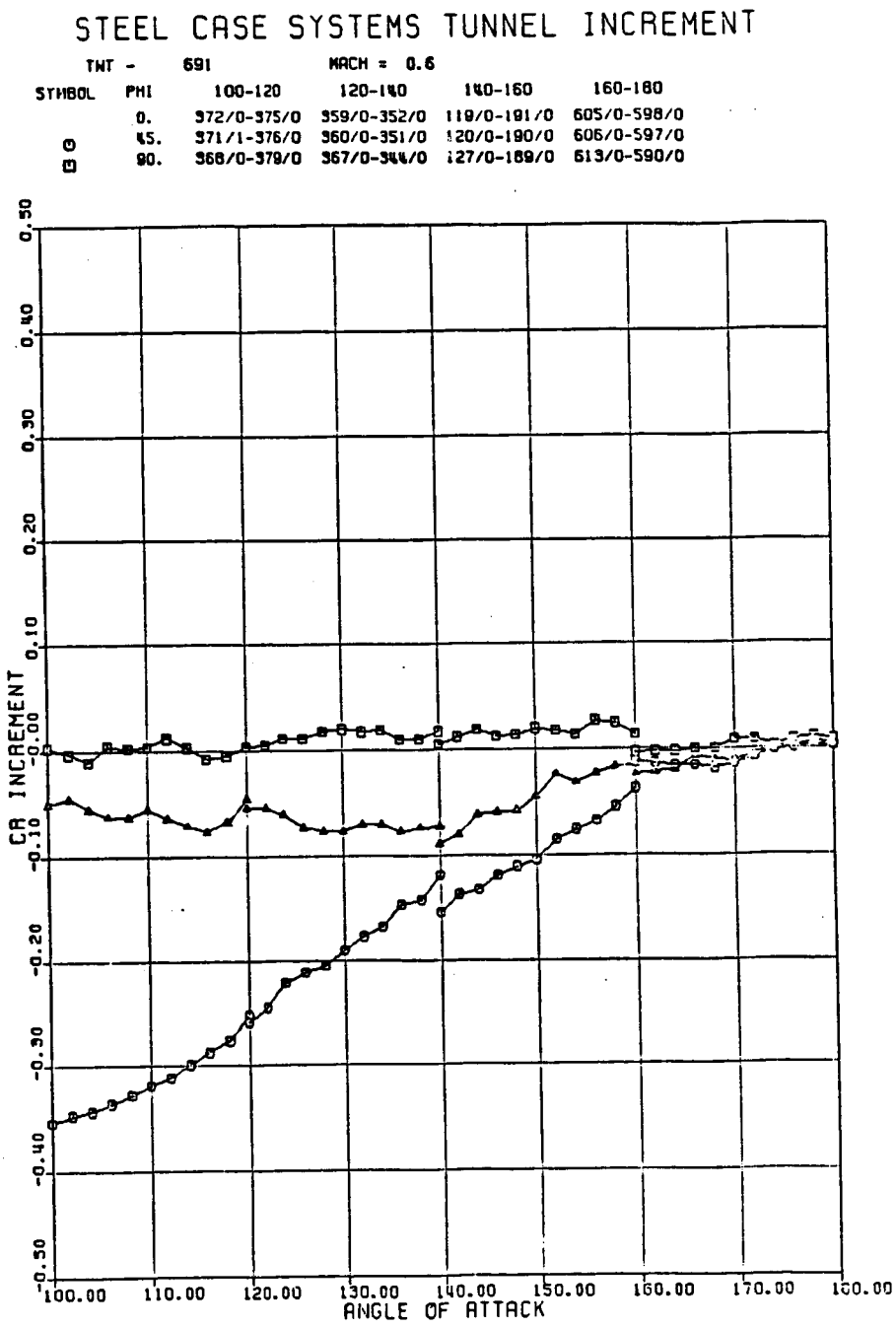

Fig. 6-10 Cross Plot of Rolling Moment Increment for Steel Case System Tunnel

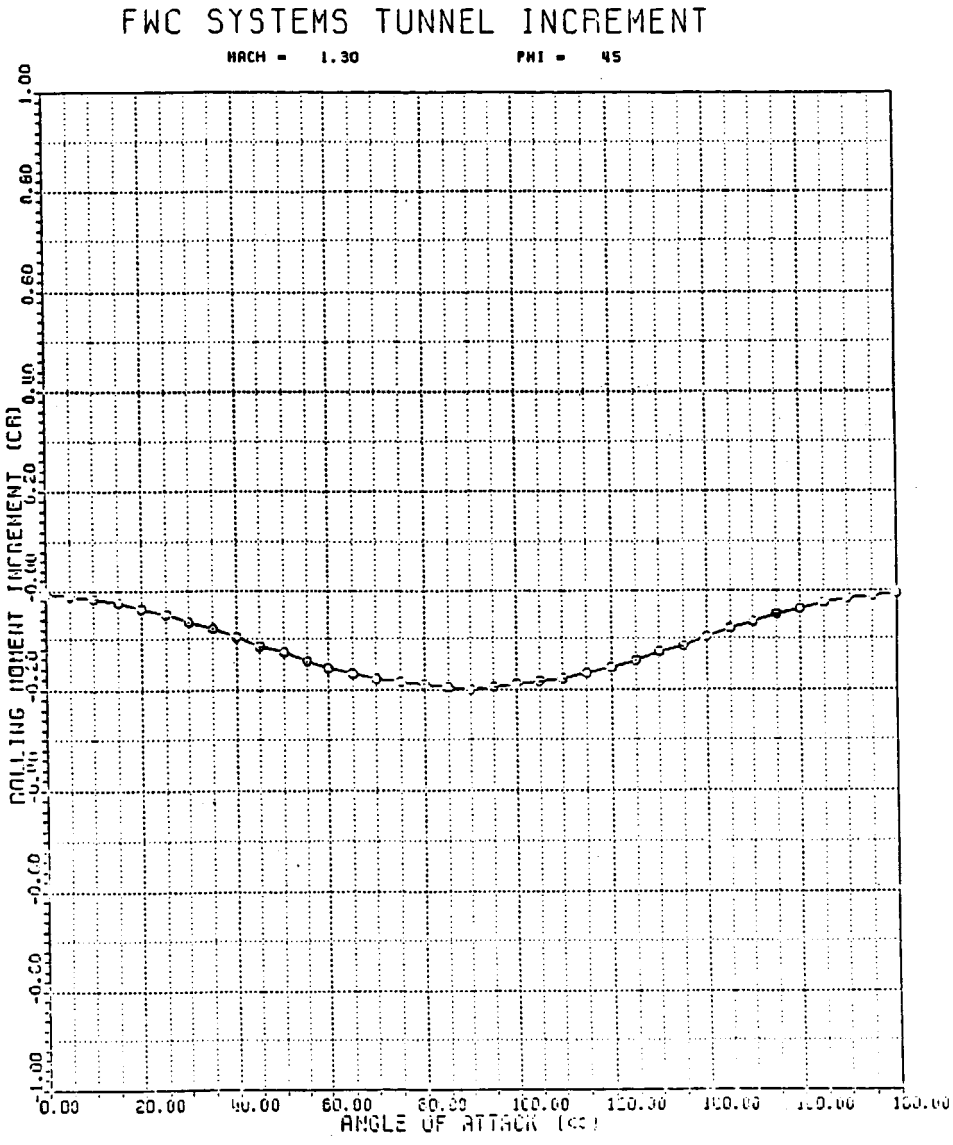

Fig. 6-11 Sample Plot of Rolling Moment Increment for FWC Systems Tunnel

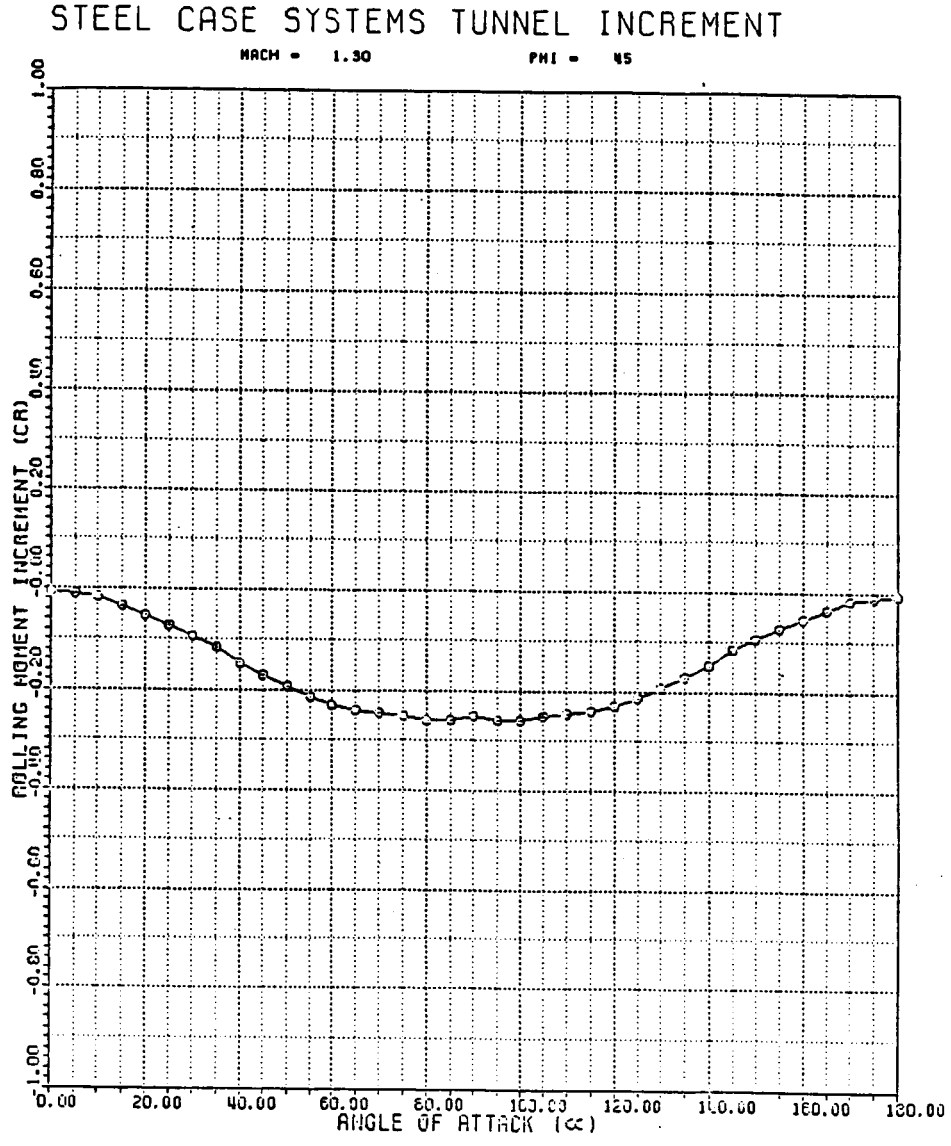

Fig. 6-12 Sample Plot of Rolling Moment Increment for Steel Case Systems Tunnel

tunnel increments versus angle of attack for the FWC and steel case SRBs. Tables 6-5 and 6-6 provide examples of the tabular data available in Appendix A of both the FWC and steel case systems tunnel increments. There is data in Appendix A for Mach numbers of 0.6, 0.9, 1.1, 1.3, and 2.99 and for roll angles of 0, 45, and 90 deg.

6.3 ET ATTACH RING INCREMENTS

Increments for both the steel case and FWC ET attach ring configurations have been developed. The configurations used to develop these increments from the TWT 691 test are pictured in Fig. 5-4b. These increments are probably the least significant of the protuberances in the respect that the difference between the two configurations is so small.

Figures 6-13 and 6-14 show sample plots of the ET attach ring increments for the FWC and steel case configurations. Tables 6-7 and 6-8 present samples of the tabular data for each of these increments as they appear in Appendix A. Each increment is presented in the appendix for Mach Numbers of 0.6, 0.9, 1.1, 1.3, and 2.99 and roll angles of 0, 45, and 90 degrees.

6.4 STIFFENER RINGS INCREMENTS

Lockheed has developed increments for the steel case and FWC aft segment stiffener rings. The configurations used to develop these increments from the TWT 691 test are presented in Fig. 5-4c. The axial force coefficient is the most important of the stiffener rings increments because it has the largest contribution to the aerodynamic characteristics of the SRBs.

Figures 6-15 and 6-16 show sample plots of the stiffener rings increments for the FWC and steel case configurations. Tables 6-9 and 6-10 present examples of each of these increments as they are presented in tabular form in Appendix A. In the appendix each increment is presented for Mach numbers of 0.6, 0.9, 1.1, 1.3, and 2.99. The FWC stiffener rings increment

Table 6-5 SAMPLE OF TABULAR DATA IN APPENDIX A FOR THE FWC SYSTEMS TUNNEL INCREMENTS

FWC SYSTEMS TUNNEL INCREMENT

DREF=146 IN
LREF=1789.6 IN
MRP=.59*LREF (STA 1255.9)

MACH= 0.60
PHI= 0.

ALPHA	CN	CM	CY	CYM	CA	CR
0.	0.00000000	0.00000000	0.00000000	0.00000000	0.00000000	-0.00940000
5.	0.00000000	0.00000000	0.00000000	0.00000000	0.00000000	-0.01290000
10.	0.00000000	0.00000000	0.00000000	0.00000000	0.00000000	-0.01520000
15.	0.00000000	0.00000000	0.00000000	0.00000000	0.00000000	-0.01520000
20.	0.00000000	0.00000000	0.00000000	0.00000000	0.00000000	-0.01500000
25.	0.00000000	0.00000000	0.00000000	0.00000000	0.00000000	-0.02490000
30.	0.00000000	0.00000000	0.00000000	0.00000000	0.00000000	-0.03740000
35.	0.00000000	0.00000000	0.00000000	0.00000000	0.00000000	-0.05840000
40.	0.00000000	0.00000000	0.00000000	0.00000000	0.00000000	-0.07510000
45.	0.00000000	0.00000000	0.00000000	0.00000000	0.00000000	-0.06090000
50.	0.00000000	0.00000000	0.00000000	0.00000000	0.00000000	-0.05240000
55.	0.00000000	0.00000000	0.00000000	0.00000000	0.00000000	-0.04990000
60.	0.00000000	0.00000000	0.00000000	0.00000000	0.00000000	-0.04320000
65.	0.00000000	0.09950000	0.00000000	0.00000000	0.00000000	-0.05230000
70.	0.00000000	0.20050000	0.00000000	0.00000000	0.00000000	-0.02540000
75.	-0.06500000	0.29949999	0.00000000	0.00000000	0.00000000	-0.03510000
80.	-0.14000000	0.34999999	0.00000000	0.03500000	0.00000000	-0.02950000
85.	-0.14500000	0.33300000	-0.07150000	0.22499999	0.00000000	-0.02950000
90.	-0.10500000	0.27000001	-0.19499999	0.50000000	0.00000000	-0.02950000
95.	0.00000000	0.15500000	-0.37000000	0.99980003	0.00000000	-0.02950000
100.	0.24020000	-0.06670000	-0.74360001	1.66299999	-0.02930000	-0.02950000
105.	0.55559999	-0.62419999	-1.20620000	2.54209995	-0.05410000	-0.03510000
110.	0.80229998	-0.55540001	-1.37269998	2.69560003	-0.03940000	-0.02540000
115.	0.72399998	-0.59429997	-1.35109997	1.94110000	0.01670000	-0.05230000
120.	0.23590000	-0.89700001	-2.00710011	-2.17429996	0.07190000	-0.04320000
125.	0.17470001	-1.54639995	-2.79329991	-3.57049990	0.09820000	-0.04990000
130.	0.87599999	-2.64219999	-3.38369999	-4.21659994	0.07840000	-0.05240000
135.	2.23749995	-0.02880000	-2.60360003	-4.05000019	0.04430000	-0.06090000
140.	1.98740005	1.45710003	-2.66389990	-3.79010010	0.01460000	-0.07510000
145.	1.64470005	1.67019999	-1.60029995	-1.52149999	0.01150000	-0.05840000
150.	1.07179999	0.95609999	-1.68050003	-0.76880002	0.01390000	-0.03740000
155.	0.78320003	0.69199997	-1.39230001	-0.39730000	0.00800000	-0.02490000
160.	0.60159999	1.01779997	-0.23909999	-0.21250001	-0.01070000	-0.01500000
165.	0.30379999	0.64490002	-0.09940000	-0.19080000	0.00430000	-0.01520000
170.	0.09200000	0.18709999	-0.02030000	0.04620000	-0.01460000	-0.01520000
175.	0.00230000	0.00860000	-0.00980000	0.02490000	-0.00490000	-0.01290000
180.	-0.01120000	-0.01710000	0.00320000	0.02930000	-0.00310000	-0.00940000

Table 6-6 SAMPLE OF TABULAR DATA IN APPENDIX A FOR THE STEEL CASE SYSTESM TUNNEL INCREMENTS

STEEL CASE SYSTEMS TUNNEL INCREMENTS

DREF=146 IN
LREF=1789.6 IN
MRP=.59*LREF (STA 1255.9)

MACH= 0.60
PHI= 0.

ALPHA	CN	CM	CY	CYM	CA	CR
0.	0.00000000	0.00000000	0.00000000	0.00000000	0.00000000	0.00090000
5.	0.00000000	0.00000000	0.00000000	0.00000000	0.00000000	0.00180000
10.	0.00000000	0.00000000	0.00000000	0.00000000	0.00000000	-0.01070000
15.	0.00000000	0.00000000	0.00000000	0.00000000	0.00000000	-0.01270000
20.	0.00000000	0.00000000	0.00000000	0.00000000	0.00000000	-0.02360000
25.	0.00000000	0.00000000	0.00000000	0.00000000	0.00000000	-0.02680000
30.	0.00000000	0.00000000	0.00000000	0.00000000	0.00000000	-0.04470000
35.	0.00000000	0.00000000	0.00000000	0.00000000	0.00000000	-0.06040000
40.	0.00000000	0.00000000	0.00000000	0.00000000	0.00000000	-0.07200000
45.	0.00000000	0.00000000	0.00000000	0.00000000	0.00000000	-0.07360000
50.	0.00000000	0.00000000	0.00000000	0.00000000	0.00000000	-0.07660000
55.	0.00000000	0.00000000	0.00000000	0.00000000	0.00000000	-0.06670000
60.	0.00000000	0.00000000	0.00000000	0.00000000	0.00000000	-0.05380000
65.	0.00000000	0.00000000	0.00000000	0.00000000	0.00000000	-0.07390000
70.	0.00000000	0.00000000	-0.00300000	0.00000000	0.00000000	-0.05330000
75.	0.00000000	0.00000000	-0.07500000	0.05000000	0.00000000	-0.05090000
80.	0.00000000	0.00000000	-0.19000000	0.19499999	0.00000000	-0.04990000
85.	0.00000000	-0.00300000	-0.37500000	0.31999999	0.00000000	-0.04990000
90.	0.00000000	-0.10000000	-0.60000002	0.61000001	0.00000000	-0.04990000
95.	0.10000000	-0.30000001	-0.81999999	1.00000000	0.00000000	-0.04990000
100.	0.30300000	-0.64770001	-1.28079998	1.60150003	-0.01350000	-0.04990000
105.	0.63090003	-1.03260005	-1.75999999	2.48259997	-0.05970000	-0.05090000
110.	0.92570001	-0.88849998	-2.03160000	2.40540004	-0.05310000	-0.05530000
115.	0.69510000	-0.98790002	-2.43490005	1.35590005	-0.00200000	-0.07390000
120.	0.44560000	-1.17229998	-2.98230004	-2.57489991	0.06060000	-0.05300000
125.	0.37220001	-2.08890009	-3.53500009	-4.00199986	0.09240000	-0.06670000
130.	1.15050006	-3.36299992	-3.58999991	-4.26999998	0.06080000	-0.07660000
135.	2.28749990	0.38330001	-3.42499995	-4.03999996	0.03930000	-0.07360000
140.	2.06089997	1.56270003	-3.22720003	-3.76259995	0.01330000	-0.07200000
145.	1.55970001	1.46679997	-2.34870005	-2.24169993	0.01110000	-0.06040000
150.	1.17400002	1.00000000	-2.13210011	-1.79999995	0.00200000	-0.04470000
155.	0.91189998	0.85409999	-1.00720000	-1.39180005	0.02010000	-0.02680000
160.	0.69029999	1.09940004	-0.19120000	-0.62210000	0.00940000	-0.02360000
165.	0.40430000	0.77179998	-0.06150000	-0.19030000	0.02470000	-0.01270000
170.	0.14350000	0.29100001	0.00110000	0.09550000	0.01710000	-0.01070000
175.	0.02250000	0.06680000	-0.01560000	0.03890000	0.01440000	0.00180000
180.	0.01240000	0.04250000	-0.01270000	0.00950000	0.01560000	0.00090000

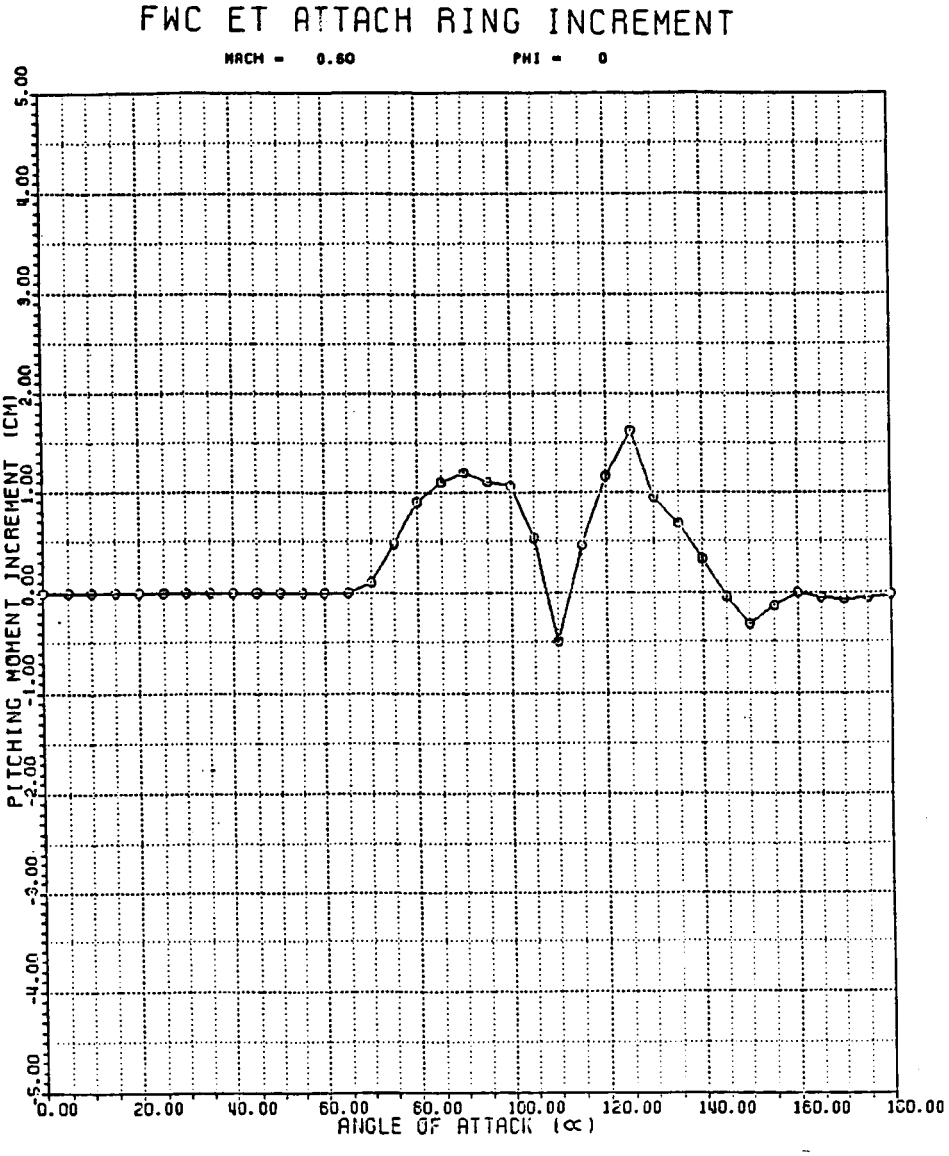

Fig. 6-13 Sample Plot of Pitching Moment Increment for FWC ET Attach Ring

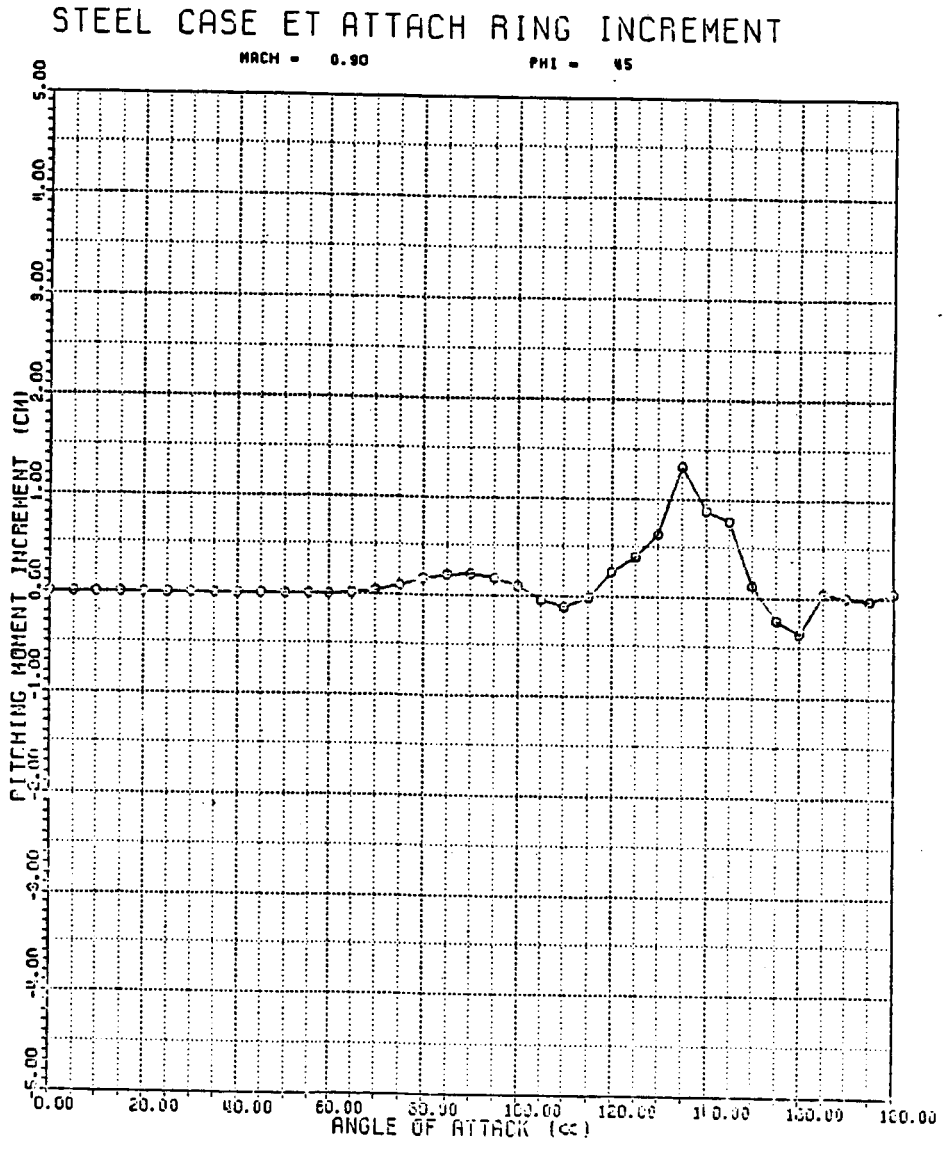

Fig. 6-14 Sample Plot of Pitching Moment Increment for Steel Case ET Attach Ring

Table 6-7 SAMPLE OF TABULAR DATA IN APPENDIX A FOR THE FWC ET ATTACH RING INCREMENTS

FWC ET ATTACH RING INCREMENT

DREF=146 IN
LREF=1789.6 IN
MRP=.59*LREF (STA 1255.9)

MACH= 0.60
PHI= 0.

ALPHA	CN	CM	CY	CYM	CA	CR
0.	0.00000000	0.00000000	0.00000000	0.00000000	0.00000000	0.00000000
5.	0.00000000	0.00000000	0.00000000	0.00000000	0.00000000	0.00000000
10.	0.00000000	0.00000000	0.00000000	0.00000000	0.00000000	0.00000000
15.	0.00000000	0.00000000	0.00000000	0.00000000	0.00000000	0.00000000
20.	0.00000000	0.00000000	0.00000000	0.00000000	0.00000000	0.00000000
25.	0.00000000	0.00000000	0.00000000	0.00000000	0.00000000	0.00000000
30.	0.00000000	0.00000000	0.00000000	0.00000000	0.00000000	0.00000000
35.	0.00000000	0.00000000	0.00000000	0.00000000	0.00000000	0.00000000
40.	0.00000000	0.00000000	0.00000000	0.00000000	0.00000000	0.00000000
45.	0.00000000	0.00000000	0.00000000	0.00000000	0.00000000	0.00000000
50.	0.00000000	0.00000000	0.00000000	0.00000000	0.00000000	0.00000000
55.	0.00000000	0.00000000	0.00000000	0.00000000	0.00000000	0.00000000
60.	0.00000000	0.00000000	0.00000000	0.00000000	0.00000000	0.00000000
65.	0.00000000	0.00000000	0.00000000	0.00000000	0.00000000	0.00000000
70.	0.00000000	0.10000000	0.00000000	0.00000000	0.00000000	0.00000000
75.	0.00000000	0.47999999	0.00000000	0.10000000	0.00000000	0.00000000
80.	-0.02000000	0.89999998	0.00000000	0.34999999	0.00000000	0.00000000
85.	-0.07000000	1.10000002	-0.05000000	0.60000002	-0.05000000	0.00000000
90.	-0.10000000	1.20000005	-0.18000001	0.98000002	-0.08000000	0.00000000
95.	-0.13000000	1.10000002	-0.31000000	1.60000002	-0.06000000	0.00000000
100.	-0.15279999	1.06120002	-0.54769999	2.43330002	-0.02070000	0.00000000
105.	-0.17050000	0.53820002	-0.79939997	3.02080011	0.05130000	0.00000000
110.	-0.48249999	-0.48840001	-0.19620000	3.04999995	0.07900000	0.00000000
115.	-0.09930000	0.46280000	-0.07460000	2.94720006	0.06160000	0.00000000
120.	0.16410001	1.16410005	-0.40210000	2.07500000	0.01270000	0.00000000
125.	0.24680001	1.63160002	-0.98820001	1.63000001	-0.04180000	0.00000000
130.	-0.06950000	0.95150000	-0.33190000	0.23440000	-0.06710000	0.00000000
135.	0.01110000	0.67519999	0.95609999	-0.31369999	-0.06840000	0.00000000
140.	-0.22640000	0.32690001	-0.10080000	-0.93760002	-0.11280000	0.00000000
145.	-0.34930000	-0.04410000	0.29330000	-1.96500003	-0.11630000	0.00000000
150.	-0.33280000	-0.31880000	0.01130000	-1.81400001	-0.12350000	0.00000000
155.	-0.08930000	-0.13550000	0.09170000	-1.36080003	-0.15640000	0.00000000
160.	0.16550000	-0.00240000	0.42080000	-0.26570001	-0.14540000	0.00000000
165.	0.06490000	-0.05140000	0.18080001	0.01200000	-0.06210000	0.00000000
170.	-0.01610000	-0.06760000	-0.02040000	0.01550000	-0.00660000	0.00000000
175.	-0.01690000	-0.05050000	0.02360000	0.04100000	0.04790000	0.00000000
180.	-0.01050000	-0.02580000	0.03380000	0.06240000	0.04990000	0.00000000

Table 6-8 SAMPLE OF TABULAR DATA IN APPENDIX A FOR THE STEEL CASE ET ATTACH RING INCREMENTS

STEEL CASE ET ATTACH RING INCREMENTS

DREF=146 IN
LREF=1789.6 IN
MRP=.59*LREF (STA 1255.9)

MACH= 0.60
PHI= 0.

ALPHA	CN	CM	CY	CYM	CA	CR
0.	0.00000000	0.00000000	0.00000000	0.00000000	0.00000000	0.00000000
5.	0.00000000	0.00000000	0.00000000	0.00000000	0.00000000	0.00000000
10.	0.00000000	0.00000000	0.00000000	0.00000000	0.00000000	0.00000000
15.	0.00000000	0.00000000	0.00000000	0.00000000	0.00000000	0.00000000
20.	0.00000000	0.00000000	0.00000000	0.00000000	0.00000000	0.00000000
25.	0.00000000	0.00000000	0.00000000	0.00000000	0.00000000	0.00000000
30.	0.00000000	0.00000000	0.00000000	0.00000000	0.00000000	0.00000000
35.	0.00000000	0.00000000	0.00000000	0.00000000	0.00000000	0.00000000
40.	0.00000000	0.00000000	0.00000000	0.00000000	0.00000000	0.00000000
45.	0.00000000	0.00000000	0.00000000	0.00000000	0.00000000	0.00000000
50.	0.00000000	0.00000000	0.00000000	0.00000000	0.00000000	0.00000000
55.	0.00000000	0.00000000	0.00000000	0.00000000	0.00000000	0.00000000
60.	0.00000000	0.00000000	0.00000000	0.00000000	0.00000000	0.00000000
65.	0.00000000	0.00000000	0.00000000	0.00000000	0.00000000	0.00000000
70.	0.00000000	0.20000000	0.00000000	0.00000000	0.00000000	0.00000000
75.	0.00000000	0.68000001	0.00000000	0.05000000	0.00000000	0.00000000
80.	0.00000000	1.04999995	-0.05000000	0.19000000	0.00000000	0.00000000
85.	0.00000000	1.29999995	-0.12000000	0.55000001	0.00000000	0.00000000
90.	-0.02000000	1.39999998	-0.20000000	1.25000000	0.00000000	0.00000000
95.	-0.04000000	1.35000002	-0.38000000	1.89999998	0.00000000	0.00000000
100.	-0.10570000	1.11459994	-0.54949999	2.70000005	-0.01190000	0.00000000
105.	-0.18430001	0.48570001	-0.77429998	2.81999993	0.04070000	0.00000000
110.	-0.49149999	-0.52929997	-0.31290001	2.82999992	0.08440000	0.00000000
115.	-0.10540000	0.46939999	-0.26789999	2.76690006	0.05980000	0.00000000
120.	0.28999999	1.14470005	-0.54799998	2.49329996	-0.01060000	0.00000000
125.	0.39969999	1.61020005	-1.10119998	1.70299995	-0.06780000	0.00000000
130.	0.10060000	1.20239997	-0.99039997	0.69929999	-0.09350000	0.00000000
135.	0.13680001	0.71820003	0.99080002	-0.43000001	-0.08960000	0.00000000
140.	-0.14790000	0.12470000	-0.13630000	-1.53909995	-0.14839999	0.00000000
145.	-0.30489999	-0.16140001	0.32089999	-1.76699996	-0.12080000	0.00000000
150.	-0.26850001	-0.34089999	0.32380000	-1.32729995	-0.09400000	0.00000000
155.	-0.10060000	-0.14260000	0.11470000	-0.80309999	-0.11520000	0.00000000
160.	0.09190000	-0.06410000	0.10660000	-0.54210001	-0.11030000	0.00000000
165.	0.09620000	-0.00420000	0.13140000	0.08970000	-0.05970000	0.00000000
170.	0.02410000	-0.03020000	-0.02030000	0.04320000	-0.00310000	0.00000000
175.	-0.00590000	-0.02900000	0.01580000	0.03300000	0.03400000	0.00000000
180.	0.01160000	0.02200000	0.01870000	0.02410000	0.04560000	0.00000000

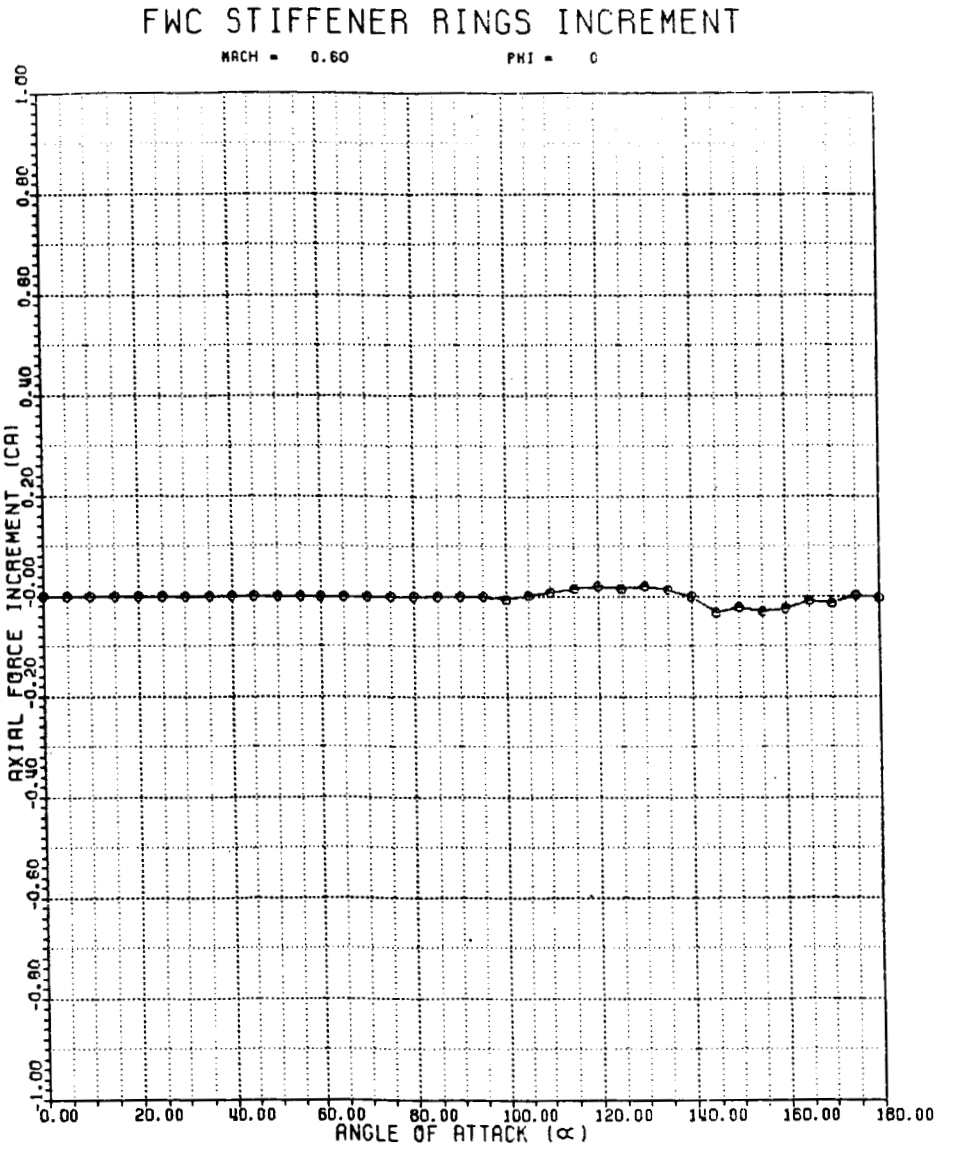

Fig. 6-15 Sample Plot of Axial Force Increment for FWC Stiffener Rings

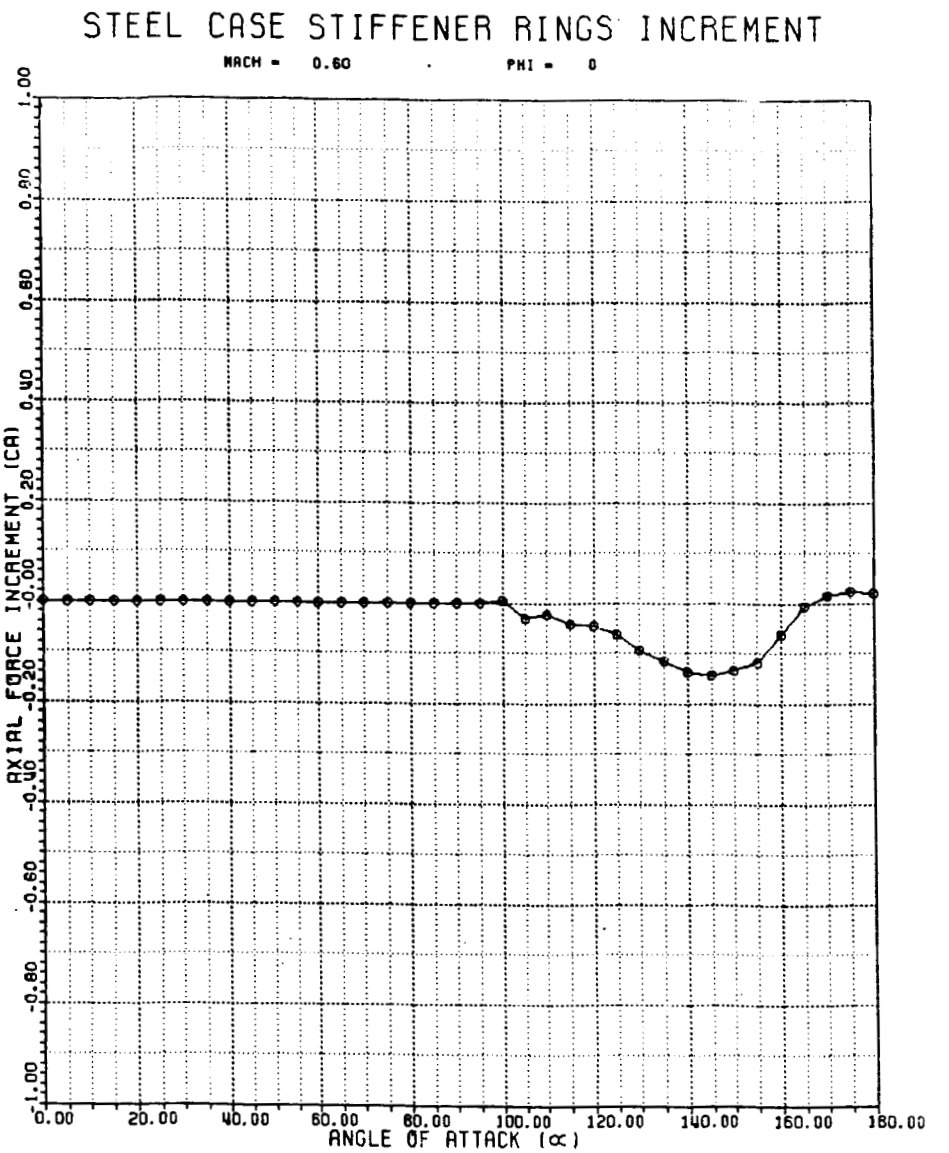

Fig. 6-16 Sample Plot of Axial Force Incremet
fot Steel Case Stiffener Rings

Table 6-9 SAMPLE OF TABULAR DATA IN APPENDIX A FOR THE FWC STIFFENER RINGS INCREMENTS

FWC STIFFENER RINGS INCREMENT

DREF=146 IN
LREF=1789.6 IN
MRP=.59*LREF (STA 1255.9)

MACH= 0.60
PHI= 0.

ALPHA	CN	CM	CY	CYM	CA	CR
0.	0.00000000	0.00000000	0.00000000	0.00000000	0.00000000	0.00000000
5.	0.00000000	0.00000000	0.00000000	0.00000000	0.00000000	0.00000000
10.	0.00000000	0.00000000	0.00000000	0.00000000	0.00000000	0.00000000
15.	0.00000000	0.00000000	0.00000000	0.00000000	0.00000000	0.00000000
20.	0.00000000	0.00000000	0.00000000	0.00000000	0.00000000	0.00000000
25.	0.00000000	0.00000000	0.00000000	0.00000000	0.00000000	0.00000000
30.	0.00000000	0.00000000	0.00000000	0.00000000	0.00000000	0.00000000
35.	0.00000000	0.00000000	0.00000000	0.00000000	0.00000000	0.00000000
40.	0.00000000	0.00000000	0.00000000	0.00000000	0.00000000	0.00000000
45.	0.00000000	0.00000000	0.00000000	0.00000000	0.00000000	0.00000000
50.	0.00000000	0.00000000	0.00000000	0.00000000	0.00000000	0.00000000
55.	0.00000000	0.00000000	0.00000000	0.00000000	0.00000000	0.00000000
60.	0.00000000	0.00000000	0.00000000	0.00000000	0.00000000	0.00000000
65.	0.00000000	0.05000000	0.00000000	0.00000000	0.00000000	0.00000000
70.	0.00000000	0.10500000	0.00000000	0.00270000	0.00000000	0.00000000
75.	0.00000000	0.20500000	0.00000000	0.00800000	0.00000000	0.00000000
80.	0.00000000	0.35600001	-0.02750000	0.20999999	0.00000000	0.00000000
85.	0.00000000	0.50000000	-0.00500000	0.40849999	0.00000000	0.00000000
90.	0.00000000	0.58350003	-0.14500000	0.57999998	0.00000000	0.00000000
95.	0.05500000	0.59899998	-0.20000000	0.70499998	0.00000000	0.00000000
100.	0.13410001	0.50830001	-0.23080000	0.69340003	-0.00570000	0.00000000
105.	0.18089999	0.37729999	-0.21430001	0.67159998	0.00190000	0.00000000
110.	0.10110000	0.16230001	-0.08160000	0.16820000	0.00890000	0.00000000
115.	0.00150000	0.02580000	-0.00460000	0.23920000	0.01530000	0.00000000
120.	-0.13150001	-0.12100000	-0.19410001	0.41220000	0.02100000	0.00000000
125.	-0.21870001	-0.19490001	0.00930000	0.25880000	0.01530000	0.00000000
130.	-0.13339999	-0.20500000	0.19499999	0.40500000	0.02070000	0.00000000
135.	0.00370000	-0.20050000	0.29499999	0.74000001	0.01360000	0.00000000
140.	0.12070000	-0.13800000	0.26089999	0.71670002	0.00000000	0.00000000
145.	0.17299999	-0.05500000	0.24200000	0.57569999	-0.03230000	0.00000000
150.	0.04500000	-0.04300000	0.25510001	0.47499999	-0.02230000	0.00000000
155.	0.02190000	-0.04720000	0.13750000	0.38000000	-0.03030000	0.00000000
160.	0.03070000	0.03630000	0.08690000	0.26449999	-0.02280000	0.00000000
165.	-0.04720000	-0.05120000	0.01040000	0.04590000	-0.00920000	0.00000000
170.	-0.02160000	-0.04190000	-0.00360000	0.02610000	-0.01440000	0.00000000
175.	-0.01220000	-0.03520000	0.00930000	-0.01040000	0.00100000	0.00000000
180.	-0.01460000	-0.02170000	0.01890000	0.02650000	-0.00320000	0.00000000

Table 6-10 SAMPLE OF TABULAR DATA IN APPENDIX A FOR THE STEEL CASE STIFFENER RINGS INCREMENTS

STEEL CASE STIFFENER RINGS INCREMENT

DREF=146 IN
LREF=1789.6 IN
MRP=.59*LREF (STA 1255.9)

MACH= 0.60
PHI= 0.

ALPHA	CN	CM	CY	CYM	CA	CR
0.	0.00000000	0.00000000	0.00000000	0.00000000	0.00000000	0.00000000
5.	0.00000000	0.00000000	0.00000000	0.00000000	0.00000000	0.00000000
10.	0.00000000	0.00000000	0.00000000	0.00000000	0.00000000	0.00000000
15.	0.00000000	0.00000000	0.00000000	0.00000000	0.00000000	0.00000000
20.	0.00000000	0.00000000	0.00000000	0.00000000	0.00000000	0.00000000
25.	0.00000000	0.00000000	0.00000000	0.00000000	0.00000000	0.00000000
30.	0.00000000	0.00000000	0.00000000	0.00000000	0.00000000	0.00000000
35.	0.00000000	0.00000000	0.00000000	0.00000000	0.00000000	0.00000000
40.	0.00000000	0.00000000	0.00000000	0.00000000	0.00000000	0.00000000
45.	0.00000000	0.00000000	0.00000000	0.00000000	0.00000000	0.00000000
50.	0.00000000	0.00000000	0.00000000	0.00000000	0.00000000	0.00000000
55.	0.00000000	0.00000000	0.00000000	0.00000000	0.00000000	0.00000000
60.	0.00000000	0.00000000	0.00000000	0.00000000	0.00000000	0.00000000
65.	0.00000000	0.00000000	0.00000000	0.00000000	0.00000000	0.00000000
70.	0.00000000	0.00000000	0.00000000	0.00000000	0.00000000	0.00000000
75.	0.00000000	0.00000000	0.00000000	0.11000000	0.00000000	0.00000000
80.	0.00000000	0.00000000	0.00000000	0.25999999	0.00000000	0.00000000
85.	0.00000000	-0.04000000	0.05000000	0.36000001	0.00000000	0.00000000
90.	0.05000000	-0.09000000	0.08000000	0.41999999	0.00000000	0.00000000
95.	0.10000000	-0.08000000	0.07000000	0.50000000	0.00000000	0.00000000
100.	0.07380000	-0.03110000	-0.01510000	0.45490000	0.00490000	0.00000000
105.	0.07710000	0.11980000	-0.14200000	0.35260001	-0.02950000	0.00000000
110.	-0.04870000	0.24500000	-0.16249999	-0.00190000	-0.02220000	0.00000000
115.	0.05890000	0.05100000	-0.39250001	0.41549999	-0.04010000	0.00000000
120.	0.02130000	0.15160000	-0.41870001	1.25000000	-0.04530000	0.00000000
125.	-0.19100000	-0.39930001	0.25040001	1.33749998	-0.06200000	0.00000000
130.	-0.16689999	-0.63830000	0.58740002	1.32000005	-0.09230000	0.00000000
135.	0.29899999	-0.69999999	0.41000000	1.20000005	-0.11460000	0.00000000
140.	0.12780000	-0.72000003	0.18189999	0.52469999	-0.13660000	0.00000000
145.	0.02690000	-0.49380001	0.36449999	-1.00029997	-0.14320000	0.00000000
150.	0.12510000	0.36690000	1.04970002	-0.63080001	-0.13440000	0.00000000
155.	0.10020000	0.24540000	0.97509998	0.46959999	-0.11800000	0.00000000
160.	0.00000000	0.08000000	0.23960001	0.32499999	-0.06200000	0.00000000
165.	-0.00570000	0.01650000	0.03550000	0.05410000	-0.00520000	0.00000000
170.	-0.01000000	-0.03490000	0.00130000	-0.00850000	0.01620000	0.00000000
175.	-0.00380000	-0.04390000	0.01230000	0.00490000	0.02420000	0.00000000
180.	-0.00290000	0.01890000	0.00900000	-0.04450000	0.02049000	0.00000000

presented for roll angles of 0, 45, and 90 degrees while the steel case increment is only presented for a roll angle of zero degrees. If the mutual interference between the stiffener rings and other protuberances is assumed to be zero, the FWC stiffener ring increment is then assumed to not vary with roll angle. Analysis of the steel case data shows this assumption to be valid.

7. CONCLUSIONS

The efforts of this contract have resulted in a better understanding of the aerodynamic characteristics of the SRBs during reentry and the effects the individual protuberances have upon the reentry aerodynamics. This knowledge should have a significant effect in aiding development of aerodynamic data for future flight vehicle configurations.

Data Tape 7 provides the best available reentry aerodynamic definition of the current baseline right side steel case SRB without nozzle extension. These data should be used to develop reentry trajectories and dynamic behavior of the steel case SRB.

Data Tape 8 was developed to provide the reentry aerodynamics for the baseline Filament Wound Case (FWC) right side SRB without nozzle extension. This tape should be used to analyze the reentry characteristics of the FWC SRB.

The TWT 691 wind tunnel test program did not model the thermal heat shield on the FWC SRB configuration therefore Data Tape 8 provides the reentry aerodynamics of the FWC SRB without the heat shield. The heat shield has a significant effect upon the axial force coefficients. Absence of the heat shield causes an increase in negative axial force resulting in a higher drag at the high angles of attack encountered during reentry. The magnitude of the heat shield effect is much greater than what was measured in previous tests. All data tapes prior to Data Tape 8 modeled the heat shield. Due to the uncertainty of the presence of the heat shield during reentry, this difference should be addressed to ensure an accurate representation of the SRB reentry aerodynamic characteristics.

Seven sets of increments were developed for the predominant steel case and FWC protuberances. These protuberances are: the high performance motor nozzle extension, the FWC and steel case systems tunnel, the FWC and steel case ET attach rings, and the FWC and steel case stiffener rings. The high performance nozzle increment contributes significantly to the longitudinal data. The difference between the FWC and steel case systems tunnels has the greatest effect upon the rolling moment coefficients, while the difference in stiffener rings contribute mainly to the axial force coefficients. The configuration of the ET attach ring has the least effect of all protuberances due to the close simularities between the FWC and steel case configurations.

8. REFERENCES

1. Sharp, R.S., and W.F. Braddock, "Right Side SRB Reentry Aerodynamics Revised Baseline Data Tape 7," LMSC-HREC TR D867290, Lockheed Missiles & Space Company, Huntsville, Ala., September 1983 (also Appendixes A and B).

2. Conine, B., and W.W. Boyle, "Space Shuttle Solid Rocket Booster Sting Interference Wind Tunnel Test Analysis," NSI TDR-230-2042, September 1981 (and Appendix D dated August 1982).

3. Hengel, J.E., "Post-Test Report for an Investigation to Determine the Reentry Aerodynamic Static Stability Characteristics for the Filament Wound Case STB in the MSFC 14 x 14-Inch TWT," MSFC Memorandum ED32-84-17, April 1984.

4. Gerry, G.B., "Post-Test Report for an Aerodynamic Roll study of a 0.00548 Scale Model of the Space Shuttle 146-Inch Diameter SRB with FWC Systems Tunnel and ET Attack Ring at Reentry Attitudes in the MSFC 14-Inch TWT (TWT 694)," MSFC Memorandum ED32-84-16, April 1984.

5. Hoerner, S.F., Fluid-Dynamic Drag, published by the author, Millard Park, N.J., 1965, pp. 16-13 to 16-17.

6. Wiegmann, B.M., "Updated SRB Reentry Static Stability Increments Due to Addition of High Performance Motor Nozzle Extension," MSFC memorandum ED32-82-17, December 1982.

7. Culberson, R.N., "SRB Aerodynamic Data Analysis Report," unpublished report dated November 1974.

END

DATE

JUN. 30, 1987